Tomas Mares

Fragments of curvilinear elasticity of fibre composites

Keep things simple!

Occam's razor

Reviewers

ISBN 80-...

Contents

CHAPTER 1

Anisotropic elasticity in curvilinear coordinates

1. Introduction

Elasticity is a branch of physics which studies the behaviour of materials that are deformed under stress (or, say, external forces), but then return to their original shape when the stress is removed. The amount of deformation is specified by strain.[1]

The strain is a measure that characterizes change of shape and dimensions (Fig. 1).[2] There is a fable[3]

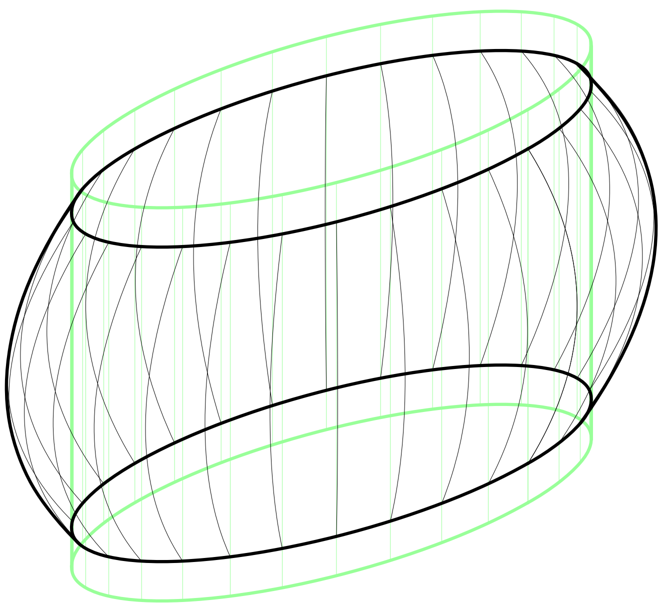

FIGURE 1. Change of shape

that features an oak as motionlessly standing under blasts of wind and a willow as vigorously swaying. At the end of a storm the oak lies fallen on ground but the willow still stays upright.

There are two questions and one suggestion. The questions first: What is strong? When do we speak about strength and when about elasticity? Then the suggestion: We are strongly used to connect deformation with force. The search for a relationship of stress (force) and strain (deformation) is the scope of a science called rheology and the model of elastic material is one of the most elementary models of rheology. The concept of elasticity is built on the classical works of PETTY and HOOKE.[4]

If we accept the thought that

$$\text{deformation} = f(\text{force})$$

than we must look at the forces (Figs. 2, 3). Let us assume that

$$F = \int_A \boldsymbol{t}\,\mathrm{d}A,$$

[1]http://en.wikipedia.org/wiki/Elasticity_(physics), 2007-01-10.

[2][**Cau27b**]

[3]The genre invented with Ezop (Aesop, *Αἴσωπος*) 6th century BC. Cf. http://www.mythfolklore.net/aesopica/.

[4]SIR WILLIAM PETTY (London, 1674), *…a new Hypothesis of Springing or Elastique Motions*, and ROBERT HOOKE (London, 1678/1660), *De Potentiâ Restitutiva*.

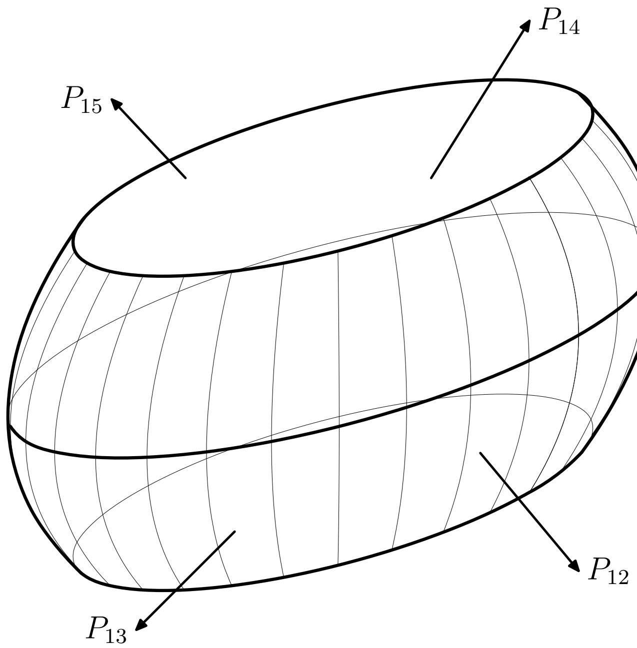

FIGURE 2. Force cause deformation

where the traction, $\boldsymbol{t}$ was defined by A. L. CAUCHY in 1823 as[5]

$$\boldsymbol{t} = \lim_{A \to 0} \frac{F}{A}$$

Inasmuch as (see Fig. 3)

$$F \neq F_1 \;\Rightarrow\; F = f(A),$$

A being the area of cross-section, and

$$F \neq P \;\Rightarrow\; F = g(\boldsymbol{n}),$$

where $\boldsymbol{n}$ is a normal to the cross-section, we can define, for $A \to 0$, a stress, σ, via

$$F = \boldsymbol{t}A = \sigma(\boldsymbol{A}),\;\; \boldsymbol{A} = A\boldsymbol{n}.$$

Let us look at the properties of σ. We isolate an infinitesimal but long element from the body (Fig. 4) and sum the acting forces (the forces on the smallest faces are neglected)[6]

$$\boldsymbol{F} = \sigma(\boldsymbol{A}) + \sigma(\boldsymbol{B}) + \sigma(\boldsymbol{C}),$$

where $\boldsymbol{A} = A\boldsymbol{n}, \boldsymbol{B}, \boldsymbol{C}$ are normals with lengths equal to the magnitudes of the respective areas. As

$$\lim_{x \to 0} \frac{\text{area}(x^2)}{\text{volume}(x^3)} = \infty$$

and

$$\frac{\text{area}}{\text{volume}} \propto \frac{\boldsymbol{F}}{\text{mass}} = \text{acceleration}$$

holds true, the implication

$$\boldsymbol{F} \neq \boldsymbol{0} \Rightarrow \text{acceleration} \to \infty \quad \text{(which is not true)}$$

leads to

$$\boldsymbol{F} = \boldsymbol{0},$$

i.e.,

$$\sigma(\boldsymbol{A}) + \sigma(\boldsymbol{B}) + \sigma(\boldsymbol{C}) = 0.$$

By definition,

$$\sigma(k\boldsymbol{A}) = k\sigma(\boldsymbol{A}) \tag{1}$$

[5]See [**Cau27a**].
[6][**Wan05**]

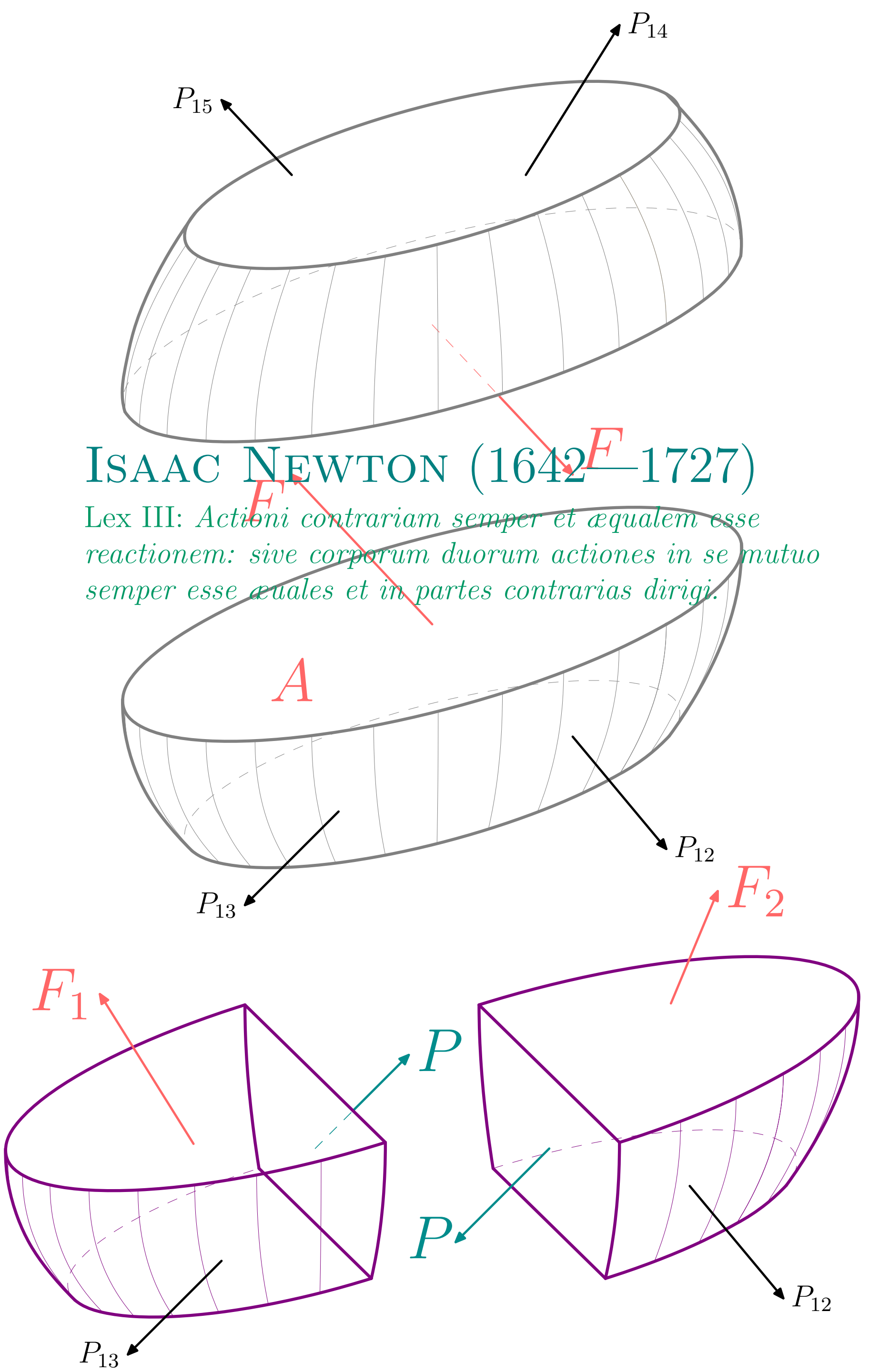

ISAAC NEWTON (1642—1727)

Lex III: *Actioni contrariam semper et æqualem esse reactionem: sive corporum duorum actiones in se mutuo semper esse æquales et in partes contrarias dirigi.*

FIGURE 3. Internal force

and consequently

$$\sigma(-\boldsymbol{C}) = -\sigma(\boldsymbol{C}) = \sigma(\boldsymbol{A}) + \sigma(\boldsymbol{B}).$$

Using geometry, *i.e.*

$$\boldsymbol{A} + \boldsymbol{B} + \boldsymbol{C} = 0,$$

the last relation takes the form

$$\sigma(\boldsymbol{A} + \boldsymbol{B}) = \sigma(\boldsymbol{A}) + \sigma(\boldsymbol{B}). \tag{2}$$

The relations (1) and (2) mean that σ is a linear vector operator, that is a *tensor*,[7] mapping a set of normals onto a set of forces. Thus we can write

$$F^a = t^a A = A\sigma^{ab} n_b$$

[7] [**Lov27**]

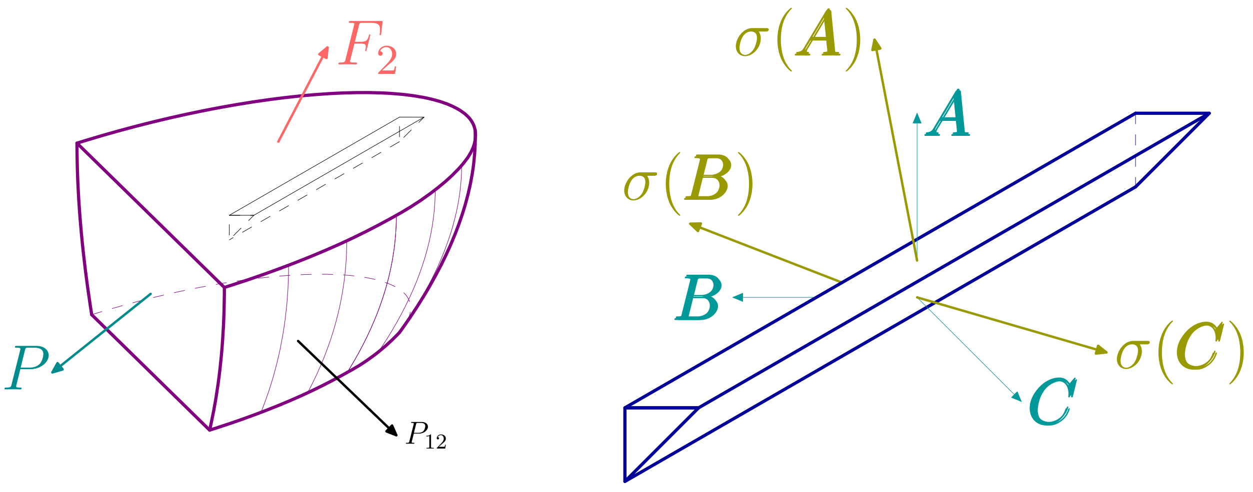

FIGURE 4. Internal force

and thus

$$t^a = \sigma^{ab} n_b.$$

2. A brief account of the tensor calculus

As the stress is a tensor we must take a look at tensor calculus.[8] Nothing is more natural than to measure distances. What happens if a surface is distorted like at Fig. 5? For a metric, $\mathrm{d}s_o$, in the undeformed body (with Cartesian coordinate system) we can write

$$\mathrm{d}s_o^2 = \left(\mathrm{d}\xi^1\right)^2 + \left(\mathrm{d}\xi^2\right)^2,$$

i.e.,

$$\mathrm{d}s_o^2 = \begin{pmatrix} \mathrm{d}\xi^1 & \mathrm{d}\xi^2 \end{pmatrix} \begin{pmatrix} 1 & 0 \\ 0 & 1 \end{pmatrix} \begin{pmatrix} \mathrm{d}\xi^1 \\ \mathrm{d}\xi^2 \end{pmatrix}$$

or, using Einstein summation convention,

$$\mathrm{d}s_o^2 = \delta_{ab} \mathrm{d}\xi^a \mathrm{d}\xi^b,$$

where δ_{ab} is the well known Kronecker symbol.[9]

By analogy, in the case of deformed surface, we may write

$$\mathrm{d}s^2 = g_{ab} \mathrm{d}\xi^a \mathrm{d}\xi^b,$$

meaning that we replace $\mathrm{d}s_o$ with the metric $\mathrm{d}s$ and Kronecker symbol δ_{ab} with a metric tensor g_{ab}.

Now, we must determine the metric tensor via expressing the length $\mathrm{d}s$ on a surface embedded in a three dimensional Euclidean space with a Cartesian coordinate system, x^a (see Fig. 6)

Consider a surface determined by mapping[10]

$$\theta : \mathbb{R}^2 \ni \omega \to \mathbb{R}^3$$

and let us look at two points on the surface defined by

$$\boldsymbol{x}_o = \theta(\xi^a)$$

and

$$\boldsymbol{x} = \theta(\xi^a + \mathrm{d}\xi^a).$$

From vector algebra it follows that

$$\mathrm{d}\boldsymbol{r} = \boldsymbol{g}_1 \mathrm{d}\xi^1 + \boldsymbol{g}_2 \mathrm{d}\xi^2, \tag{3}$$

$$\mathrm{d}\boldsymbol{r} = \boldsymbol{x} - \boldsymbol{x}_o,$$

$$\mathrm{d}\boldsymbol{r} = \theta(\xi^a + \mathrm{d}\xi^a) - \theta(\xi^a).$$

[8] [**SS78**], [**LR89**].

[9] LEOPOLD KRONECKER (1823—1891)

[10] Cf. [**CGM06**], [**CL03**] and [**Cia05**].

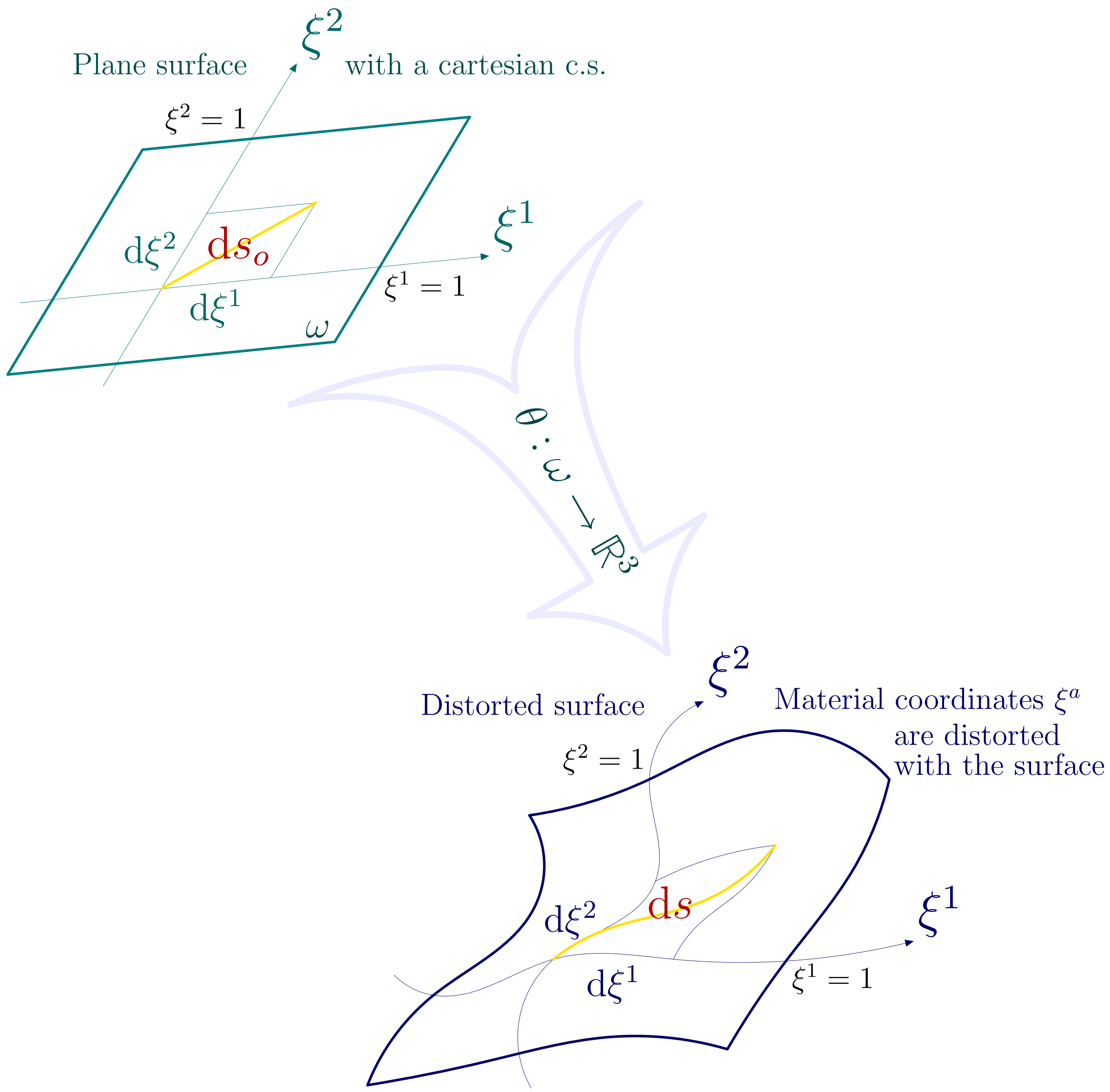

Figure 5. Distortion of a surface

From vector analysis we have (for $\mathrm{d}\xi^a \to 0$)

$$\mathrm{d}\boldsymbol{r} = \frac{\partial\theta}{\partial\xi^1}\mathrm{d}\xi^1 + \frac{\partial\theta}{\partial\xi^2}\mathrm{d}\xi^2, \tag{4}$$

$$\mathrm{d}s^2 = \mathrm{d}\boldsymbol{r}\cdot\mathrm{d}\boldsymbol{r} = \left(\frac{\partial\theta}{\partial\xi^1}\mathrm{d}\xi^1\right)^2 + 2\frac{\partial\theta}{\partial\xi^1}\frac{\partial\theta}{\partial\xi^2}\mathrm{d}\xi^1\mathrm{d}\xi^2 + \left(\frac{\partial\theta}{\partial\xi^2}\mathrm{d}\xi^2\right)^2$$

and using Einstein summation convention

$$\mathrm{d}s^2 = \frac{\partial\theta}{\partial\xi^a}\frac{\partial\theta}{\partial\xi^b}\mathrm{d}\xi^a\mathrm{d}\xi^b. \tag{5}$$

From above stated definition we may write

$$\mathrm{d}s^2 = g_{ab}\mathrm{d}\xi^a\mathrm{d}\xi^b. \tag{6}$$

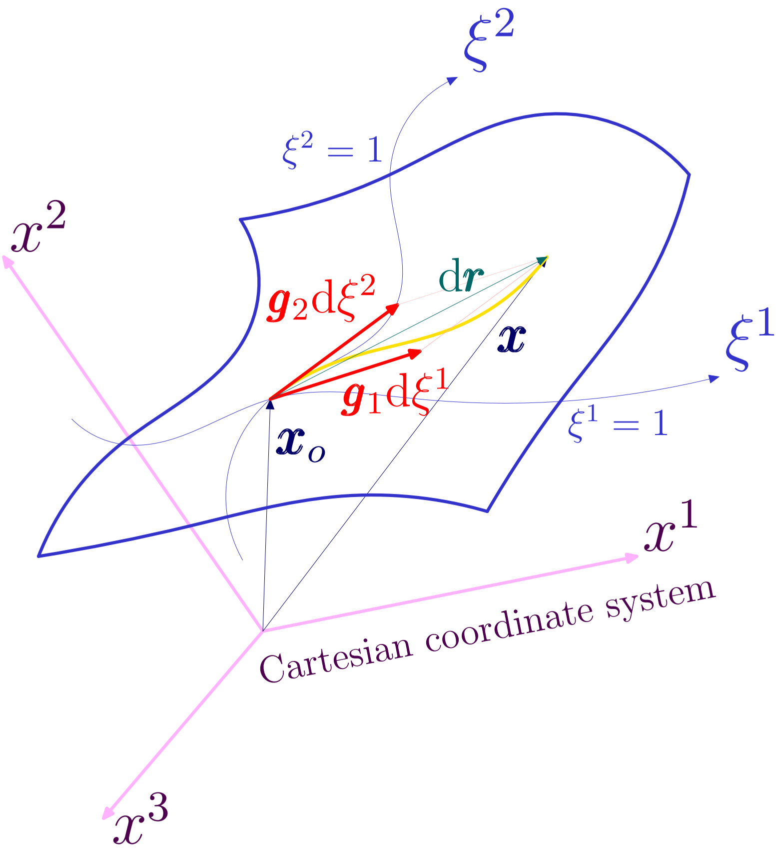

FIGURE 6. A surface embedded in a three dimensional Euclidean space

Now, (3) and (4) imply

$$\boldsymbol{g}_a = \frac{\partial \theta}{\partial \xi^a}$$

and (5) and (6) imply

$$g_{ab} = \frac{\partial \theta}{\partial \xi^a} \frac{\partial \theta}{\partial \xi^b}.$$

As a conclusion we can state that metric tensor is symmetric,

$$g_{ab} = g_{ba},$$

but the base vectors are not generally orthonormal, *i.e.*,

$$\boldsymbol{g}_a \cdot \boldsymbol{g}_b = g_{ab} \neq \delta_{ab}.$$

Any vector can be represented as a linear combination of a set of vectors, $\boldsymbol{e}_a$, selected in an appropriate manner, *i.e.*

$$\boldsymbol{a} = a^1 \boldsymbol{e}_1 + a^2 \boldsymbol{e}_2 = a^a \boldsymbol{e}_a.$$

Such a set is called a base and the vectors of the set base vectors.

In the case of a Cartesian coordinate system (Fig. 7) we are used to base vectors that are unitary and perpendicular to each other,

$$\boldsymbol{e}_a \cdot \boldsymbol{e}_b = \delta_{ab}. \tag{7}$$

In the case of a curvilinear coordinate system (or, generally, in the case of non-euclidean space, Fig. 8) the base vectors are not, always, unitary and perpendicular[11]

$$\boldsymbol{g}_a \cdot \boldsymbol{g}_b = g_{ab} \neq \delta_{ab}.$$

As we would like to hold on to some properties following the relation (7) we need to introduce a new base, $\boldsymbol{g}^a$, signified with superscript, such that

$$\boldsymbol{g}_b \cdot \boldsymbol{g}^a = \delta^a_b.$$

[11] [**GZ54**] and [**Tab04**]

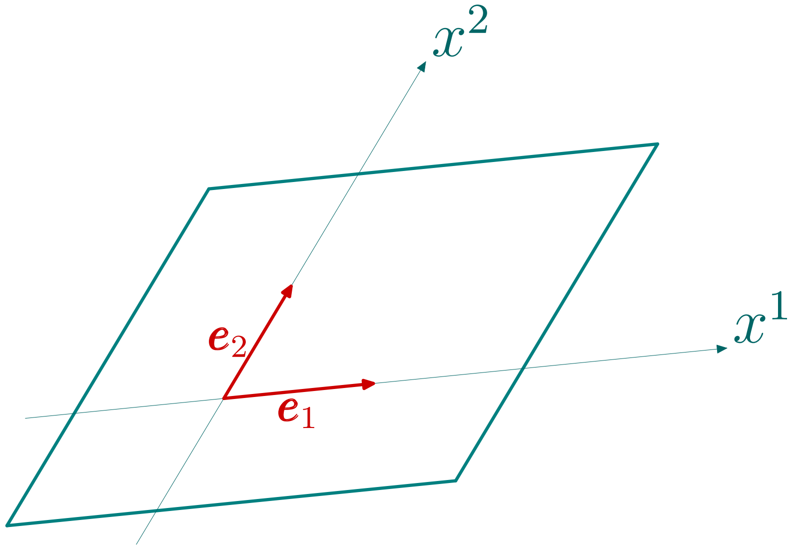

FIGURE 7. Euclidean space with a Cartesian coordinate system

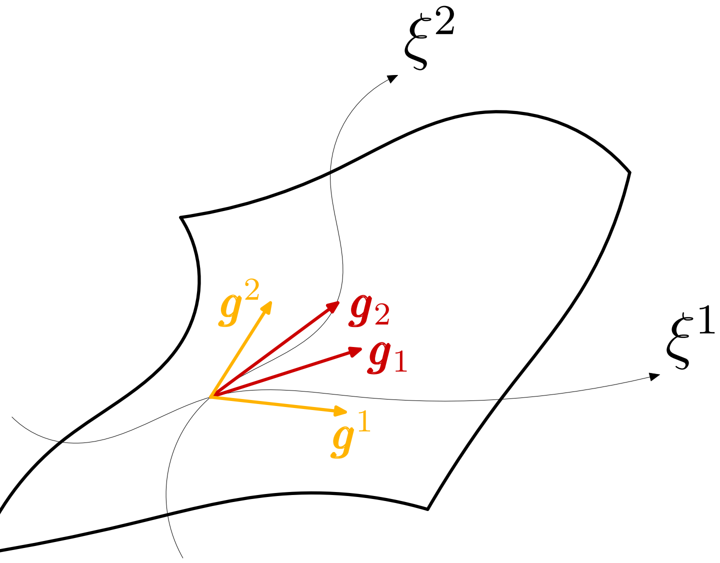

FIGURE 8. A curvilinear coordinate system (in a non-euclidean space)

Now we may, for vector

$$\boldsymbol{a} = a_a \boldsymbol{g}^a = a^a \boldsymbol{g}_a,$$

write, *e.g.*, the scalar product

$$\boldsymbol{a} \cdot \boldsymbol{a} = (a_a \boldsymbol{g}^a) \cdot (a_b \boldsymbol{g}^b) = (a_a \boldsymbol{g}^a) \cdot (a^b \boldsymbol{g}_b) = a_a a^b \boldsymbol{g}^a \cdot \boldsymbol{g}_b = a_a a^a$$

or vector addition

$$\boldsymbol{a} + \boldsymbol{b} = a_a \boldsymbol{g}^a + b_a \boldsymbol{g}^a = (a_a + b_a)\, \boldsymbol{g}^a,$$

in a form we are used to. These relations, together with, for example, the tensor equation

$$\boldsymbol{T} = \boldsymbol{a} \otimes \boldsymbol{b} \quad \Leftrightarrow \quad T^{ab} \boldsymbol{g}_a \otimes \boldsymbol{g}_b = (a^a \boldsymbol{g}_a) \otimes (b^b \boldsymbol{g}_b) = a^a b^b \boldsymbol{g}_a \otimes \boldsymbol{g}_b,$$

lead us to a thought to leave out the base vectors and write only the left-hand sides of the following relations:

$$a_a a^a = \boldsymbol{a} \cdot \boldsymbol{a}, \quad a^a + b^a \Leftrightarrow \boldsymbol{a} + \boldsymbol{b}, \quad a^a b^b \Leftrightarrow \boldsymbol{a} \otimes \boldsymbol{b}.$$

In this way we have passed up the information about the coordinate system we are using. This means we have abstracted the notation, and thus this very effective form of writing tensors is called the abstract index notation.

Let us define a contravariant metric tensor[12] (in effect this tensor is not a metric tensor and thus more rigorously it is called the inverse to metric tensor)

$$g^{ab} = (g_{ab})^{-1} \tag{8}$$

and multiply both sides of the equation

$$a_a \boldsymbol{g}^a = a^a \boldsymbol{g}_a$$

with $\boldsymbol{g}_b$, giving

$$a_a \boldsymbol{g}^a \cdot \boldsymbol{g}_b = a^a \boldsymbol{g}_a \cdot \boldsymbol{g}_b$$

and

$$a_b = a_a \delta^a_b = a^a g_{ab},$$

which is the rule of lowering of indices. Now, multiply both sides with g^{bd}, and using the definition (8), we get the rule of raising of indices

$$g^{bd} a_b = a^d.$$

Let us express the derivative of a vector

$$\frac{\partial \boldsymbol{a}}{\partial x^a} = \frac{\partial}{\partial x^a}(a^b \boldsymbol{g}_b) = (\partial_a a^b)\boldsymbol{g}_b + a^b \frac{\partial \boldsymbol{g_b}}{\partial x^a},$$

introducing the notation

$$\partial_a = \frac{\partial}{\partial x^a}.$$

Naturally, we would like the derivative to be a linear combination of base vectors, *i.e.*, something like

$$\frac{\partial \boldsymbol{a}}{\partial x^a} = \nabla_a a^b \boldsymbol{g}_b.$$

It turns out that such a ∇_a exists and it holds

$$\nabla_a a^b = \partial_a a^b + \Gamma^b_{ac} a^c$$

and is called the covariant derivative. The Christoffel symbols of the second kind are

$$\Gamma^d_{ab} = g^{dc} \frac{1}{2}(g_{ac,b} + g_{cb,a} - g_{ab,c})$$

with the partial derivative

$$g_{ab,c} = \partial_c g_{ab} = \frac{\partial g_{ab}}{\partial x^c}.$$

The well known differential operators are expressed as

$$\operatorname{grad} \varphi = \nabla_a \varphi \, \boldsymbol{g}^a = \partial_a \varphi \, \boldsymbol{g}^a,$$

$$\operatorname{div} \boldsymbol{v} = \nabla \boldsymbol{v} = \nabla_a v^a,$$

$$\operatorname{rot} \boldsymbol{A} = \nabla \times \boldsymbol{A} = \epsilon^{abc} \nabla_a A_b \, \boldsymbol{g}^c$$

and

$$\nabla^2 \varphi = \operatorname{div} \operatorname{grad} \varphi.$$

Let us very briefly mention the transformation rules for vectors (contravariant tensors)[13]

$$\mathrm{d}x^a = \frac{\partial x^a}{\partial \xi^b} \mathrm{d}\xi^b$$

and covectors (covariant tensors)

$$\frac{\partial \phi}{\partial x^a} = \frac{\partial \xi^b}{\partial x^a} \frac{\partial \phi}{\partial \xi^b},$$

where $\mathrm{d}x^a, \mathrm{d}\xi^b$ stand for contravariant tensors and $\dfrac{\partial \phi}{\partial x^a}, \dfrac{\partial \phi}{\partial \xi^b}$ for covariant tensors.

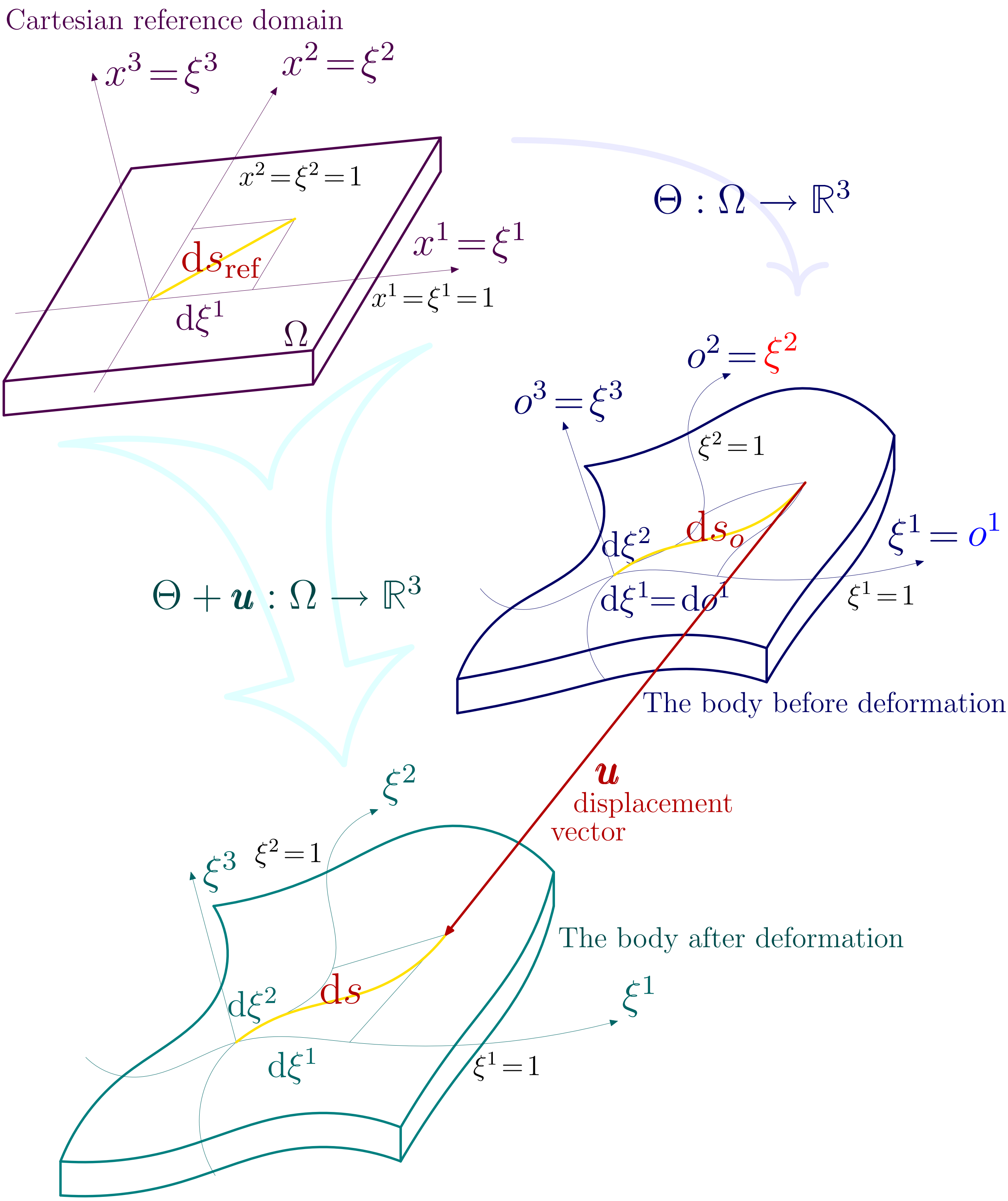

FIGURE 9. Deformed body and coordinate systems

3. Deformation tensor

Let us see (Fig. 9) how a body described with coordinates ranging in a fictitious rectangular domain, Ω, behaves under imposed deformation. A point has before deformation the same coordinates, $o^a = \xi^a$, in

[12][**SS78**], [**LR89**]

[13]For more thorough discussion see, *e.g.*, [**LR89**], [**GZ54**], [**Ham55**], [**SS78**], [**Tab04**], [**Tot05**], [**Wal84**], [**Wan05**], [**Was75**].

both the space coordinate system, o, the system frozen in space, and the material coordinate system, ξ, the system frozen in a material, *i.e.*, coordinate system that deforms with the deformed body.[14]

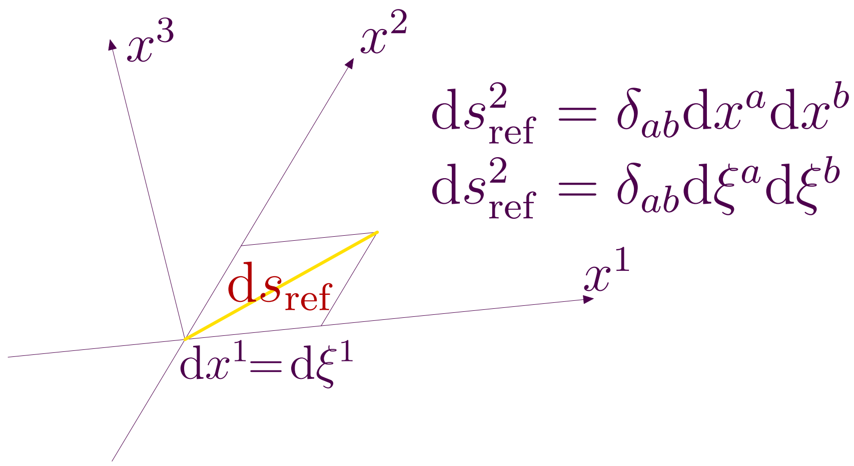

Figure 10. Cartesian reference domain

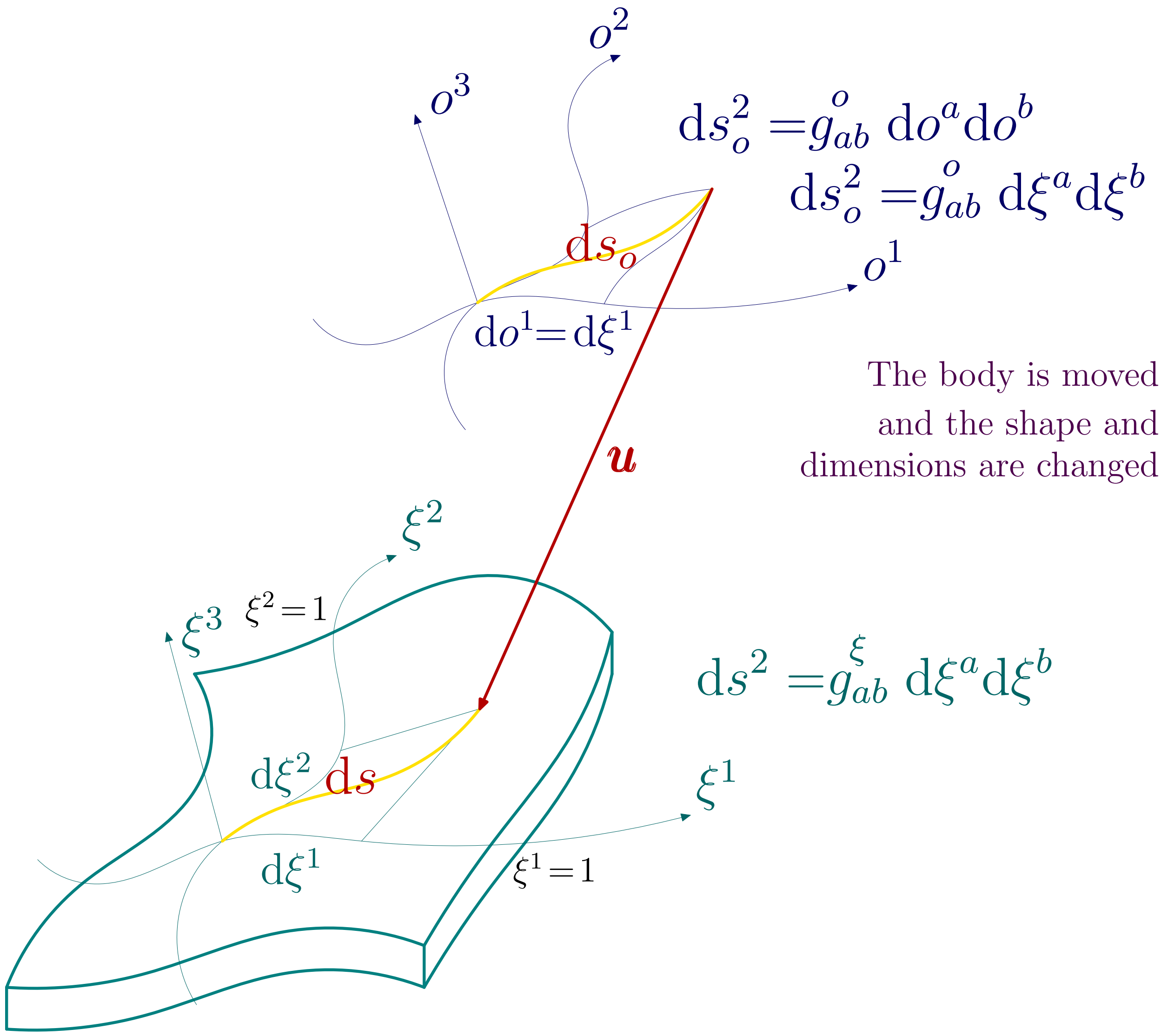

Figure 11. Space coordinate system, o, and material coordinate system, ξ

[14][**GZ54**], [**Ant05**], [**Cia05**].

The deformation is a measure of a change of dimensions and shape.[15] The dimensions and shape are described by coordinate systems. Let us look once more at these, this time at Figs. 10 and 11 and the square of the distance between two points. Before deformation it is

$$\mathrm{d}s_o^2 = \overset{o}{g}_{ab}\, \mathrm{d}o^a \mathrm{d}o^b$$

and after deformation the distance squared is

$$\mathrm{d}s^2 = \overset{\xi}{g}_{ab}\, \mathrm{d}\xi^a \mathrm{d}\xi^b.$$

$\overset{o}{g}_{ab}$ denotes a metric of the space coordinate system o and $\overset{\xi}{g}_{ab}$ is a metric of the material coordinate system ξ. The metric $\overset{\xi}{g}_{ab}$ is a function of time; it changes during the process of loading and at the end it is stabilized in the state of static equilibrium. At the beginning it is supposed that the space and material coordinate systems coincide, *i.e.*

$$\left.\overset{\xi}{g}_{ab}\right|_{t=0} = \overset{o}{g}_{ab}\ .$$

The coordinates o^a at the undeformed state and ξ^a both at the deformed and undeformed state are both from the same interval Ω_r ($o^a \in \Omega_r$, $\xi^a \in \Omega_r$). The element of the volume before deformation is

$$\mathrm{d}\Omega_o = \left|\overset{o}{g}_{ab}\right|^{\frac{1}{2}} \mathrm{d}\Omega_r$$

and after deformation

$$\mathrm{d}\Omega = \left|\overset{\xi}{g}_{ab}\right|^{\frac{1}{2}} \mathrm{d}\Omega_r,$$

with

$$\mathrm{d}\Omega_r = \mathrm{d}^3\xi = \mathrm{d}^3 o.$$

Now, the last expression for the square of deformed body distance can be written as

$$\mathrm{d}s^2 = \overset{\xi}{g}_{ab}\, \mathrm{d}o^a \mathrm{d}o^b.$$

The deformation is characterized by a change of the distance, that is by the change of the element length. Let us express this as

$$\mathrm{d}s^2 - \mathrm{d}s_o^2 = (\overset{\xi}{g}_{ab} - \overset{o}{g}_{ab})\mathrm{d}o^a \mathrm{d}o^b.$$

Now, the relation

$$\mathrm{d}s^2 - \mathrm{d}s_o^2 = 2\, \overset{o}{E}_{ab}\, \mathrm{d}o^a \mathrm{d}o^b$$

defines the Green-Lagrange-St. Venant strain, $\overset{o}{E}_{ab}$, and thus

$$\overset{o}{E}_{ab} = \frac{1}{2}(\overset{\xi}{g}_{ab} - \overset{o}{g}_{ab}).$$

If o, and consequently also $\overset{o}{\xi}$ are Cartesian coordinate systems, *i.e.* $\overset{o}{g}_{ab} = \delta_{ab}$, then we may write $o^a = \xi^a + \overset{o}{u}^a$ and

$$\overset{\xi}{g}_{ab} = \frac{\partial o^c}{\partial \xi^a}\frac{\partial o^d}{\partial \xi^b}\, \overset{o}{g}_{cd} = (\delta^c_a + \partial_a\, \overset{o}{u}^c)(\delta^d_b + \partial_b\, \overset{o}{u}^d)\delta_{cd} = \delta_{ab} + \partial_a\, \overset{o}{u}_b + \partial_b\, \overset{o}{u}_a + \partial_a\, \overset{o}{u}^c\, \partial_b\, \overset{o}{u}_c$$

and

$$\overset{o}{E}_{ab} = \frac{1}{2}(\overset{\xi}{g}_{ab} - \delta_{ab}) = \frac{1}{2}(\partial_a\, \overset{o}{u}_b + \partial_b\, \overset{o}{u}_a + \partial_a\, \overset{o}{u}^c\, \partial_b\, \overset{o}{u}_c)$$

becomes the well known finite strain tensor in Lagrangian description. In this case ($\overset{o}{g}_{ab} = \delta_{ab}$) the metric $\overset{\xi}{g}_{ab}$ is called Cauchy-Green strain.

Let us also mention the Almansi-Euler strain tensor

$$\overset{\xi}{E}^{ab} = \frac{\partial \xi^c}{\partial o^a}\frac{\partial \xi^d}{\partial o^b}\, \overset{o}{E}^{cd}\ .$$

[15] [**Ant05**], [**GZ54**], [**Cia05**]

4. Small strain tensor

By linearizing the Green-Lagrange-St. Venant strain (expressed in Cartesian coordinates)

$$\overset{o}{E}_{ab}=\frac{1}{2}(\partial_a u_b+\partial_b u_a+\partial_a u^c\partial_b u_c),$$

i.e., by ignoring the quadratic term, $\partial_a u^c\partial_b u_c$, we arrive at the small strain tensor[16]

$$\varepsilon_{ab}=\frac{1}{2}(\partial_a u_b+\partial_b u_a).$$

If we would like to return to the curvilinear coordinates then we must replace the partial derivative, ∂_a, with the covariant derivative, ∇_a:[17]

$$\varepsilon_{ab}=\frac{1}{2}(\overset{\xi}{g}_{ab}-\overset{o}{g}_{ab})\bigg|_{\text{lin.}}=\frac{1}{2}(\nabla_a u_b+\nabla_b u_a).$$

5. Stress tensor

One way as to introduce the stress tensor is to define it as a tensor conjugate to a strain tensor. To this end let us express the following statements. For the elastic energy density in the reference state it holds that

$$\mathrm{d}w=\varrho_o\mathrm{d}u$$

and for the elastic energy density in the deformed state

$$\mathrm{d}\tilde{w}=\varrho\mathrm{d}u$$

holds, where u is the specific internal energy. The specific internal energy may be regarded either as a function of the Green-Lagrange-St Venant strain, $\overset{o}{E}_{ab}$, or as a function of the Euler-Almansi strain, $\overset{\xi}{E}_{ab}$. Then

$$\mathrm{d}u=\frac{\mathrm{d}w}{\varrho_o}=\frac{\partial w}{\varrho_o\partial\overset{o}{E}_{ab}}\mathrm{d}\overset{o}{E}_{ab} \tag{9}$$

and also

$$\mathrm{d}u=\frac{\mathrm{d}\tilde{w}}{\varrho}=\frac{\partial\tilde{w}}{\varrho\partial\overset{\xi}{E}_{ab}}\mathrm{d}\overset{\xi}{E}_{ab}\ . \tag{10}$$

As

$$\mathrm{d}\overset{\xi}{E}_{ab}=\frac{\partial o^c}{\partial\xi^a}\frac{\partial o^d}{\partial\xi^b}\mathrm{d}\overset{o}{E}_{cd}$$

holds we have, from the equality (9) to (10),

$$\frac{\partial\tilde{w}}{\varrho\partial\overset{\xi}{E}_{ab}}\frac{\partial o^c}{\partial\xi^a}\frac{\partial o^d}{\partial\xi^b}=\frac{\partial w}{\varrho_o\partial\overset{o}{E}_{cd}}. \tag{11}$$

Now,

$$m=\int\limits_{\Omega_r}\varrho\left|\overset{\xi}{g}_{ab}\right|^{\frac{1}{2}}\mathrm{d}^3\xi=\int\limits_{\Omega_r}\varrho_o\left|\overset{o}{g}_{ab}\right|^{\frac{1}{2}}\mathrm{d}^3\xi$$

and thus

$$\frac{\varrho_o}{\varrho}=\frac{\left|\overset{\xi}{g}_{ab}\right|^{\frac{1}{2}}}{\left|\overset{o}{g}_{ab}\right|^{\frac{1}{2}}}. \tag{12}$$

---

[16] See [**Lov27**], [**Was75**] and [**Cia05**]. The origin of this tensor is connected with Kelvin, Tait, Kirchhoff, Saint-Venant, Pearson and von Kármán.

[17] [**Wal84**]

Using (12) in (11) yields

$$\overset{\xi}{\sigma}{}^{ab}\,\frac{\partial o^c}{\partial \xi^a}\frac{\partial o^d}{\partial \xi^b}\frac{\left|\overset{\xi}{g}_{ab}\right|^{\frac{1}{2}}}{\left|\overset{o}{g}_{ab}\right|^{\frac{1}{2}}} = \overset{o}{S}{}^{cd}, \tag{13}$$

where[18]

$$\overset{o}{S}{}^{ab} = \frac{\partial w}{\partial \overset{o}{E}_{ab}}$$

is the well known 2$^{\text{nd}}$ Piola-Kirchhoff stress tensor and

$$\overset{\xi}{\sigma}{}^{ab} = \frac{\partial \tilde{w}}{\partial \overset{\xi}{E}_{ab}}$$

is the Cauchy stress tensor.

Multiplying the transformation rule (13) with $\overset{o}{g}_{ak}\overset{o}{g}_{bl}$ we arrive at the transformation rule for covariant components of the stress tensors

$$\overset{\xi}{\sigma}_{ab}\,\frac{\left|\overset{\xi}{g}_{ab}\right|^{\frac{1}{2}}}{\left|\overset{o}{g}_{ab}\right|^{\frac{1}{2}}} = \frac{\partial o^k}{\partial \xi^a}\frac{\partial o^l}{\partial \xi^b}\,\overset{o}{S}_{kl},$$

which is the well known transformation rule for the case of a cartesian space coordinate system

$$\boldsymbol{FSF}^T = J\boldsymbol{\sigma}.$$

6. The minimum principles

Let us state the well known minimum principles used in elasticity.[19]

6.1. The minimum principle of total potential energy. It became commonly known and used[20] that the real state of a deformed body, $\hat{u}_a$, minimizes the total potential energy

$$\Pi(u_a) = a(u_a) - l(u_a)$$

on a set of admissible states, $\mathbb{U}$, where the elastic strain energy

$$a(u_a) = \frac{1}{2}\int_{\Omega} E^{abcd}\varepsilon_{ab}(u_a)\varepsilon_{cd}(u_a)\mathrm{d}\Omega$$

and the potential energy of the applied forces

$$-l(u_a) = -\int_{\Omega} p^a u_a \mathrm{d}\Omega - \int_{\partial_t\Omega} t^a u_a \mathrm{d}\Gamma.$$

In essence

$$\hat{u}_a = \arg\min_{u_b\in\mathbb{U}} \Pi(u_c).$$

[18] [**Cia88**]

[19] The origin of these principles is joined with such names as Maupertuis, 1746, Euler, 1744, and Lagrange, 1788.

[20] [**Mik64**], [**Was75**], [**LR89**], [**Dac89**], [**Ped00**], [**Che00**]

6.2. The minimum principle of complementary energy. The minimum principle of total potential energy leads straightforwardly to the minimum principle of complementary energy

$$\hat{\sigma}_{ab} = \arg\min_{\sigma^{ab}\in\mathbb{S}} \Pi_c(\sigma^{ab})$$

that says that equilibrium stress state, $\hat{\sigma}_{ab}$, minimizes the complementary energy

$$\Pi_c(\sigma^{ab}) = c(\sigma^{ab}) - l_u(\sigma^{ab})$$

on a set of admissible stress states

$$\mathbb{S} = \left\{\sigma^{ab} \mid \nabla_a\sigma^{ab} + p^b = 0 \text{ in } \Omega, \quad \sigma^{ab}\ell_b = t^a \text{ on } \partial_t\Omega\right\}.$$

Now the elastic stress energy[21]

$$c(\sigma^{ab}) = \frac{1}{2}\int_\Omega C_{abcd}\sigma^{ab}\sigma^{cd}\mathrm{d}\Omega$$

and work of reactions (*i.e.*, work done through kinematic boundary conditions)

$$l_u(\sigma^{ab}) = \int_{\partial_u\Omega} \sigma^{ab}\tilde{u}_a\ell_b\mathrm{d}\Gamma.$$

7. Elasticity tensor and compliance tensor

In the case of an isotropic material we may write the Hooke's law

$$\sigma_{ab} = E^{abcd}\varepsilon_{cd}$$

with elasticity tensor given by expression valid in any coordinate system

$$E^{abcd} = \lambda g^{ab}g^{cd} + \mu g^{ac}g^{bd} + \mu g^{ad}g^{bc},$$

where λ and μ are Lamé parameters.

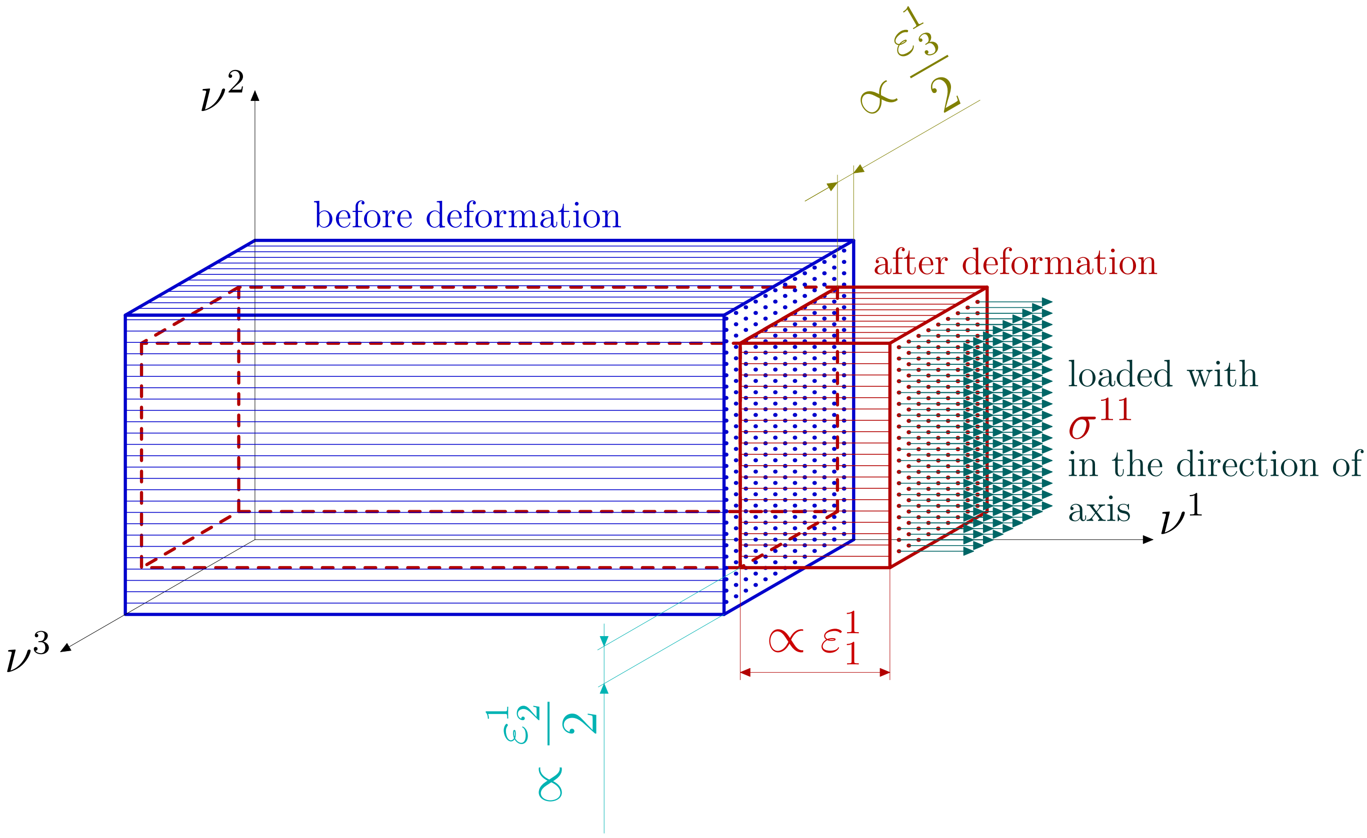

FIGURE 12. Orthotropic block

---

[21][**Sal01**] p. 487.

In the case of an orthotropic material, for example the orthotropic elementary block (designated as νth block, Figure 12) we may choose the coordinate system, ν_a, called the principal material coordinate system. The *principal* stands for *aligned with* the principal material axes of the orthotropic material.

Let us perform the following experiment: Stretch the block in the direction of ν_1 axis (*i.e.*, in the direction of fibres) in such a manner that the prescribed strain ε_1^1 does not violate the linear elasticity conditions. Now measure the stress σ_{11} with which you have pulled the block, and strains in transverse directions (*i.e.* the directions ν_2 and ν_3). These strains are designated ε_2^1 (*i.e.*, the strain in the ν_2 direction caused by the strain ε_1^1 in the ν_1 direction) and ε_3^1, with a similar meaning of the indices.

We can define the so-called principal Poisson ratios

$$\nu_{12} = -\frac{\varepsilon_2^1}{\varepsilon_1^1}, \quad \nu_{13} = -\frac{\varepsilon_3^1}{\varepsilon_1^1},$$

and the ratio

$$E_{11} = \frac{\sigma_{11}}{\varepsilon_1^1}$$

called the Hooke's law for uniaxial stress state.

In a similar way, we may arrive at the relations

$$E_{22} = \frac{\sigma^{22}}{\varepsilon_2^2}, \quad \nu_{21} = -\frac{\varepsilon_1^2}{\varepsilon_2^2}, \quad \nu_{23} = -\frac{\varepsilon_3^2}{\varepsilon_2^2}$$

and

$$E_{33} = \frac{\sigma^{33}}{\varepsilon_3^3}, \quad \nu_{31} = -\frac{\varepsilon_1^3}{\varepsilon_3^3}, \quad \nu_{32} = -\frac{\varepsilon_2^3}{\varepsilon_3^3},$$

where the meaning of the indices is analogous to those first mentioned.

It is acceptable to think about superposition, *i.e.*, to presume the total strain is a sum of the strain in direction ν_1 due to stress σ_{11} (*i.e.*, ε_1^1), the strain in direction ν_1 due to stress σ_{22} (ε_1^2), and the strain in direction ν_1 due to stress σ_{33} (ε_1^3), namely

$$\varepsilon_{11} = \varepsilon_1^1 + \varepsilon_1^2 + \varepsilon_1^3,$$

or

$$\varepsilon_{11} = \varepsilon_1^1 - \nu_{21}\varepsilon_2^2 - \nu_{31}\varepsilon_3^3,$$

and, finally

$$\varepsilon_{11} = \frac{\sigma_{11}}{E_{11}} - \nu_{21}\frac{\sigma_{22}}{E_{22}} - \nu_{31}\frac{\sigma_{33}}{E_{33}}.$$

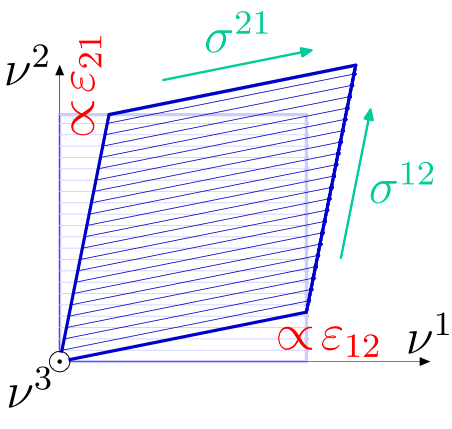

FIGURE 13. Pure shear stress

In the case of pure shear strain (Fig. 13) we have, from the above mentioned definition,

$$\varepsilon_{ab} = \varepsilon_{ba}$$

and, from equilibrium equation, we have

$$\sigma^{ab} = \sigma^{ba}.$$

The commonly accepted relation between shear stress and strain is

$$\sigma^{12} = \sigma^{12} = G_{12}(\varepsilon_{12} + \varepsilon_{21})$$

or

$$\sigma^{12} = 2\varepsilon_{12}G_{12},\ \sigma^{23} = 2\varepsilon_{23}G_{23},\ \sigma^{31} = 2\varepsilon_{31}G_{31}.$$

Now, we may write the compliance relation

$$\begin{pmatrix} \varepsilon_{11} \\ \varepsilon_{22} \\ \varepsilon_{33} \\ \varepsilon_{12} \\ \varepsilon_{23} \\ \varepsilon_{31} \end{pmatrix} = \begin{pmatrix} \frac{1}{E_{11}} & -\frac{\nu_{21}}{E_{22}} & -\frac{\nu_{31}}{E_{33}} & 0 & 0 & 0 \\ -\frac{\nu_{12}}{E_{11}} & \frac{1}{E_{22}} & -\frac{\nu_{32}}{E_{33}} & 0 & 0 & 0 \\ -\frac{\nu_{13}}{E_{11}} & -\frac{\nu_{23}}{E_{22}} & \frac{1}{E_{33}} & 0 & 0 & 0 \\ 0 & 0 & 0 & \frac{1}{2G_{12}} & 0 & 0 \\ 0 & 0 & 0 & 0 & \frac{1}{2G_{23}} & 0 \\ 0 & 0 & 0 & 0 & 0 & \frac{1}{2G_{31}} \end{pmatrix} \begin{pmatrix} \sigma^{11} \\ \sigma^{22} \\ \sigma^{33} \\ \sigma^{12} \\ \sigma^{23} \\ \sigma^{31} \end{pmatrix}$$

or in a more convenient form

$$\overset{\nu}{\varepsilon}_{ab}=\overset{\nu}{C}_{abcd}\overset{\nu}{\sigma}{}^{cd},$$

where the compliance tensor

$$\left\{\overset{\nu}{C}_{abcd}\right\}_{\{ab\lceil cd\}} = \begin{pmatrix} \frac{1}{E_{11}} & 0 & 0 & 0 & -\frac{\nu_{21}}{E_{22}} & 0 & 0 & 0 & -\frac{\nu_{31}}{E_{33}} \\ 0 & \frac{1}{4G_{12}} & 0 & \frac{1}{4G_{12}} & 0 & 0 & 0 & 0 & 0 \\ 0 & 0 & \frac{1}{4G_{13}} & 0 & 0 & 0 & \frac{1}{4G_{13}} & 0 & 0 \\ 0 & \frac{1}{4G_{12}} & 0 & \frac{1}{4G_{12}} & 0 & 0 & 0 & 0 & 0 \\ -\frac{\nu_{12}}{E_{11}} & 0 & 0 & 0 & \frac{1}{E_{22}} & 0 & 0 & 0 & -\frac{\nu_{32}}{E_{33}} \\ 0 & 0 & 0 & 0 & 0 & \frac{1}{4G_{23}} & 0 & \frac{1}{4G_{23}} & 0 \\ 0 & 0 & \frac{1}{4G_{13}} & 0 & 0 & 0 & \frac{1}{4G_{13}} & 0 & 0 \\ 0 & 0 & 0 & 0 & 0 & \frac{1}{4G_{23}} & 0 & \frac{1}{4G_{23}} & 0 \\ -\frac{\nu_{13}}{E_{11}} & 0 & 0 & 0 & -\frac{\nu_{23}}{E_{22}} & 0 & 0 & 0 & \frac{1}{E_{33}} \end{pmatrix}.$$

The ν above the tensor symbol indicates that the symbol does not symbolize an abstract tensor but that it stands for the tensor components in the ν-frame of reference and $\{ij\lceil kl\}$ indicate how the entries are stored in the array, namely that the rows belong successively to the following pairs of indices ($ij = 11, 12, 13, 21, 22, 23, 31, 32, 33$) and the pairs to the couples ($kl = 11, 12, \dots, 33$).

A little tedious arrangement leads to the generalized Hooke's law of the laminated block in the form

$$\overset{\nu}{\sigma}{}^{ab}=\overset{\nu}{E}{}^{abcd}\overset{\nu}{\varepsilon}_{cd}$$

with components of the elasticity tensor

$$\left\{\overset{\nu}{E}{}^{abcd}\right\}_{\{ab\lceil cd} = \begin{pmatrix} \Phi_{1111} & 0 & 0 & 0 & \Phi_{1122} & 0 & 0 & 0 & \Phi_{1133} \\ 0 & G_{12} & 0 & G_{12} & 0 & 0 & 0 & 0 & 0 \\ 0 & 0 & G_{13} & 0 & 0 & 0 & G_{13} & 0 & 0 \\ 0 & G_{12} & 0 & G_{12} & 0 & 0 & 0 & 0 & 0 \\ \Phi_{2211} & 0 & 0 & 0 & \Phi_{2222} & 0 & 0 & 0 & \Phi_{2233} \\ 0 & 0 & 0 & 0 & 0 & G_{23} & 0 & G_{23} & 0 \\ 0 & 0 & G_{13} & 0 & 0 & 0 & G_{13} & 0 & 0 \\ 0 & 0 & 0 & 0 & 0 & G_{23} & 0 & G_{23} & 0 \\ \Phi_{3311} & 0 & 0 & 0 & \Phi_{3322} & 0 & 0 & 0 & \Phi_{3333} \end{pmatrix},$$

where

$$\Phi_{1111} = \frac{1-\nu_{23}\nu_{32}}{N}E_{11},\quad \Phi_{1122} = \frac{\nu_{21}+\nu_{23}\nu_{31}}{N}E_{11},\quad \Phi_{1133} = \frac{\nu_{31}+\nu_{32}\nu_{21}}{N}E_{11},$$
$$\Phi_{2211} = \frac{\nu_{12}+\nu_{13}\nu_{32}}{N}E_{22},\quad \Phi_{2222} = \frac{1-\nu_{13}\nu_{31}}{N}E_{22},\quad \Phi_{2233} = \frac{\nu_{32}+\nu_{31}\nu_{12}}{N}E_{22},$$
$$\Phi_{3311} = \frac{\nu_{13}+\nu_{12}\nu_{23}}{N}E_{33},\quad \Phi_{3322} = \frac{\nu_{23}+\nu_{21}\nu_{13}}{N}E_{33},\quad \Phi_{3333} = \frac{1-\nu_{12}\nu_{21}}{N}E_{33},$$

and

$$N = 1 - \nu_{12}\nu_{21} - \nu_{23}\nu_{32} - \nu_{31}\nu_{13} - \nu_{12}\nu_{23}\nu_{31} - \nu_{13}\nu_{32}\nu_{21}.$$

It is well known, following the elastic energy expression, that in a Cartesian reference frame,[22] like the ν-frame,

$$\overset{\nu}{E}{}^{abcd}=\overset{\nu}{E}_{cdab} \quad \text{and} \quad \overset{\nu}{C}_{abcd}=\overset{\nu}{C}_{cdab}$$

[22]Compare, for instance, [**Sal01**] p. 329.

holds which means $\Phi_{1122} = \Phi_{2211}$ and $\nu_{21}E_{11} = \nu_{12}E_{22}$, *etc.* The two last equalities imply

$$\nu_{23}\nu_{31}\nu_{12} = \nu_{13}\nu_{32}\nu_{21}.$$

Similarly, for the other two cases. From

$$\sigma^{ab} = \sigma^{ba} \quad \text{and} \quad \varepsilon^{ab} = \varepsilon^{ba}$$

it follows that

$$C_{abcd} = C_{bacd}.$$

As the main frame of reference is orthogonal it is evident that covariant and contravariant tensor components coincide, *i.e.*,

$$\overset{\nu}{\boldsymbol{e}}_i \overset{\nu}{\boldsymbol{e}}{}^j = \delta_i^j,\ \overset{\nu}{\boldsymbol{e}}_i \overset{\nu}{\boldsymbol{e}}_j = \delta_{ij} = \delta_i^j \Rightarrow \overset{\nu}{\boldsymbol{e}}_j = \overset{\nu}{\boldsymbol{e}}{}^j$$

and thus, as indicated above,

$$\overset{\nu}{E}{}^{ij}{}_{kl} = \overset{\nu}{E}_{ijkl} = \overset{\nu}{E}{}^{ijkl}\ .$$

What is essential is that these tensor components are *physical* quantities, *i.e.*, quantities possessing true units, however the coordinate systems are distorted in the reference frame of computation.

8. Concept of locally orthotropic material

The above relations may be readily used in very large variety of anisotropic materials via the concept of locally orthotropic material.

The concept of locally orthotropic material is based on the idea that at every point of a material it is possible to construct a cartesian coordinate system ν_a such that the material in its infinitesimal surrounding behaves orthotropically, *i.e.*, the mentioned relations hold.

Thus we only need to perform a transformation from the main frame of orthogonality, ν^a, into a frame of computation. In the frame of the computation the tensor entries are not necessarily physical quantities.

CHAPTER 2

Analysis of thick-walled anisotropic elliptic tube

1. Introduction

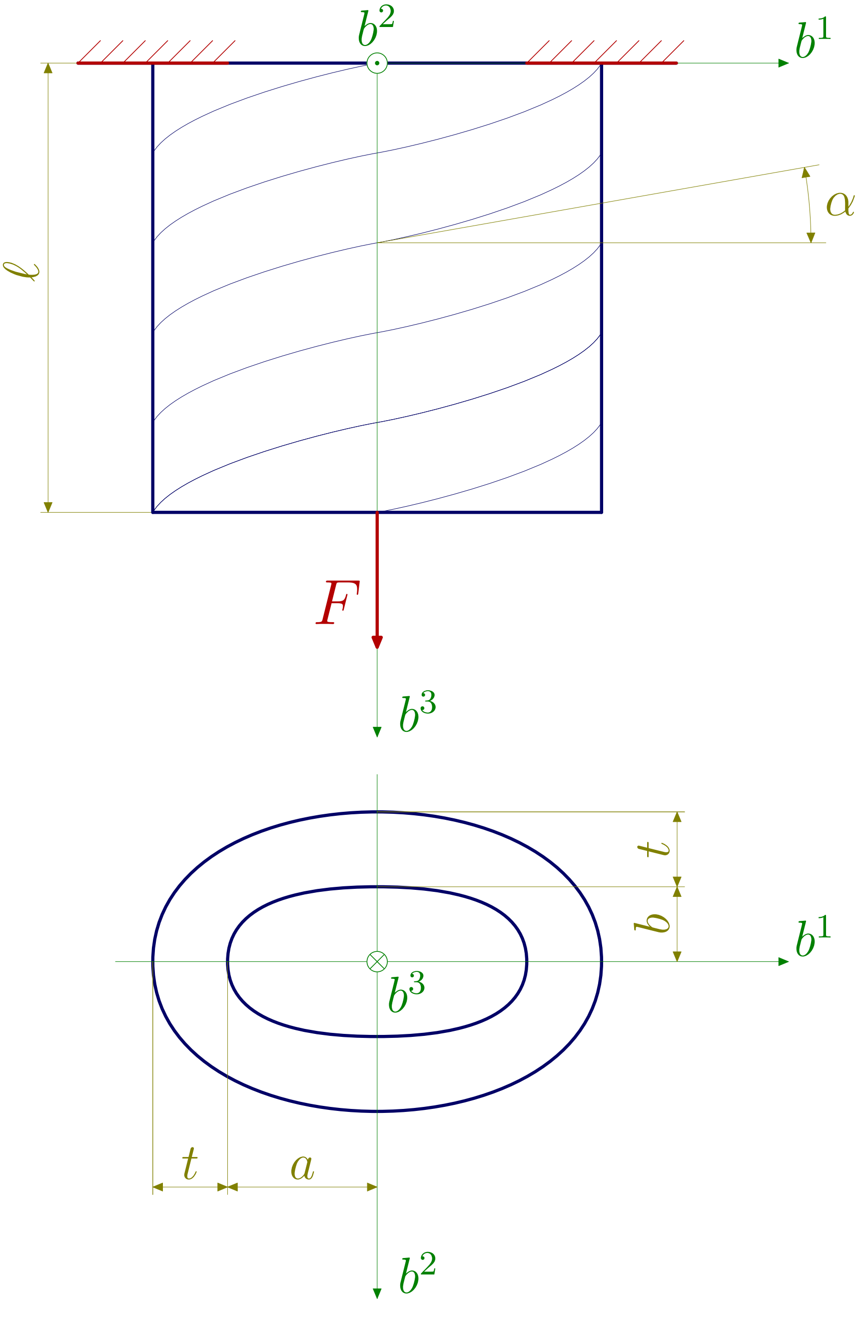

FIGURE 1. The anisotropic elliptic tube

In this chapter we focus on an analysis of a thick-walled elliptic tube which is wound by a fiber such as a laminated composite (Fig. 1). The upper end of the tube is clamped and a uniformly distributed force, F, is applied on the lower end. The fiber is wound at an angle, α. The problem is solved using the concept of locally orthotropic material, where the elasticity tensor is expressed in a local Cartesian coordinate system aligned with the principal directions of local orthotropy of the material. A system of coordinate transformations from the local Cartesian coordinate systems into a global coordinate system of computation is performed. The total potential energy of the problem is expressed in the global coordinate system. After approximating the dependent variables, representing the displacements, with Fourier series, the potential energy expression is minimized.

2. A compendium of the coordinate systems

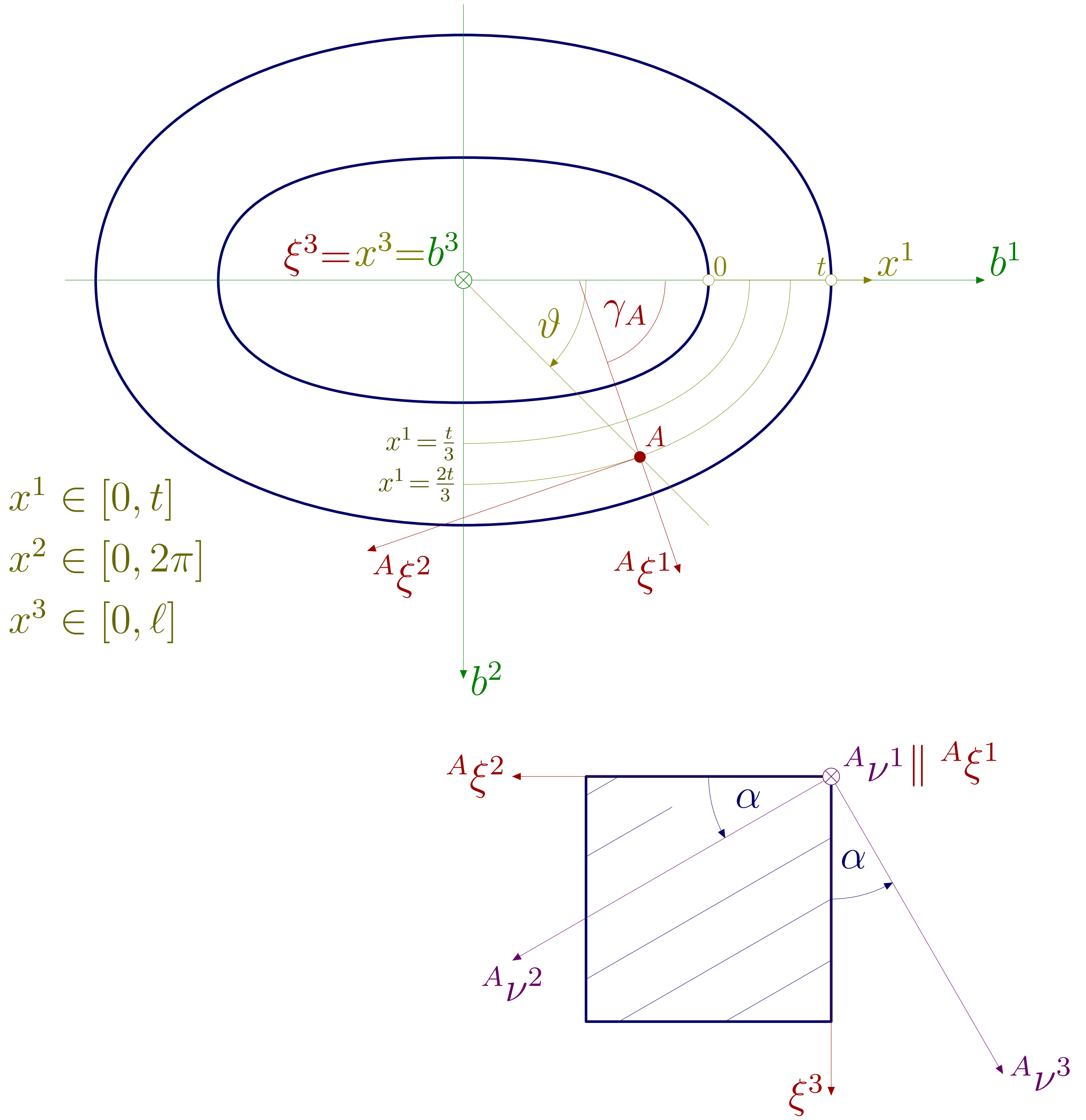

FIGURE 2. Coordinate systems

As has been said, the foremost task rests on a choice of appropriate coordinate systems and the expression of the transformations. In the case of the elliptic tube shown in Fig. 2, there are the global Cartesian coordinate system, b^a, the global elliptic coordinate system, x^a, the local Cartesian coordinate system, ξ^a, and the local coordinate system aligned with the principal directions of the local orthotropy, ν^a. The basic advantages of the elliptic coordinate system are the range of the coordinates

$$x \in [0, t], \;\; x \in [0, 2\pi], \;\; x \in [0, \ell]$$

and the known relations with the global Cartesian coordinate system b^a

$$b^1 = (a + x^1)\cos x^2,$$
$$b^2 = (b + x^1)\sin x^2,$$

and

$$b^3 = x^3.$$

3. Metric tensors of the coordinate systems

As the coordinate systems b, ξ and ν are Cartesian, the metrics are

$$\overset{b}{g}_{ab} = \delta_{ab},$$
$$\overset{\xi}{g}_{ab} = \delta_{ab},$$

and

$$\overset{\nu}{g}_{ab} = \delta_{ab}.$$

The following transformation rule

$$\overset{x}{g}_{ab} = \frac{\partial b^c}{\partial x^a}\frac{\partial b^d}{\partial x^b}\delta_{cd}$$

and the transformation matrix

$$\frac{\partial b^a}{\partial x^b} = \begin{pmatrix} \cos x^2 & -(a + x^1)\sin x^2 & 0 \\ \sin x^2 & (b + x^1)\cos x^2 & 0 \\ 0 & 0 & 1 \end{pmatrix}_{a\lceil b}$$

imply

$$\overset{x}{g}_{ab} = \begin{pmatrix} 1 & (b-a)\sin x^2\cos x^2 & 0 \\ (b-a)\sin x^2 \cos x^2 & (a+x^1)^2\sin^2 x^2 + (b+x^1)^2\cos^2 x^2 & 0 \\ 0 & 0 & 1 \end{pmatrix}.$$

4. Elasticity tensor in the global computational coordinate system

Elasticity tensor in the global computational coordinate system can be expressed via the transformation rule

$$\overset{x}{E}^{abcd} = \frac{\partial x^a}{\partial \nu^i}\frac{\partial x^b}{\partial \nu^j}\frac{\partial x^c}{\partial \nu^k}\frac{\partial x^d}{\partial \nu^l}\overset{\nu}{E}^{ijkl},$$

where $\overset{\nu}{E}^{ijkl}$ is the known elasticity tensor in the coordinate system ν aligned with the directions of the local orthotropy. For the transformation matrix, we have

$$\frac{\partial x^a}{\partial \nu^b} = \frac{\partial x^a}{\partial b^c}\frac{\partial b^c}{\partial \xi^d}\frac{\partial \xi^d}{\partial \nu^b},$$

where

$$\frac{\partial x^a}{\partial b^b} = \left(\frac{\partial b^a}{\partial x^b}\right)^{-1},$$

i.e.

$$\frac{\partial x^a}{\partial b^b} = \frac{1}{a\sin^2 x^2 + b\cos^2 x^2 + x^1}\begin{pmatrix} (b+x^1)\cos x^2 & (a+x^1)\sin x^2 & 0 \\ -\sin x^2 & \cos x^2 & 0 \\ 0 & 0 & a\sin^2 x^2 + b\cos^2 x^2 + x^1 \end{pmatrix},$$

$$\frac{\partial b^a}{\partial \xi^b} = \begin{pmatrix} \cos\gamma_A & -\sin\gamma_A & 0 \\ \sin\gamma_A & \cos\gamma_A & 0 \\ 0 & 0 & 1 \end{pmatrix}$$

and

$$\frac{\partial \xi^a}{\partial \nu^b} = \begin{pmatrix} 1 & 0 & 0 \\ 0 & \cos\alpha & -\sin\alpha \\ 0 & \sin\alpha & \cos\alpha \end{pmatrix}.$$

The determination of $\cos\gamma_A$ and $\sin\gamma_A$ is the only remaining problem. Fig. 3 indicates

$$\cos\gamma_A = (1, 0)\cdot \boldsymbol{n}$$

and

$$\sin \gamma_A = (0, 1) \cdot \boldsymbol{n}.$$

From analytical geometry we have

$$n^1 = \frac{b_t^2}{\sqrt{(b_t^1)^2 + (b_t^2)^2}}$$

and

$$n^2 = \frac{-b_t^1}{\sqrt{(b_t^1)^2 + (b_t^2)^2}},$$

where

$$b_t^a = \frac{\partial b^a}{\partial x^2}$$

and

$$b^1 = (a + x^1) \cos x^2,$$
$$b^2 = (b + x^1) \sin x^2.$$

Performing the differentiation leads to

$$\boldsymbol{n} = \frac{1}{d} \begin{pmatrix} (b + x^1) \cos x^2 \\ (a + x^1) \sin x^2 \end{pmatrix}$$

with

$$d = \sqrt{(a + x^1)^2 \sin^2 x^2 + (b + x^1)^2 \cos^2 x^2}$$

and hence

$$\cos \gamma_A = \frac{b + x^1}{d} \cos x^2$$

and

$$\sin \gamma_A = \frac{a + x^1}{d} \sin x^2.$$

5. Total potential energy of the elliptic tube

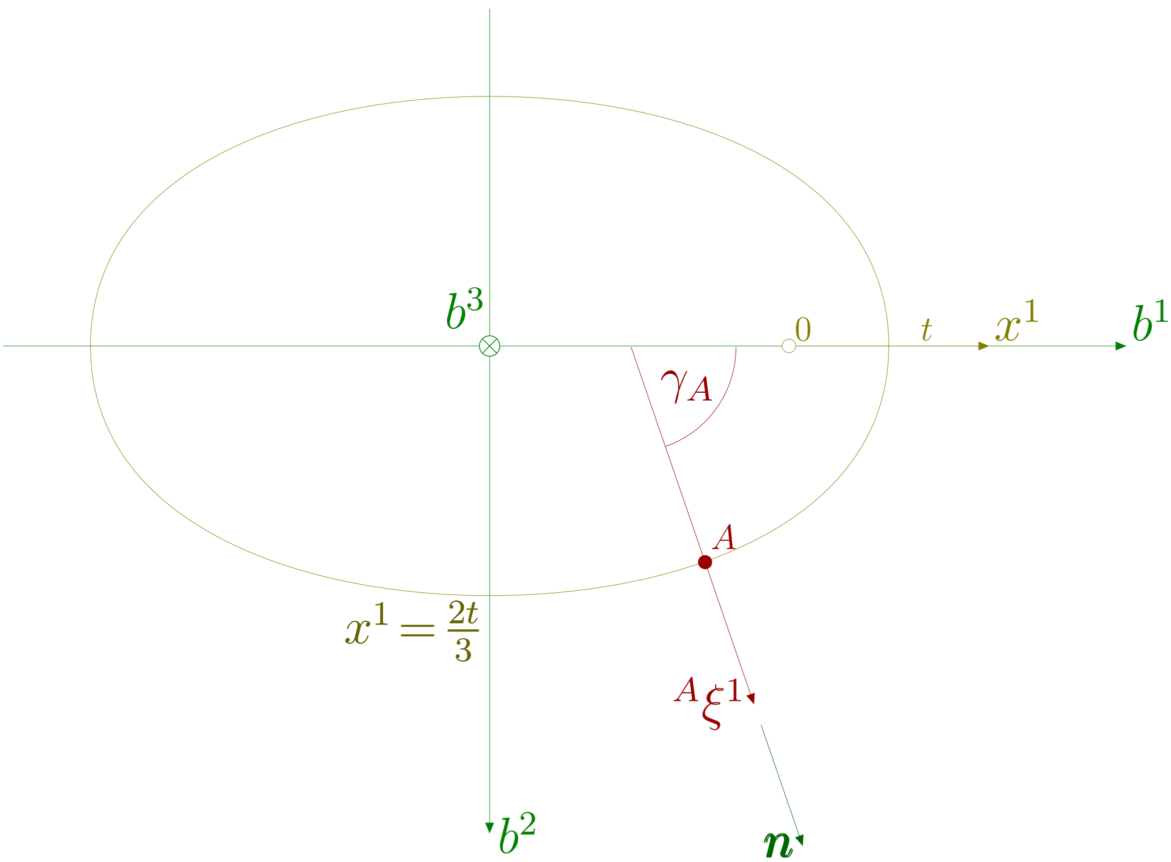

Figure 3. Normal to ellipse

It was stated already that[1]

$$\hat{u}_a = \arg\min_{u_b \in \mathbb{U}} \Pi(u_c),$$

i.e., that the real state $\hat{u}_a$ of the deformed body minimizes, on a set $\mathbb{U}$ of admissible states, the total potential energy

$$\Pi(u_a) = a(u_a) - l(u_a)$$

with the elastic strain energy

$$a(u_a) = \frac{1}{2}\int\limits_{\Omega} E^{abcd}\varepsilon_{ab}(u_a)\varepsilon_{cd}(u_a)\mathrm{d}\Omega$$

and the potential energy of the applied forces

$$-l(u_a) = -\int\limits_{\Omega} p^a u_a \mathrm{d}\Omega - \int\limits_{\partial_t\Omega} t^a u_a \mathrm{d}\Gamma.$$

Let us limit ourselves to the case of small deformations, then

$$\varepsilon_{ab} = \frac{1}{2}(\nabla_a u_b + \nabla_b u_a),$$

where[2]

$$\nabla_a u_b = \partial_a u_b - \Gamma^c_{ab} u_c$$

and Christoffel symbol of the second kind is

$$\Gamma^d_{ab} = g^{dc}\frac{1}{2}(\partial_b g_{ac} + \partial_a g_{cb} - \partial_c g_{ab}).$$

Thus

$$\overset{x}{\varepsilon}_{ab} = \frac{1}{2}(\partial_a \overset{x}{u}_b + \partial_b \overset{x}{u}_a - 2\,\Gamma^c_{ab} \overset{x}{u}_c)$$

with

$$\Gamma^c_{ab} \overset{x}{u}_c = \Gamma^1_{ab} \overset{x}{u}_1 + \Gamma^2_{ab} \overset{x}{u}_2 + \Gamma^3_{ab} \overset{x}{u}_3 .$$

Using GNU MAXIMA[3] we readily obtain (in the coordinate system x^a)

$$\Gamma^1_{12} = \Gamma^1_{21} = \frac{(a-b)\cos x^2 \sin x^2}{(b-a)\cos^2 x^2 + x^1 + a},$$

$$\Gamma^2_{12} = \Gamma^2_{21} = \frac{1}{(b-a)\cos^2 x^2 + x^1 + a},$$

$$\Gamma^1_{22} = -\frac{(x^1)^2 + x^1(a+b) + ab}{(b-a)\cos^2 x^2 + x^1 + a}$$

and

$$\Gamma^2_{22} = \frac{(a-b)\cos x^2 \sin x^2}{(b-a)\cos^2 x^2 + x^1 + a}$$

with the remaining entries equal to zero, *i.e.*,

$$\Gamma^1_{ab} = \frac{1}{J}\begin{pmatrix} 0 & (a-b)\cos x^2 \sin x^2 & 0 \\ (a-b)\cos x^2 \sin x^2 & -((x^1)^2 + x^1(a+b) + ab) & 0 \\ 0 & 0 & 0 \end{pmatrix},$$

$$\Gamma^2_{ab} = \frac{1}{J}\begin{pmatrix} 0 & 1 & 0 \\ 1 & (a-b)\cos x^2 \sin x^2 & 0 \\ 0 & 0 & 0 \end{pmatrix}$$

and

$$\Gamma^3_{ab} = 0,$$

where

$$J = (b-a)\cos^2 x^2 + x^1 + a.$$

Now, as

$$E^{abcd} = E^{bacd}$$

[1] [**Mik64**], [**Was75**], [**LR89**], [**Dac89**], [**Ped00**] and [**Che00**].

[2] [**SS78**], [**LR89**].

[3] http://sourceforge.net/projects/maxima

we can replace $\overset{x}{\varepsilon}_{ab}$ with $\partial_a \overset{x}{u}_b - \Gamma^c_{ab} \overset{x}{u}_c$ and write the total potential energy at the form

$$a = \frac{1}{2} \int\limits_{\Omega} \left(\partial_a \overset{x}{u}_b - \Gamma^p_{ab} \overset{x}{u}_p\right) \overset{x}{E}{}^{abcd} \left(\partial_c \overset{x}{u}_d - \Gamma^p_{cd} \overset{x}{u}_p\right) \left|\overset{x}{g}_{ab}\right|^{\frac{1}{2}} \mathrm{d}^3 x.$$

The elasticity tensor in the x-coordinates

$$\overset{x}{E}{}^{abcd} = \frac{\partial x^a}{\partial \nu^i} \frac{\partial x^b}{\partial \nu^j} \frac{\partial x^c}{\partial \nu^k} \frac{\partial x^d}{\partial \nu^l} \overset{\nu}{E}{}^{ijkl}$$

can be very easily performed in GNU Octave[4] syntax as

```
xnu=xb*bxi*xinu
Ex=kron(xnu,xnu)*Enu*kron(xnu',xnu')
```

6. Solution approximated by the Fourier series

Let us approximate the solution by a Fourier series that satisfies the boundary conditions

$$x^3 = 0 : \overset{x}{u}_1 = 0,\ \overset{x}{u}_2 = 0,\ \overset{x}{u}_3 = 0.$$

Such a series is, for example,

$$\overset{x}{u}_1 = \sum_{j,k,m=-K}^{K} a_1^{jkm} x^3 e^{i\left(jx^1 \frac{2\pi}{t} + kx^2 + mx^3 \frac{2\pi}{\ell}\right)},$$

$$\overset{x}{u}_2 = \sum_{j,k,m=-K}^{K} a_2^{jkm} x^3 e^{i\left(jx^1 \frac{2\pi}{t} + kx^2 + mx^3 \frac{2\pi}{\ell}\right)},$$

$$\overset{x}{u}_3 = \sum_{j,k,m=-K}^{K} a_3^{jkm} x^3 e^{i\left(jx^1 \frac{2\pi}{t} + kx^2 + mx^3 \frac{2\pi}{\ell}\right)},$$

where, ideally, $K = \infty$ but in practice, $K = 3$.

Provided that we denote

$$\overset{x}{u}_{1,2,3} = \Sigma\, a_{1,2,3}\, \varphi \quad (\varphi = x^3 \phi)$$

we can write

$$\partial_b \overset{x}{u}_a = \frac{\partial \overset{x}{u}_a}{\partial x^b} = \begin{pmatrix} \Sigma\, a_1\, \varphi\, ij \frac{2\pi}{t} & \Sigma\, a_1\, \varphi\, ik & \Sigma\, a_1\, (\varphi\, im \frac{2\pi}{\ell} + \phi) \\ \Sigma\, a_2\, \varphi\, ij \frac{2\pi}{t} & \Sigma\, a_2\, \varphi\, ik & \Sigma\, a_2\, (\varphi\, im \frac{2\pi}{\ell} + \phi) \\ \Sigma\, a_3\, \varphi\, ij \frac{2\pi}{t} & \Sigma\, a_3\, \varphi\, ik & \Sigma\, a_3\, (\varphi\, im \frac{2\pi}{\ell} + \phi) \end{pmatrix}.$$

As

$$\varphi = \varphi^{jkm} = x^3 e^{ijx^1 \frac{2\pi}{t}} \cdot e^{ikx^2} \cdot e^{imx^3 \frac{2\pi}{\ell}}$$

we can write, in GNU Octave syntax,

```
j=(-3:1:3); k=(-3:1:3); m=(-3:1:3);
phi=x3*kron(kron(exp(i*j*x1*2*pi/t),exp(i*k*x2)),exp(i*m*x3*2*pi/ell));
ux=[phi,zeros(1,686);zeros(1,343),phi,zeros(1,343);zeros(1,686),phi]*A;
```

where `A` is a vector of unknown coefficients a_a^{jkl} and `ux` stands for

$$\mathtt{ux} = \begin{pmatrix} \overset{x}{u}_1 \\ \overset{x}{u}_2 \\ \overset{x}{u}_3 \end{pmatrix}.$$

Writing

$$\left\{ \frac{\partial \overset{x}{u}_a}{\partial x^b} \right\}_{ab\lceil} = \mathtt{B*A}$$

the matrix `B` is computed via[5]

[4] http://www.octave.org/

[5] Presented just to demonstrate the simplicity of the numerical realisation of the solution.

```
B=[i*2*pi/t*phi.*kron(kron(j,jedna),jedna),zeros(1,343),zeros(1,343);
  i*phi.*kron(kron(jedna,k),jedna),zeros(1,343),zeros(1,343);
  i*2*pi/ell*phi.*kron(kron(jedna,jedna),m)+varphi,zeros(1,686);
  zeros(1,343),i*2*pi/t*phi.*kron(kron(j,jedna),jedna),zeros(1,343);
  zeros(1,343),i*phi.*kron(kron(jedna,m),jedna),zeros(1,343);
  zeros(1,343),i*2*pi/ell*phi.*kron(kron(je,je),m)+varphi,zeros(1,343);
  zeros(1,343),zeros(1,343),i*2*pi/t*phi.*kron(kron(j,jedna),jedna);
  zeros(1,343),zeros(1,343),i*phi.*kron(kron(jedna,k),jedna);
  zeros(1,686),i*2*pi/ell*phi.*kron(kron(jedna,jedna),m)+varphi];
```

As the part of the deformation gradient containing the Christoffel symbols

$$\Gamma^c_{ab} \overset{x}{u}_c = \Gamma^1_{ab} \overset{x}{u}_1 + \Gamma^2_{ab} \overset{x}{u}_2 + \Gamma^3_{ab} \overset{x}{u}_3$$

is expressible in the form

$$\left\{\Gamma^p_{ab} \overset{x}{u}_p\right\}_{ab\lceil} = \left\{\Gamma^1_{ab}\right\}_{ab\lceil} \texttt{*[phi,zeros(1,686)]*A} + \left\{\Gamma^2_{ab}\right\}_{ab\lceil} \texttt{*[zeros(1,343),phi,zeros(1,343)]*A}$$

we may write for the whole deformation gradient

$$\left(\partial_a \overset{x}{u}_b - \Gamma^p_{ab} \overset{x}{u}_p\right) = \texttt{(B-Gam)*A}$$

where

```
   J=(b-a)*(cos(x2))**2+x1+a;
   G1=1/J*[0,(a-b)*cos(x2)*sin(x2),0;
           (a-b)*cos(x2)*sin(x2),-((x1)**2+{x1}*(a+b)+a*b),0;0,0,0];
   G2=1/J*[0,1,0;1,(a-b)*cos(x2)*sin(x2),0;0,0,0];
Gam=vec(G1')*[phi,zeros(1,686)]+vec(G2')*[zeros(1,343),phi,zeros(1,343)];
```

7. Results

Thus, we can write for the elastic energy

$$a = \frac{1}{2}\, \mathtt{A}^T K \mathtt{A}$$

with the stiffness matrix

$$K = \int_0^{\ell}\int_0^{2\pi}\int_0^{t} \texttt{(B-Gam)'*Ex*(B-Gam)*sqrt(det(gx))}\, \mathrm{d}x^1 \mathrm{d}x^2 \mathrm{d}x^3$$

where `gx=(xb**(-1))'*xb**(-1)` and the integration is performed numerically.

The work of the applied force

$$l = \int_S \frac{F}{S} \overset{x}{u}_3 \,\mathrm{d}S$$

may be expressed as

$$l = \mathtt{P}' * \mathtt{A}$$

with

$$P = \begin{pmatrix} \texttt{zeros(343,1)} \\ \texttt{zeros(343,1)} \\ \int_0^{2\pi}\int_0^{t} \frac{F}{S}\texttt{phi'*sqrt(det(gx))}\, \mathrm{d}x^1 \mathrm{d}x^2 \end{pmatrix}$$

the integration being once more performed numerically.

The resulting displacements, `ub`, in the global coordinate system, b, obtained easily, at a given point `(x1,x2,x3)`, via a few lines at GNU Octave syntax

```
 A=K**(-1)*P
 phi=x3*kron(kron(exp(i*j*x1*2*pi/t),...
 ux=real([phi,zeros(1,siz),zeros(1,...
 xb=1/(a*(sin(x2))**2+b*(cos(x2))**2+...
 ub=xb*ux
```

are demonstrated in Fig. 4.

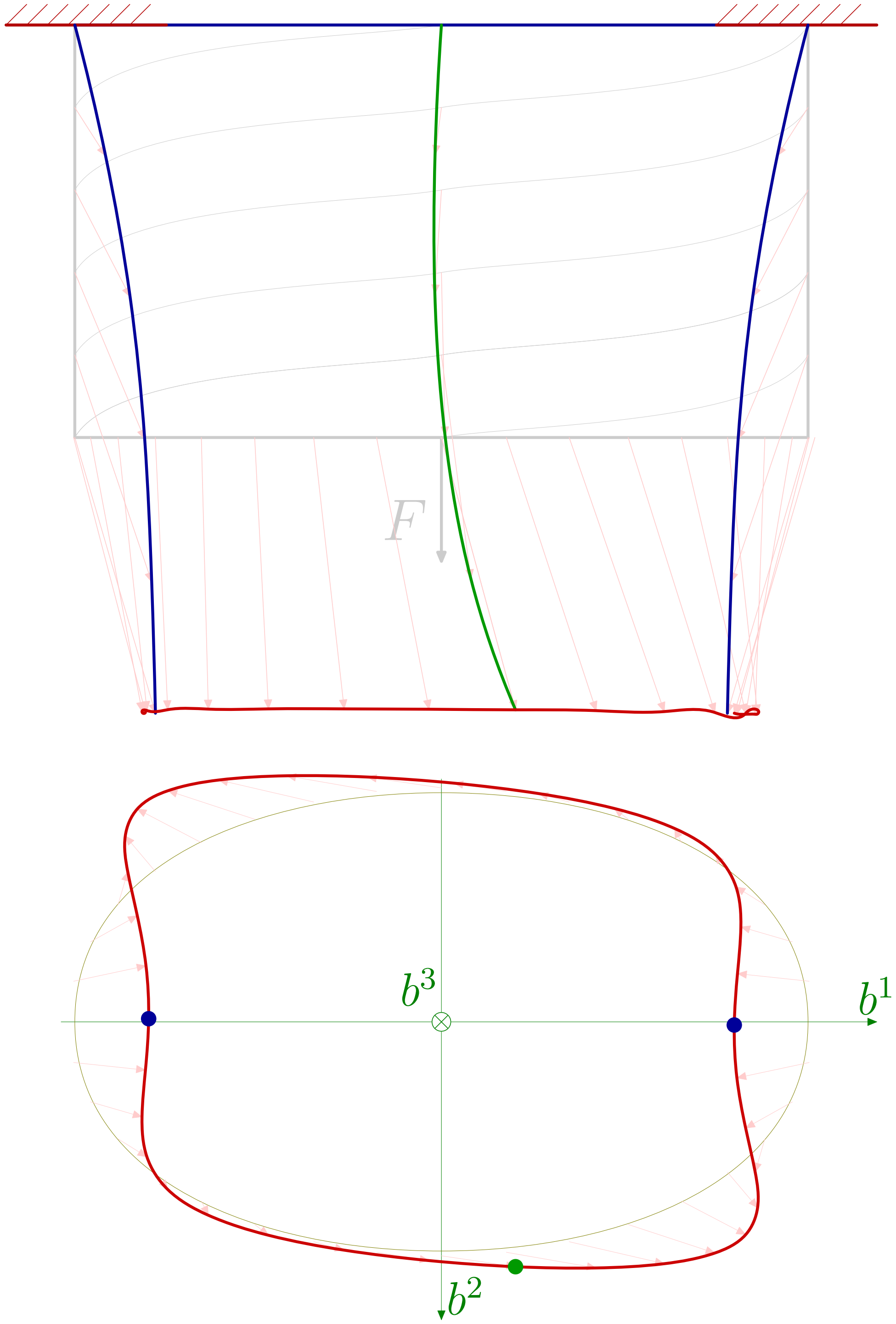

FIGURE 4. deformation of the elliptic tube

CHAPTER 3

Intervertebral disk

1. Anatomy and histology of the intervertebral disk

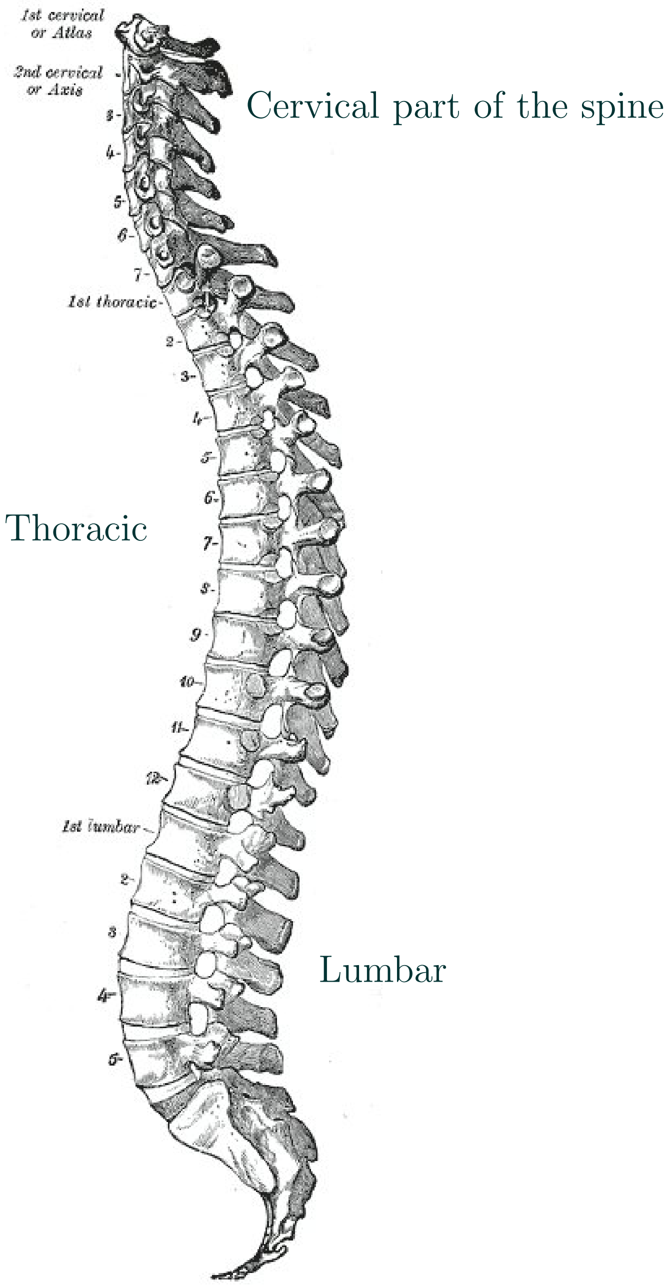

Figure 1. The vertebral column

The intervertebral disks (or intervertebral fibrocartilage) lie between adjacent vertebrae in the spine. The spine (vertebral column or backbone) is a column comprising besides the intervertebral disks and twenty-four vertebrae also the sacrum and the coccyx; Fig. 1.[1] Each disk forms a cartilaginous joint to allow slight movement of the vertebrae, and acts as a ligament to hold the vertebrae together, Fig. 2.

[1] [**Gra18**]

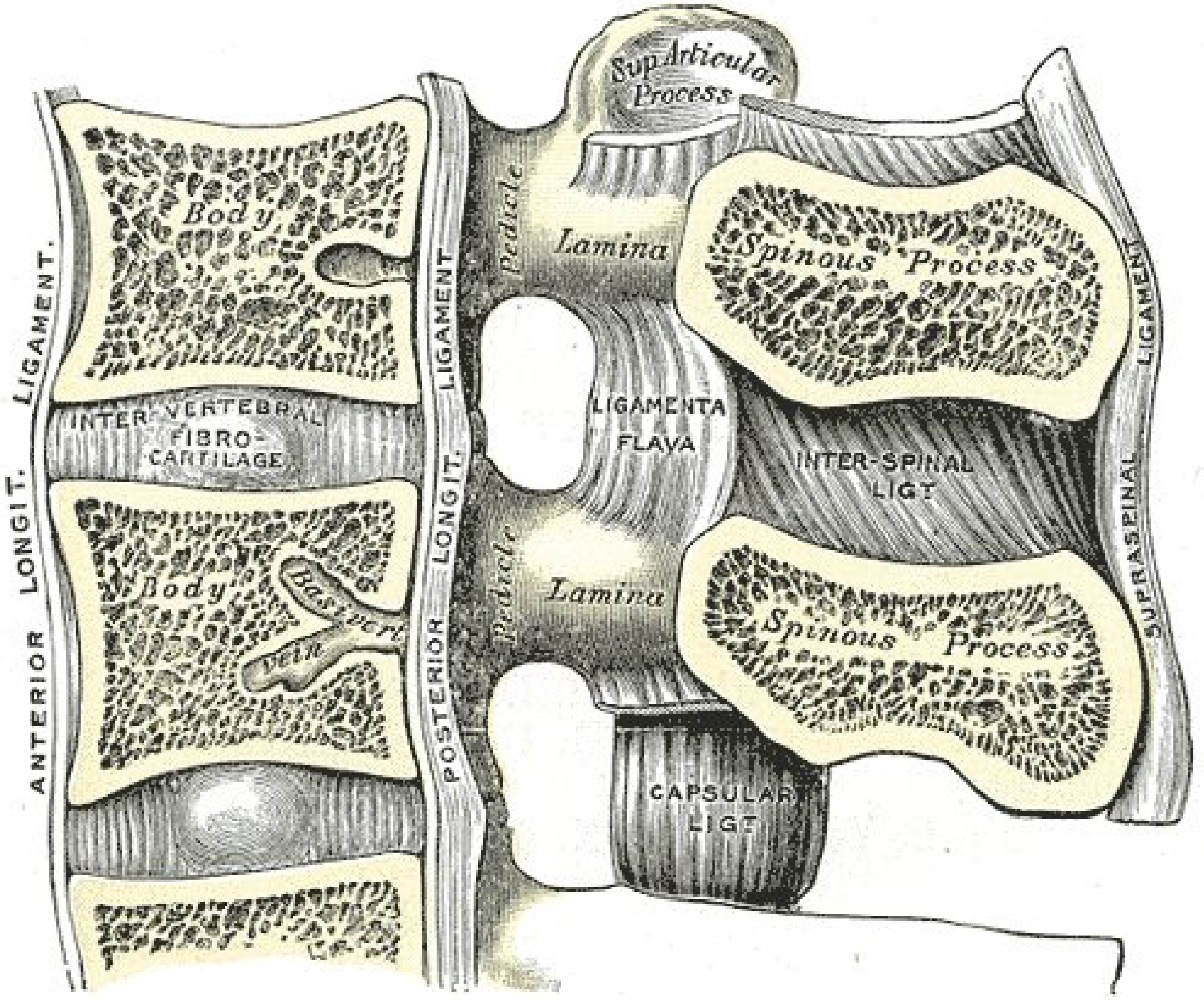

FIGURE 2. Section of lumbar vertebrae

The Intervertebral disk consists of an outer annulus fibrosus, which surrounds the inner nucleus pulposus. The annulus fibrosus consists of several layers of fibrocartilage and may be modeled as sequence of elastic locally orthotropic lamellae with rheological description that was discussed above,

$$\overset{\nu}{\sigma}^{ij}=\overset{\nu}{E}^{ijkl}\overset{\nu}{\varepsilon}_{kl},$$

$$\overset{\nu}{E}^{ijkl}=\begin{pmatrix} \Phi_{11} & 0 & 0 & 0 & \Phi_{12} & 0 & 0 & 0 & \Phi_{13} \\ 0 & G_{12} & 0 & G_{12} & 0 & 0 & 0 & 0 & 0 \\ 0 & 0 & G_{13} & 0 & 0 & 0 & G_{13} & 0 & 0 \\ 0 & G_{12} & 0 & G_{12} & 0 & 0 & 0 & 0 & 0 \\ \Phi_{21} & 0 & 0 & 0 & \Phi_{22} & 0 & 0 & 0 & \Phi_{23} \\ 0 & 0 & 0 & 0 & 0 & G_{23} & 0 & G_{23} & 0 \\ 0 & 0 & G_{13} & 0 & 0 & 0 & G_{13} & 0 & 0 \\ 0 & 0 & 0 & 0 & 0 & G_{23} & 0 & G_{23} & 0 \\ \Phi_{31} & 0 & 0 & 0 & \Phi_{32} & 0 & 0 & 0 & \Phi_{33} \end{pmatrix}_{\{ij\lceil kl\}},$$

and viscoelastic isotropic layers described by a three element viscoelastic model whose both variants are treated in the following section.

The strong annular fibres contain the nucleus pulposus that contains loose fibers suspended in a mucoprotein gel the consistency of jelly. This tissue can be once more modeled as a three element viscoelastic isotropic material (Fig. 3).

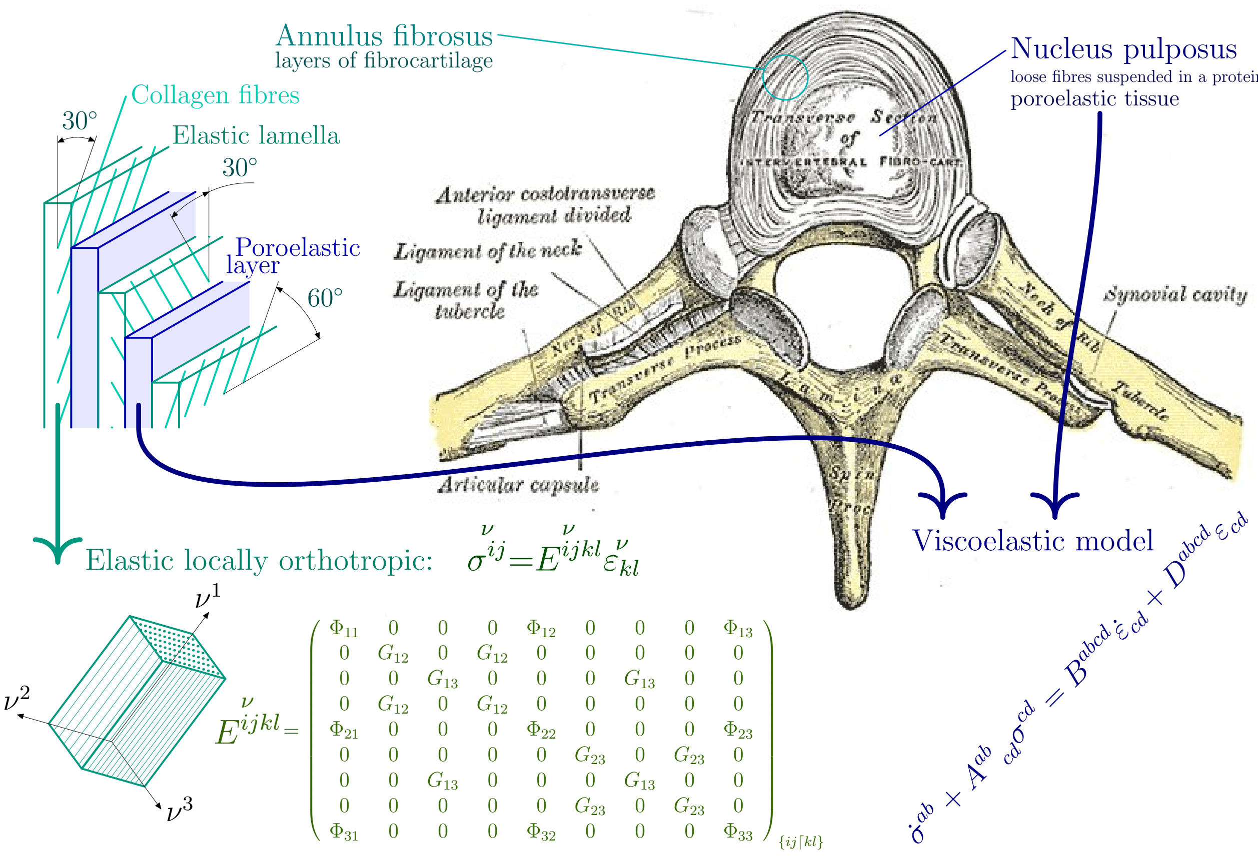

FIGURE 3. Transversal section of the intervertebral disk

2. Three element viscoelastic models

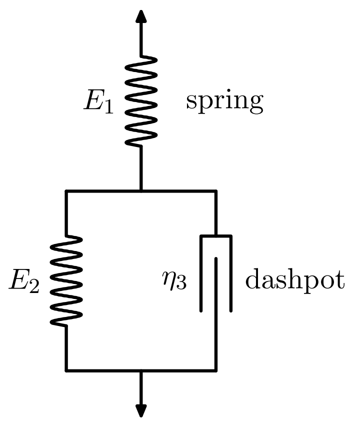

$$\dot{\sigma}+\frac{E_1+E_2}{\eta_3}\sigma=E_1\dot{\varepsilon}+\frac{E_1E_2}{\eta_3}\varepsilon$$

FIGURE 4. Poynting-Thompson model

2.1. Poynting-Thompson viscoelastic model. Rheological description of Poynting-Thompson model will be formulated using the free model diagram where the stress and strain is labeled as indicated in Fig. 4. Thus

$$\sigma=\sigma_1=\sigma_2+\sigma_3 \tag{14}$$

and

$$\varepsilon=\varepsilon_1+\varepsilon_2,\ \ \varepsilon_2=\varepsilon_3. \tag{15}$$

Using the well known relations for elastic model and viscoelastic model

$$\sigma=E\epsilon$$

and

$$\sigma = \eta\dot{\epsilon},$$

respectively, we have

(16) $$\sigma = E_1\varepsilon_1$$

and

(17) $$\sigma = E_2\varepsilon_2 + \eta_3\dot{\varepsilon}_2.$$

From (15) a (17)

$$\sigma = E_2\left(\varepsilon - \varepsilon_1\right) + \eta_3\left(\dot{\varepsilon} - \dot{\varepsilon}_1\right)$$

and using (16) the Poynting-Thompson model takes the form

(18) $$\dot{\sigma} + \frac{E_1 + E_2}{\eta_3}\,\sigma = E_1\dot{\varepsilon} + \frac{E_1E_2}{\eta_3}\,\varepsilon.$$

Such a differential equation has the general solutions

$$\sigma = e^{-\frac{E_1+E_2}{\eta_3}t}\left(\int_{t_0}^{t} e^{\frac{E_1+E_2}{\eta_3}\tau}\left(E_1\dot{\varepsilon} + \frac{E_1E_2}{\eta_3}\varepsilon\right)\,\mathrm{d}\tau + e^{\frac{E_1+E_2}{\eta_3}t_0}\sigma(t_0)\right)$$

and

$$\varepsilon = e^{-\frac{E_2}{\eta_3}t}\left(\int_{t_0}^{t} e^{\frac{E_2}{\eta_3}\tau}\left(\frac{1}{E_1}\dot{\sigma} + \frac{E_1+E_2}{E_1\eta_3}\sigma\right)\,\mathrm{d}\tau + e^{\frac{E_2}{\eta_3}t_0}\varepsilon(t_0)\right),$$

where $\sigma(t_0) = E_1\varepsilon(t_0)$.

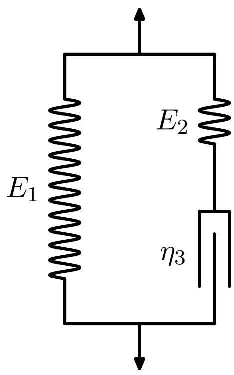

$$\dot{\sigma} + \frac{E_2}{\eta_3}\,\sigma = \left(E_1 + E_2\right)\dot{\varepsilon} + \frac{E_1E_2}{\eta_3}\,\varepsilon$$

FIGURE 5. Zener model

2.2. Zener viscoelastic model. Reological description of the Zener model, Fig. 5, is obtained in a way similar to the previous case. From the free model diagram we have

(19) $$\sigma = \sigma_1 + \sigma_2 \quad \text{and} \quad \sigma_2 = \sigma_3.$$

The compatibility condition has the form

(20) $$\varepsilon = \varepsilon_1 = \varepsilon_2 + \varepsilon_3.$$

Then

$$\dot{\varepsilon} = \dot{\varepsilon}_2 + \dot{\varepsilon}_3 = \frac{\dot{\sigma}_2}{E_2} + \frac{\sigma_3}{\eta_3}$$

and, with the aid of (19) and $\sigma_1 = E_1\varepsilon$, the Zener model has the form

(21) $$\dot{\sigma} + \frac{E_2}{\eta_3}\,\sigma = \left(E_1 + E_2\right)\dot{\varepsilon} + \frac{E_1E_2}{\eta_3}\,\varepsilon.$$

The solutions are once more

$$\sigma = e^{-\frac{E_2}{\eta_3}t}\left(\int_{t_0}^{t} e^{\frac{E_2}{\eta_3}\tau}\left((E_1+E_2)\dot{\varepsilon} + \frac{E_1E_2}{\eta_3}\varepsilon\right)\,\mathrm{d}\tau + e^{\frac{E_2}{\eta_3}t_0}\sigma(t_0)\right)$$

and

$$\varepsilon = e^{-\frac{E_1 E_2}{(E_1+E_2)\eta_3}t}\left(\int\limits_{t_0}^{t} e^{\frac{E_1 E_2}{(E_1+E_2)\eta_3}\tau}\left(\dot\sigma + \frac{E_2}{\eta_3}\sigma\right)\frac{\mathrm{d}\tau}{E_1+E_2} + e^{\frac{E_1 E_2}{(E_1+E_2)\eta_3}t_0}\varepsilon(t_0)\right),$$

where $\sigma(t_0) = (E_1+E_2)\varepsilon(t_0)$.

2.3. General three element viscoelastic model. Both of these models may be written as

$$\dot\sigma + a\sigma = b\dot\varepsilon + c\varepsilon$$

with the solution for stress

$$\sigma = e^{-at}\left(\int\limits_{t_0}^{t} e^{a\tau}(b\dot\varepsilon + c\varepsilon)\,\mathrm{d}\tau + \sigma(t_0)e^{at_0}\right) \tag{22}$$

and strain

$$\varepsilon = e^{-\frac{c}{b}t}\left(\int\limits_{t_0}^{t} e^{\frac{c}{b}\tau}(\dot\sigma + a\sigma)\,\frac{\mathrm{d}\tau}{b} + \varepsilon(t_0)e^{\frac{c}{b}t_0}\right), \tag{23}$$

where

$$\sigma(t_0) = b\varepsilon(t_0)$$

with $b = E_1 + E_2$ for the Zener model and $b = E_1$ for the Poynting-Thompson model.

The one-dimensional model can be straightforwardly generalized into three-dimensional model

$$\dot\sigma^{ab} + A^{ab}{}_{cd}\sigma^{cd} = B^{abcd}\dot\varepsilon_{cd} + D^{abcd}\varepsilon_{cd},$$

where in the isotropic case

$$\begin{aligned} A^{ab}{}_{cd} &= \alpha_1 g^{ab}g_{cd} + \alpha_2\left(\delta^a_c\delta^b_d + \delta^a_d\delta^b_c\right),\\ B^{abcd} &= \beta_1 g^{ab}g^{cd} + \beta_2\left(g^{ac}g^{bd} + g^{ad}g^{bc}\right),\\ D^{abcd} &= \gamma_1 g^{ab}g^{cd} + \gamma_2\left(g^{ac}g^{bd} + g^{ad}g^{bc}\right). \end{aligned}$$

The general solution of this differential equation has a form

$$\sigma^{ab} = U^{ab}{}_{cd}\Lambda^{cd}{}_{ij}\left(\int \mathfrak{L}^{ij}{}_{kl}\mathfrak{U}^{kl}{}_{mn}\left(B^{mnop}\dot\varepsilon_{op} + D^{mnop}\varepsilon_{op}\right)\mathrm{d}t\right) + c^{ab},$$

where

$$U^{ab}{}_{cd} = \left(\left\{M_1^{ab}\right\}_{ab\lceil}, \left\{M_2^{ab}\right\}_{ab\lceil}, \ldots, \left\{M_9^{ab}\right\}_{ab\lceil}\right)_{ab\lceil cd},$$

$$U^{ab}{}_{cd}\mathfrak{U}^{cd}{}_{kl} = \delta^a_k\delta^b_l,$$

$$\Lambda^{ab}{}_{cd} = \begin{pmatrix} e^{\lambda_1 t} & \ldots & 0\\ \vdots & \ddots & \vdots\\ 0 & \ldots & e^{\lambda_9 t}\end{pmatrix}_{ab\lceil cd}$$

and

$$\mathfrak{L}^{ab}{}_{cd} = \begin{pmatrix} e^{-\lambda_1 t} & \ldots & 0\\ \vdots & \ddots & \vdots\\ 0 & \ldots & e^{-\lambda_9 t}\end{pmatrix}_{ab\lceil cd}$$

with λ, M^{ab} being the solution of the eigenvalue problem[2]

$$\left(-A^{ab}{}_{cd} - \lambda\delta^a_c\delta^b_d\right)M^{cd} = 0,$$

and c^{ab} is a constant tensor.

[2]Using Octave, Maxima, *etc.* these are eigenvalues and eigenvectors, respectively, of the matrix $\left\{-A^{ab}{}_{cd}\right\}_{ab\lceil cd}$.

3. Geometrical model of the intervertebral disk

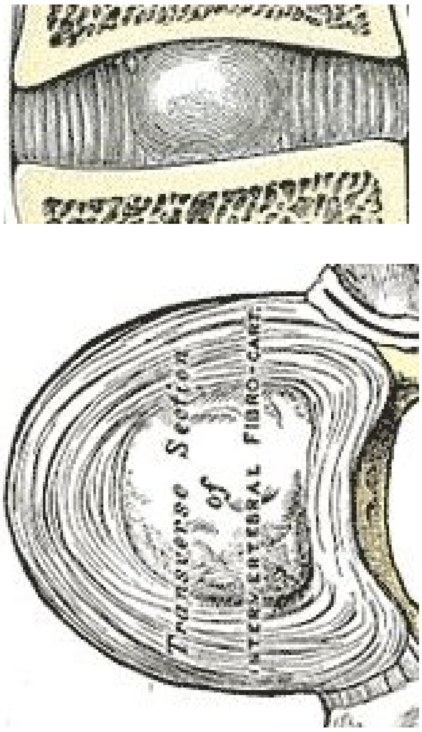

FIGURE 6. Real geometry of the intervertebral disk

The real geometry, Fig. 6, can be modeled as an epicycloidal cylinder, Fig. 7, parametrically defined by

$$b^1 = 2r_x x^1 \cos x^2 - d_x x^1 \cos 2x^2,$$
$$b^2 = 2r_y x^1 \sin x^2 - d_y x^1 \sin 2x^2,$$
$$b^3 = x^3,$$

with parameters

$$0 \leq x^1 \leq 1,$$
$$0 \leq x^2 \leq 2\pi,$$
$$0 \leq x^3 \leq h$$

called the epicycloidal coordinate system.

The metric tensor of this coordinate system is given by the transformation of the metric tensor, $\overset{b}{g}_{cd} = \delta_{cd}$, of the global cartesian coordinate system b:

$$\overset{x}{g}_{ab} = \frac{\partial b^c}{\partial x^a}\frac{\partial b^d}{\partial x^b}\,\overset{b}{g}_{cd},$$

where the transformation matrix

$$\frac{\partial b^a}{\partial x^b} = \begin{pmatrix} 2r_x \cos x^2 - d_x \cos 2x^2 & 2d_x x^1 \sin 2x^2 - 2r_x x^1 \sin x^2 & 0 \\ 2r_y \sin x^2 - d_y \sin 2x^2 & 2r_y x^1 \cos x^2 - 2d_y x^1 \cos 2x^2 & 0 \\ 0 & 0 & 1 \end{pmatrix}.$$

4. Elasticity tensor of the elastic lamellae

The elastic part of annulus fibrosus consists of collagen fibre lamellae modeled as a locally orthotropic material with the known elasticity tensor $\overset{\nu}{E}{}^{ijkl}$ expressed in the the principal material axes ν^a. As the computation is to be performed in the epicycloidal coordinate system, x, we need to transform the elasticity tensor in accord with the rule

$$\overset{x}{E}{}^{abcd} = \frac{\partial x^a}{\partial \nu^i}\frac{\partial x^b}{\partial \nu^j}\frac{\partial x^c}{\partial \nu^k}\frac{\partial x^d}{\partial \nu^l}\,\overset{\nu}{E}{}^{ijkl}$$

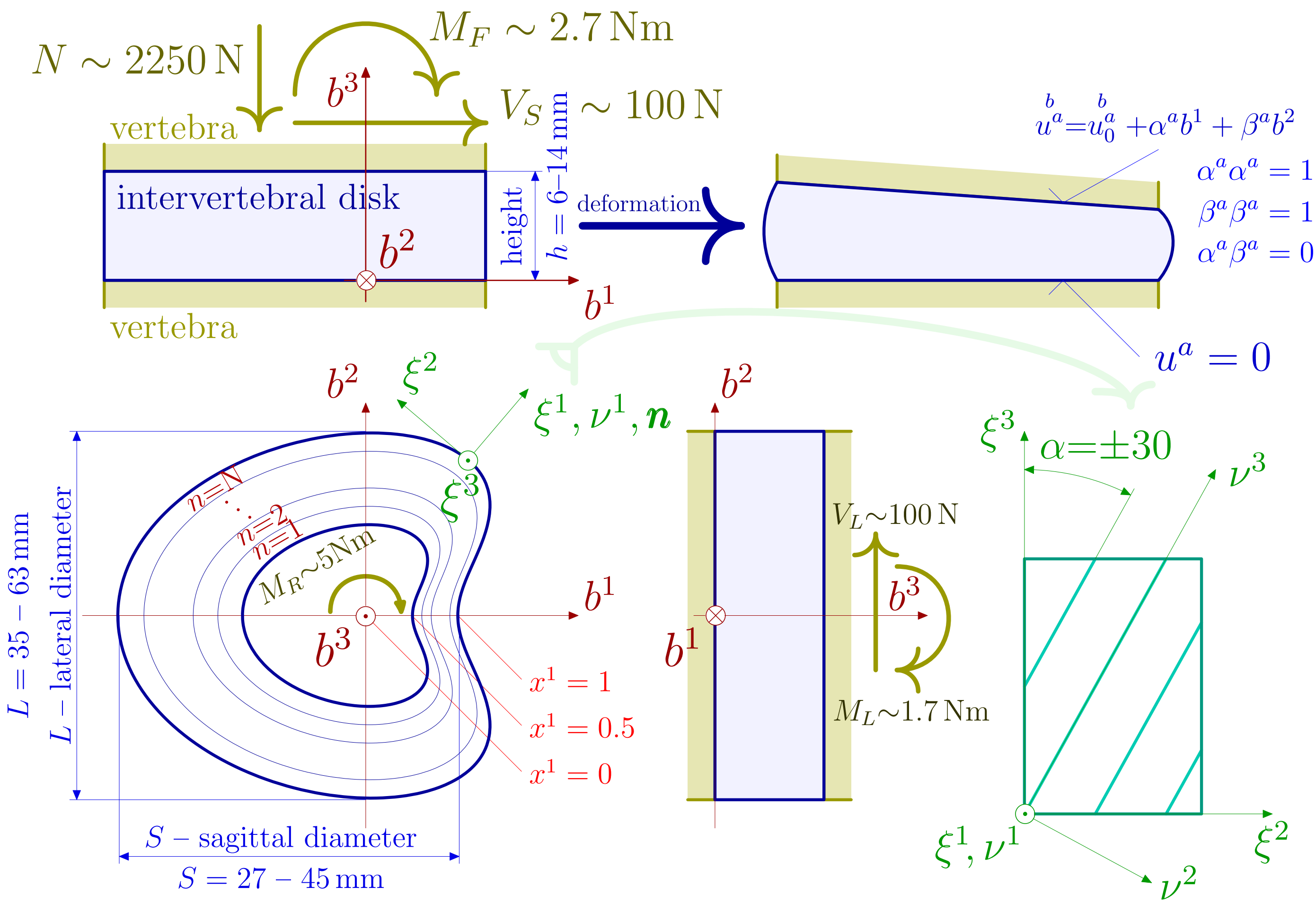

Figure 7. Geometrical model of the intervertebral disk

with the transformation matrix

$$\frac{\partial x^a}{\partial \nu^i} = \frac{\partial x^a}{\partial b^b}\frac{\partial b^b}{\partial \xi^c}\frac{\partial \xi^c}{\partial \nu^i},$$

where

$$\frac{\partial x^a}{\partial b^b} = \left(\frac{\partial b^a}{\partial x^b}\right)^{-1},$$

$$\frac{\partial \xi^a}{\partial \nu^b} = \begin{pmatrix} 1 & 0 & 0 \\ 0 & \cos\alpha & \sin\alpha \\ 0 & -\sin\alpha & \cos\alpha \end{pmatrix}$$

and

$$\frac{\partial \xi^a}{\partial b^b} = \begin{pmatrix} n^1 & n^2 & 0 \\ -n^2 & n^1 & 0 \\ 0 & 0 & 1 \end{pmatrix},$$

$$\frac{\partial b^a}{\partial \xi^b} = \begin{pmatrix} n^1 & -n^2 & 0 \\ n^2 & n^1 & 0 \\ 0 & 0 & 1 \end{pmatrix},$$

$\boldsymbol{n} = \left(n^1, n^2, 0\right)$ being the normal to the epicycloid:

$$n^1 = \frac{\frac{\partial b^2}{\partial x^2}}{\sqrt{(\frac{\partial b^1}{\partial x^2})^2 + (\frac{\partial b^2}{\partial x^2})^2}},$$

$$n^2 = \frac{-\frac{\partial b^1}{\partial x^2}}{\sqrt{(\frac{\partial b^1}{\partial x^2})^2 + (\frac{\partial b^2}{\partial x^2})^2}}.$$

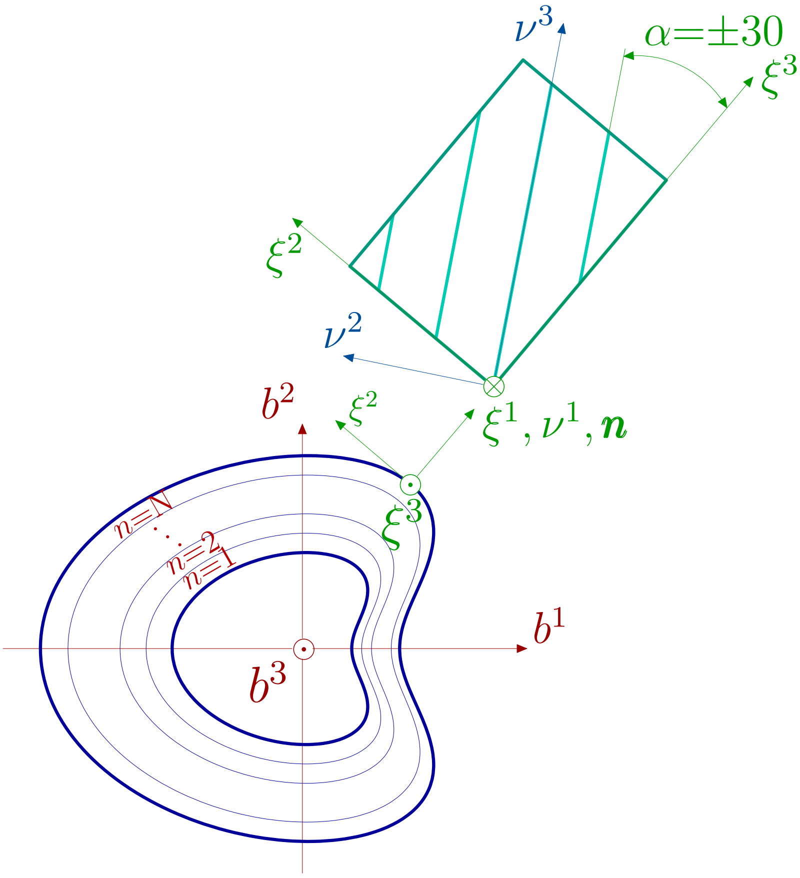

FIGURE 8. Transformation of the elasticity tensor

It holds that

$$n^1 = \frac{N^1}{d}, \ N^1 = 2r_y x^1 \cos x^2 - 2d_y x^1 \cos 2x^2,$$

$$n^2 = \frac{N^2}{d}, \ N^2 = 2r_x x^1 \sin x^2 - 2d_x x^1 \sin 2x^2$$

with

$$d = \sqrt{(N^1)^2 + (N^2)^2}.$$

Once the transformation matrices are known the GNU OCTAVE code is very simple:

```
xnu=xb*bxi*xinu
Ex=kron(xnu,xnu)*Enu*kron(xnu',xnu')
```

5. Computational models

Regarding the geometrical and material models described above, there are at least four possible computational models:

(1) Small deformations and elastic nucleus pulposus. In this model the small deformations are only considered. The elastic part of the annulus fibrosus is described as proposed in the last section and the poroelastic nucleus pulposus as well as the poroelastic lamellae of the annulus fibrosus are regarded only as an isotropic elastic, very soft and almost incompressible material with elastic tensor

$$E^{abcd}_{\text{pulpos}} = \lambda g^{ab} g^{cd} + \mu g^{ac} g^{bd} + \mu g^{ad} g^{bc}.$$

Such a model of the nucleus pulposus can be viewed as an appropriate one at least in the case of short-time loading.

This model can be solved using the principle of the total potential energy minimum.

(2) Small deformations and viscoelastic nucleus pulposus. Once more only small deformations and locally orthotropic elastic part of the annulus fibrosus are considered while the poroelastic parts are modeled as an isotropic three element viscoelastic material

$$\dot{\sigma}^{ab} + A^{ab}{}_{cd}\sigma^{cd} = B^{abcd}\dot{\varepsilon}_{cd} + D^{abcd}\varepsilon_{cd}.$$

This model could be solved using Galerkin method applied to the equations

$$\nabla_a \sigma^{ab} = 0,$$

$$2\varepsilon_{ab} = \nabla_a u_b + \nabla_b u_a$$

with the appropriate material model and base functions fulfilling the boundary conditions.

(3) Large deformations and elastic nucleus pulposus. This model is identical with the first one but the considered deformations are the large ones. Thus

$$2E_{ab} = \nabla_a u_b + \nabla_b u_a + \nabla_a u^c \nabla_b u_c$$

and

$$E^{abcd}_{\mathrm{pulpos}} = \lambda g^{ab} g^{cd} + \mu g^{ac} g^{bd} + \mu g^{ad} g^{bc}.$$

The solution is sought through minimization of the total elastic energy.

(4) Large deformations and viscoelastic nucleus pulposus. This is essentially the second model with large deformations taken into respect. Consequently, for the nucleus pulposus and the poroelastic lamellae, the material model is

$$\dot{S}^{ab} + A^{ab}{}_{cd} S^{cd} = B^{abcd}\dot{E}_{cd} + D^{abcd} E_{cd}$$

and the solution of the problem could be found using Galerkin method applied to the equations

$$2E_{ab} = \nabla_a u_b + \nabla_b u_a + \nabla_a u^c \nabla_b u_c$$

and

$$\nabla_a S^{ab} = 0$$

with base functions fulfilling appropriate boundary conditions.

At the following we will concentrate on the case where the small deformations and elastic nucleus pulposus are taken into account.

6. Small deformations and elastic nucleus pulposus

At this section we are going to analyse the deformation of the intervertebral disk in the case of small deformations when the elastic part of the annulus fibrosus is described as the locally orthotropic material and both the poroelastic nucleus pulposus and the poroelastic lamellae of the annulus fibrosus as isotropic elastic, very soft and almost incompressible material.

6.1. Total potential energy of the intervertebral disk. As we are going to use the principle of the potential energy minimum we must express the total potential energy

$$\Pi(u_a) = a(u_a) - l(u_a)$$

with elastic strain energy

$$a(u_a) = \frac{1}{2}\int\limits_{\Omega} E^{abcd}\varepsilon_{ab}(u_a)\varepsilon_{cd}(u_a)\mathrm{d}\Omega$$

and the work of the applied forces

$$l(u_a) = \int\limits_{\Omega} p^a u_a \mathrm{d}\Omega + \int\limits_{\partial_t \Omega} t^a u_a \mathrm{d}\Gamma.$$

The small strain tensor

$$\varepsilon_{ab} = \frac{1}{2}(\nabla_a u_b + \nabla_b u_a)$$

is defined by the covariant derivative of the displacement

$$\nabla_a u_b = \partial_a u_b - \Gamma^c_{ab} u_c$$

with the Christoffel symbol of the 2$^{\mathrm{nd}}$

$$\Gamma^d_{ab} = g^{dc}\frac{1}{2}(\partial_b g_{ac} + \partial_a g_{cb} - \partial_c g_{ab}).$$

We can write

$$\overset{x}{\varepsilon}_{ab}= \frac{1}{2}(\partial_a \overset{x}{u}_b + \partial_b \overset{x}{u}_a - 2\,\Gamma^c_{ab} \overset{x}{u}_c)$$

and

$$\Gamma^c_{ab} \overset{x}{u}_c = \Gamma^1_{ab} \overset{x}{u}_1 + \Gamma^2_{ab} \overset{x}{u}_2 + \Gamma^3_{ab} \overset{x}{u}_3,$$

where Christoffel symbols for the epicycloidal coordinate system x are[3]

$$\Gamma^1_{ab} = \begin{pmatrix} 0 & 0 & 0 \\ 0 & \Gamma^1_{22} & 0 \\ 0 & 0 & 0 \end{pmatrix},$$

$$\Gamma^2_{ab} = \begin{pmatrix} 0 & \Gamma^2_{12} & 0 \\ \Gamma^2_{21} & \Gamma^2_{22} & 0 \\ 0 & 0 & 0 \end{pmatrix},$$

$$\Gamma^3_{ab} = 0,$$

with

$$\Gamma^2_{12} = \Gamma^2_{21} = \frac{1}{x^1},$$

$$\Gamma^1_{22} = -\frac{(2d_x r_y + 4d_y r_x)\sin x^2 \sin 2x^2 + (4d_x r_y + 2d_y r_x)\cos x^2 \cos 2x^2 - 2r_x r_y - 4d_x d_y}{(2d_x r_y + d_y r_x)\sin x^2 \sin 2x^2 + (d_x r_y + 2d_y r_x)\cos x^2 \cos 2x^2 - 2r_x r_y - d_x d_y}\, x^1$$

and

$$\Gamma^2_{22} = -\frac{3d_y r_x \cos x^2 \sin 2x^2 - 3d_x r_y \sin x^2 \cos 2x^2}{(2d_x r_y + d_y r_x)\sin x^2 \sin 2x^2 + (d_x r_y + 2d_y r_x)\cos x^2 \cos 2x^2 - 2r_x r_y - d_x d_y}.$$

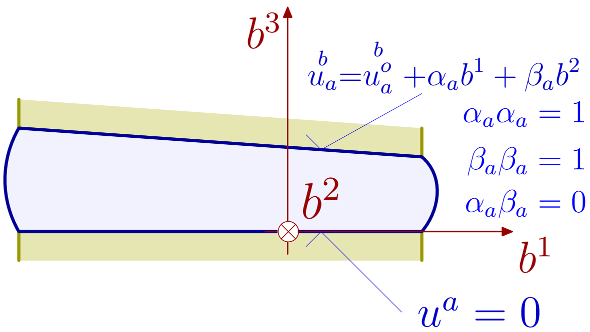

FIGURE 9. Boundary conditions

6.2. Fourier series expansion. To integrate the total potential energy, we approximate the displacement functions by the Fourier series expansion. The chosen Fourier series needs to fulfil the boundary conditions, Fig. 9. The lower vertebra is fixed and the upper vertebra moves as a rigid model, which is, for the small deformations, expressed as

$$\overset{b}{u^h_1} = \overset{b}{u^o_1} - b^2 \varphi_3,$$

$$\overset{b}{u^h_2} = \overset{b}{u^o_2} + b^1 \varphi_3,$$

$$\overset{b}{u^h_3} = \overset{b}{u^o_3} - b^1 \varphi_2 + b^2 \varphi_1,$$

where φ_1 is rotation around axis b^1, φ_2 is rotation around axis b^2, φ_3 is rotation around axis b^3 and u^o_a is displacement of the point $b^{1,2} = 0, b^3 = h$.

The convenient Fourier series fulfilling these boundary conditions is

$$\overset{x}{u}_a = \sum_{k,l=-\infty}^{\infty} \sum_{m=1}^{\infty} U^{klm}_a \left(e^{i2\pi k x^1} e^{i l x^2} x^1 + 1 \right) \sin \frac{\pi m x^3}{h} + \overset{x}{u^h_a} \frac{x^3}{h},$$

where

$$\overset{x}{u^h_a} = \frac{\partial b^b}{\partial x^a} \overset{b}{u^h_b}.$$

In the GNU OCTAVE syntax this can be written as

[3] Using GNU MAXIMA software.

```
ux=N*U
B=B(x1,x2,x3)
B=kron(kron(e.^(i*k*2*pi*x1),x1*e.^(i*l*x2)+1),sin(pi*m*x3/h))
bc=[0,0,-b(2); 0,0,b(1); b(2),-b(1),0];
N=[[B,zeros(1,K),zeros(1,K); zeros(1,K),B,zeros(1,K);
zeros(1,K),zeros(1,K),B],bx*x3/h,bx*bc*x3/h]; ## size(U)=3*K+6
```

where the infinite number of terms is replace by the number K and the unknown coefficients are

$$\mathtt{U} = \begin{pmatrix} \bar{\mathtt{U}} \\ \overset{b}{u}{}_1^0 \\ \overset{b}{u}{}_2^0 \\ \overset{b}{u}{}_3^0 \\ \varphi_1 \\ \varphi_2 \\ \varphi_3 \end{pmatrix}$$

where $\bar{\mathtt{U}}$ is a vector composed of U_a^{klm}.

6.3. Elastic energy. The expression of elastic energy

$$a(u_a) = \frac{1}{2} \int\limits_\Omega E^{abcd} \varepsilon_{ab}(u_a) \varepsilon_{cd}(u_a) \mathrm{d}\Omega$$

is a quadratic function of strain tensor

$$\varepsilon_{ab} = \frac{1}{2}(\nabla_a u_b + \nabla_b u_a)$$

with covariant derivative

$$\nabla_a u_b = \partial_a u_b - \Gamma^c_{ab} u_c.$$

As the elasticity tensor E^{abcd} is the symmetric one in indices ab and cd

$$E^{abcd} = E^{bacd} = E^{cdab},$$

we may the elastic energy, in the epicycloidal coordinate system x, write like

$$a = \frac{1}{2} \int\limits_\Omega \left(\partial_a \overset{x}{u}_b - \Gamma^p_{ab} \overset{x}{u}_p \right) \overset{x}{E}{}^{abcd} \left(\partial_c \overset{x}{u}_d - \Gamma^p_{cd} \overset{x}{u}_p \right) \left| \overset{x}{g}_{ab} \right|^{\frac{1}{2}} \mathrm{d}^3 x,$$

which in the GNU Octave syntax looks as

$$a = \frac{1}{2} \mathtt{U}' * \mathtt{K} * \mathtt{U}$$

with the stiffness matrix

$$\mathtt{K} = \int\limits_0^1 \int\limits_0^{2\pi} \int\limits_0^h (\mathtt{DG(x)}' - \mathtt{Gamma(x)}') * \mathtt{Ex(x)} * (\mathtt{DG(x)} - \mathtt{Gamma(x)}) * \mathtt{sqrt(det(gx(x)))} \mathrm{d}x^1 \mathrm{d}x^2 \mathrm{d}x^3$$

where

$$\left\{ \partial_a \overset{x}{u}_b \right\}_{ab\lceil} = \mathtt{DG} * \mathtt{U},$$

with DG constructed in GNU Octave code in a similar way as the matrix B above, and

$$\left\{ \Gamma^p_{ab} \overset{x}{u}_p \right\}_{ab\lceil} = \mathtt{Gamma} * \mathtt{U}$$

with

$$\mathtt{Gamma} = \mathtt{vec(G1')} * \mathtt{N(1,:)} + \mathtt{vec(G2')} * \mathtt{N(2,:)},$$

where

$$\mathtt{G1} = \left\{ \Gamma^1_{ab} \right\}_{a\lceil b},$$

and

$$\mathtt{G2} = \left\{ \Gamma^2_{ab} \right\}_{a\lceil b}.$$

The integration of stiffness matrix has to be performed numerically. Nevertheless, as this integration is carried out on the block

$$0 \le x^1 \le 1,\ 0 \le x^2 \le 2\pi,\ 0 \le x^3 \le h,$$

it is not great problem to perform it.

6.4. Work done by the external forces. Work done by the external forces

$$l(u_a) = \int_{\Omega} p^a u_a \mathrm{d}\Omega + \int_{\partial_t \Omega} t^a u_a \mathrm{d}\Gamma$$

is in the GNU Octave syntax expressed as

$$l = \mathtt{F} * \mathtt{U}.$$

As

$$\mathtt{U} = \begin{pmatrix} \bar{\mathtt{U}} \\ \overset{b}{u}{}_1^0 \\ \overset{b}{u}{}_2^0 \\ \overset{b}{u}{}_3^0 \\ \varphi_1 \\ \varphi_2 \\ \varphi_3 \end{pmatrix},$$

the vector F has straightforwardly the form

$$\mathtt{F} = [\mathtt{zeros}(3 * \mathtt{K}, 1); \mathtt{Vs}; \mathtt{Vl}; -\mathtt{N}; \mathtt{Ml}; \mathtt{Mf}; \mathtt{Mr}],$$

with Vs,Vl,N,Ml,Mf,Mr defined in the Fig. 7.

6.5. The necessary condition of minimum and solution of the problem. The necessary condition of the minimum of the total potential energy

$$\frac{\partial \Pi}{\partial \mathtt{U}} = 0,$$

with the total potential energy expressed in the GNU Octave syntax as

$$\Pi = \frac{1}{2}\mathtt{U}' * \mathtt{K} * \mathtt{U} - \mathtt{F} * \mathtt{U},$$

is linear

$$\mathtt{K} * \mathtt{U} = \mathtt{F}$$

with the solution of the unknown coefficients

$$\mathtt{U} = \mathtt{K}^{-1} * \mathtt{F}.$$

The displacement tensor in the epicycloidal coordinate system x

$$\overset{x}{u}_a = \mathtt{ux} = \mathtt{real}(\mathtt{N}(\mathtt{x}) * \mathtt{U})$$

and in the global cartesian system b

$$\overset{b}{u}_a = \frac{\partial x^b}{\partial b^a} \overset{x}{u}_b$$

or, in the GNU Octave syntax,

$$\mathtt{ub} = \mathtt{xb}' * \mathtt{ux}.$$

The results for different types of loading, drawn using the last (cartesian) expression of the displacement tensor, are depicted in the Figs. 10–15.

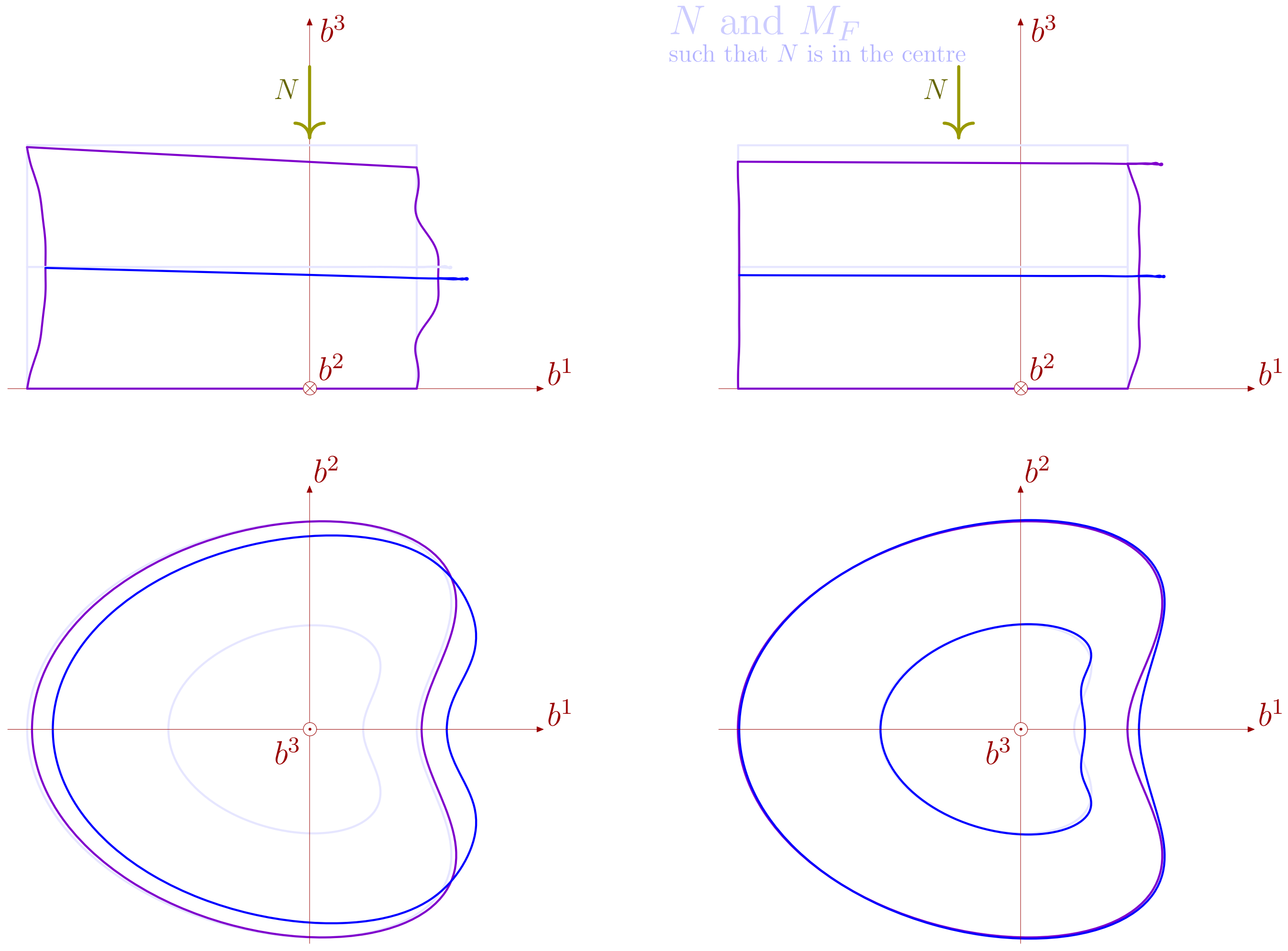

FIGURE 10. Response to the loading by N

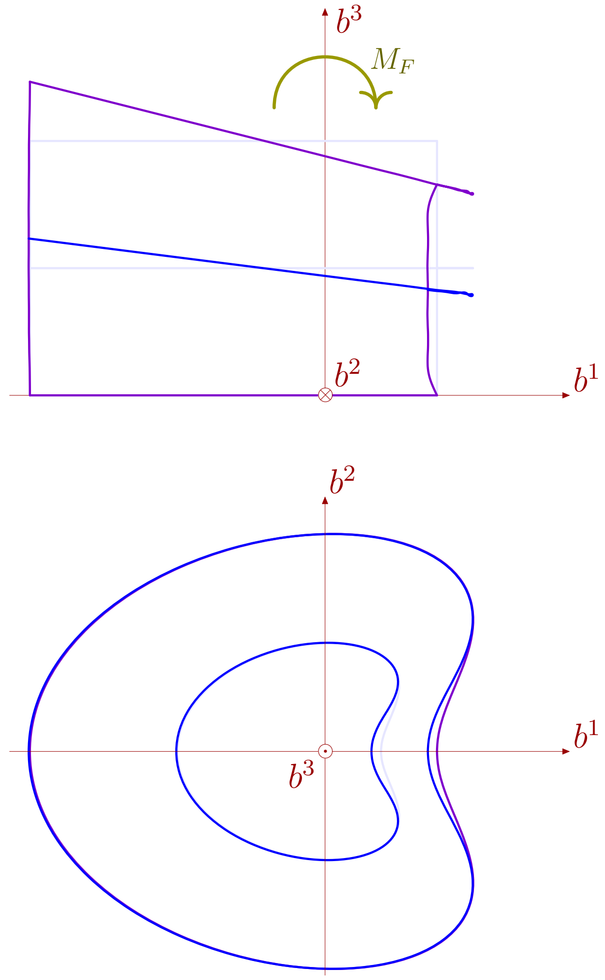

FIGURE 11. Response to the loading by M_F

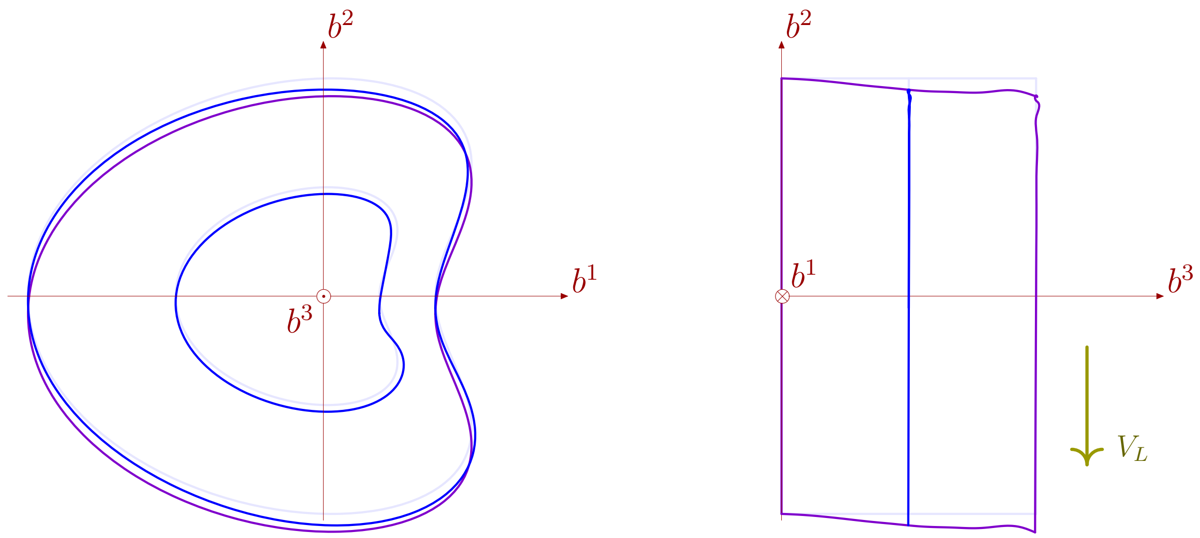

FIGURE 12. Response to the loading by V_L

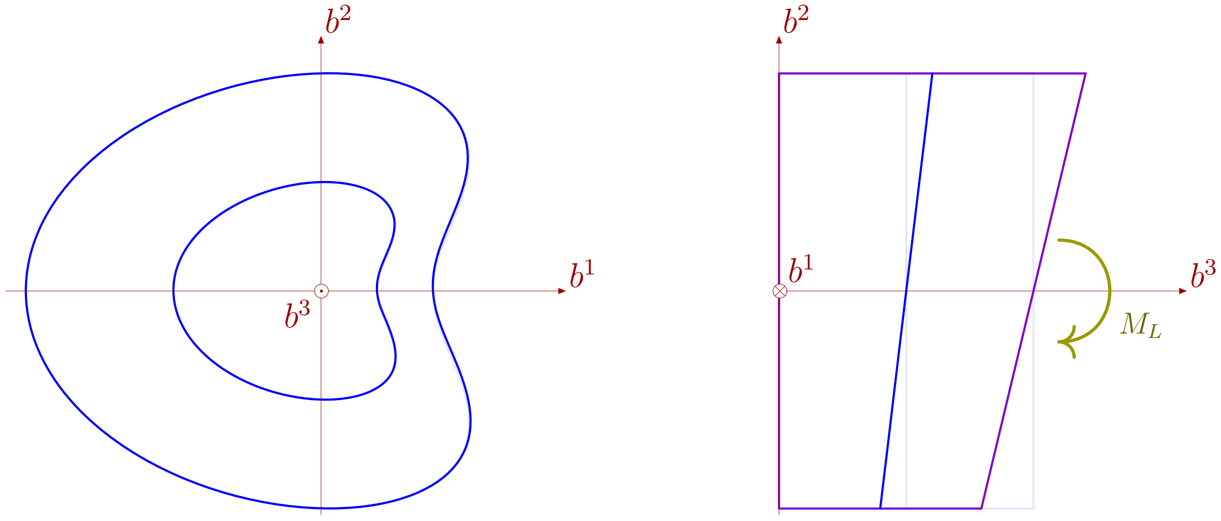

FIGURE 13. Response to the loading by M_L

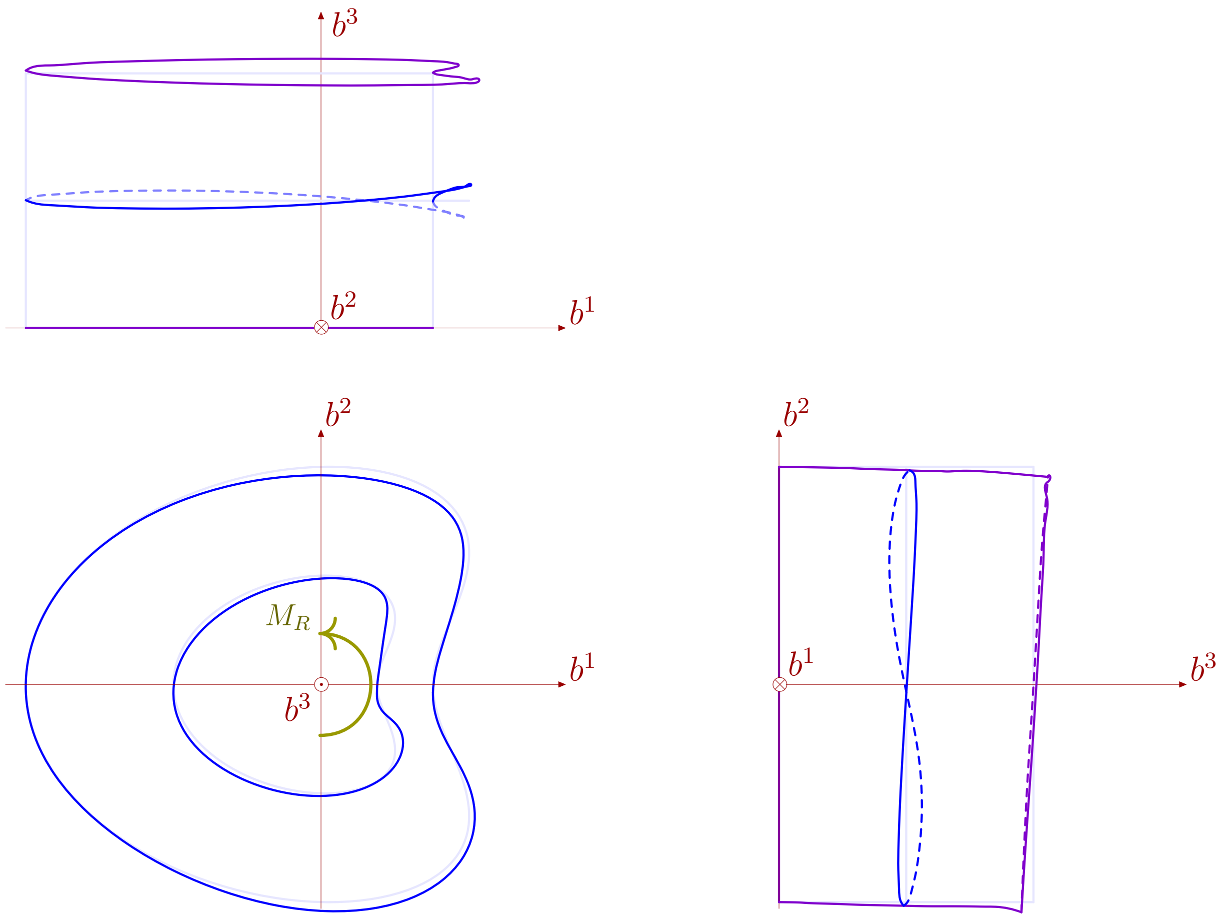

FIGURE 14. Response to the loading by M_R

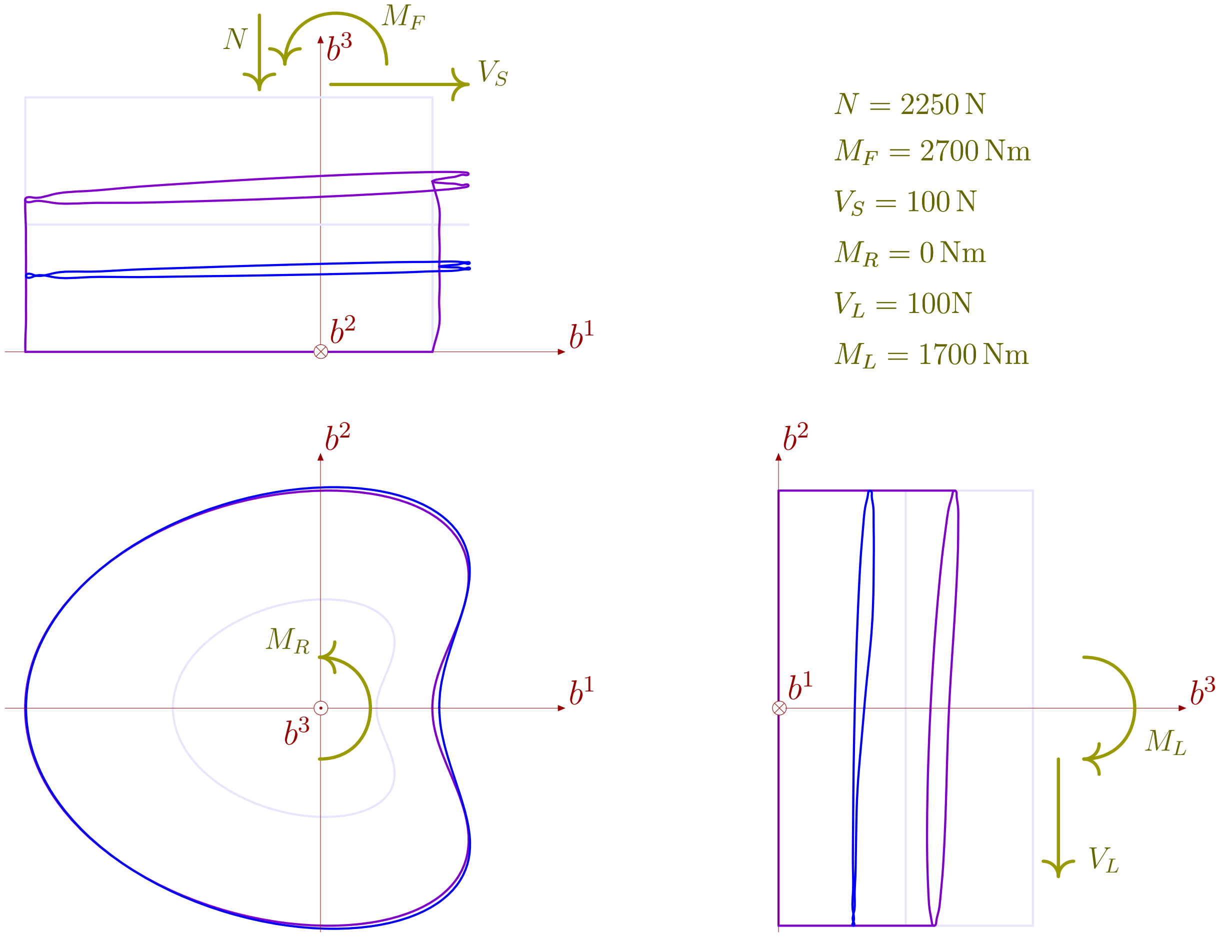

FIGURE 15. Response to the loading by the full set of loadings

CHAPTER 4

Nanomechanics of cortical bone

1. Geometry and internal structure of thigh bone

The femur,[1] the longest and strongest bone in the skeleton, is almost perfectly cylindrical in the greater part of its extent.

1.1. Geometry and nomenclature of the femur. In the following let us list some comments regarding the terms stated in Figs. 1 and 2.[2]

Proximal extremity [Upper extremity] presents for examination the head, the neck, the greater and lesser trochanter.

Caput femoris [L., head of femur] is the proximal end of the femur, articulating with the acetabulum on the *os coxae*. Called also femoral head.

Acetabulum [L., vinegar-cruet, from acetum vinegar] is the large cup-shaped cavity on the lateral surface of the *os coxae* in which the head of the femur articulates; called also acetabular bone, cotyloid cavity, and os acetabuli.

Fovea [L., a pit], *i.e.*, anatomic nomenclature for a small pit in the surface of a structure or organ.

Fovea capitis femoris, *i.e.*, fovea of head of femur: a depression in the head of the femur where the ligamentum teres is attached; called also *fossa capitis femoris* and fossa of head of femur.

Collum femoris [Femoral neck, Neck of femur] is the heavy column of bone connecting the head of the femur and the shaft. The *collum femoris* (neck) is broader laterally than medially.

Tuberculum [L., dimension of tuber], is a general term in anatomical nomenclature for a tubercle, nodule, or small eminence.

Capsula articularis [L., articular capsule] is the saclike envelope that encloses the cavity of a synovial joint by attaching to the circumference of the articular end of each involved bone; it consists of a fibrous membrane and a synovial membrane. Called also joint capsule and synovial capsule.

Linea intertrochanterica [Anterior intertrochanteric line] is a line running obliquely downward and medially from the tubercle of the femur, winding around the medial side of the body of the bone.

Musculus psoas (so'as) major [Greater psoas muscle] is a muscle with origin from the bodies of the lumbar vertebrae and the intervertebral disks from the twelfth thoracic to the fifth lumbar vertebrae and from the transverse processes of the lumbar vertebrae, with insertion into the lesser trochanter of femur, with nerve supply from the lumbar plexus, and whose action flexes the thigh or trunk.

Musculus quadriceps femoris [Quadriceps muscle of thigh] is a name applied collectively to the rectus femoris, vastus intermedius, vastus lateralis, and vastus medialis, inserting by a common tendon that surrounds the patella and ends on the tuberosity of the tibia, and acting to extend the leg upon the thigh.

Musculus vastus lateralis has origin on capsule of hip joint, lateral aspect of femur. Insertion point: patella, common tendon of quadriceps femoris. Action: extends leg.

Musculus vastus intermedius (Crureus) is the muscle for extension of the knee joint and thus extends leg. It origins at anterior and lateral surfaces of the body of the femur in its upper two-thirds and from the lower part of the lateral intermuscular septum (Septum intermusculare femoris laterale). Its fibers end in a superficial aponeurosis, which forms the deep part of the Quadriceps femoris tendon.

Musculus vastus medialis originates on medial aspect of femur. Its insertion is on patella, common tendon of quadriceps femoris. Action: extends leg.

Trochanter major [Greater trochanter] is a broad, flat process at the upper end of the lateral surface of the femur, to which several muscles are attached.

Trochanter minor [Lesser trochanter] is a short conical process projecting medially from the lower part of the posterior border of the base of the neck of the femur.

[1] [**Gra18**], *e.g.* at http://www.bartleby.com/107/59.html.

[2] Cf. [**DN03**] and A.D.A.M. Encyclopedia at http://www.mercksource.com.

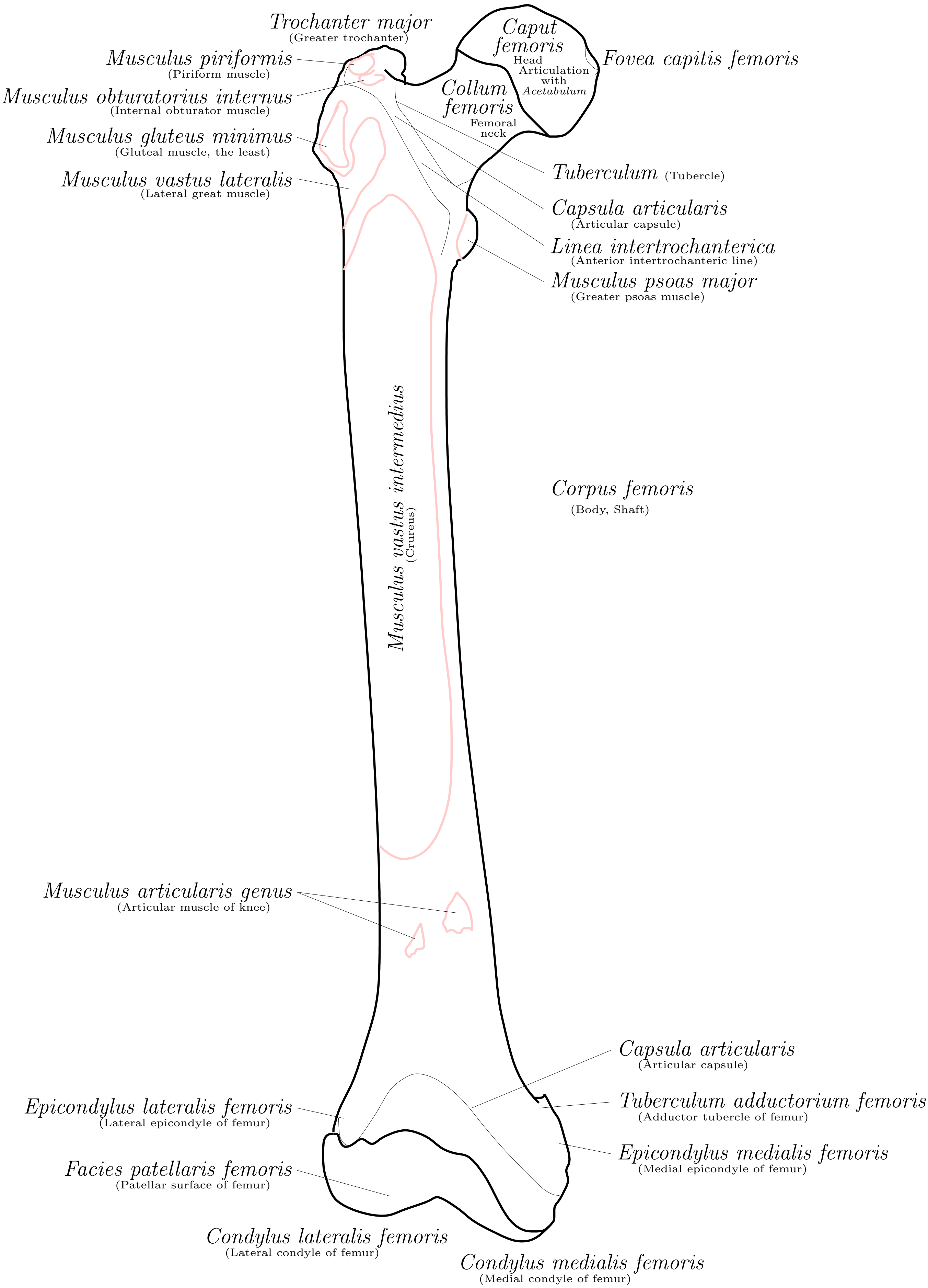

Figure 1. Right femur—Anterior surface

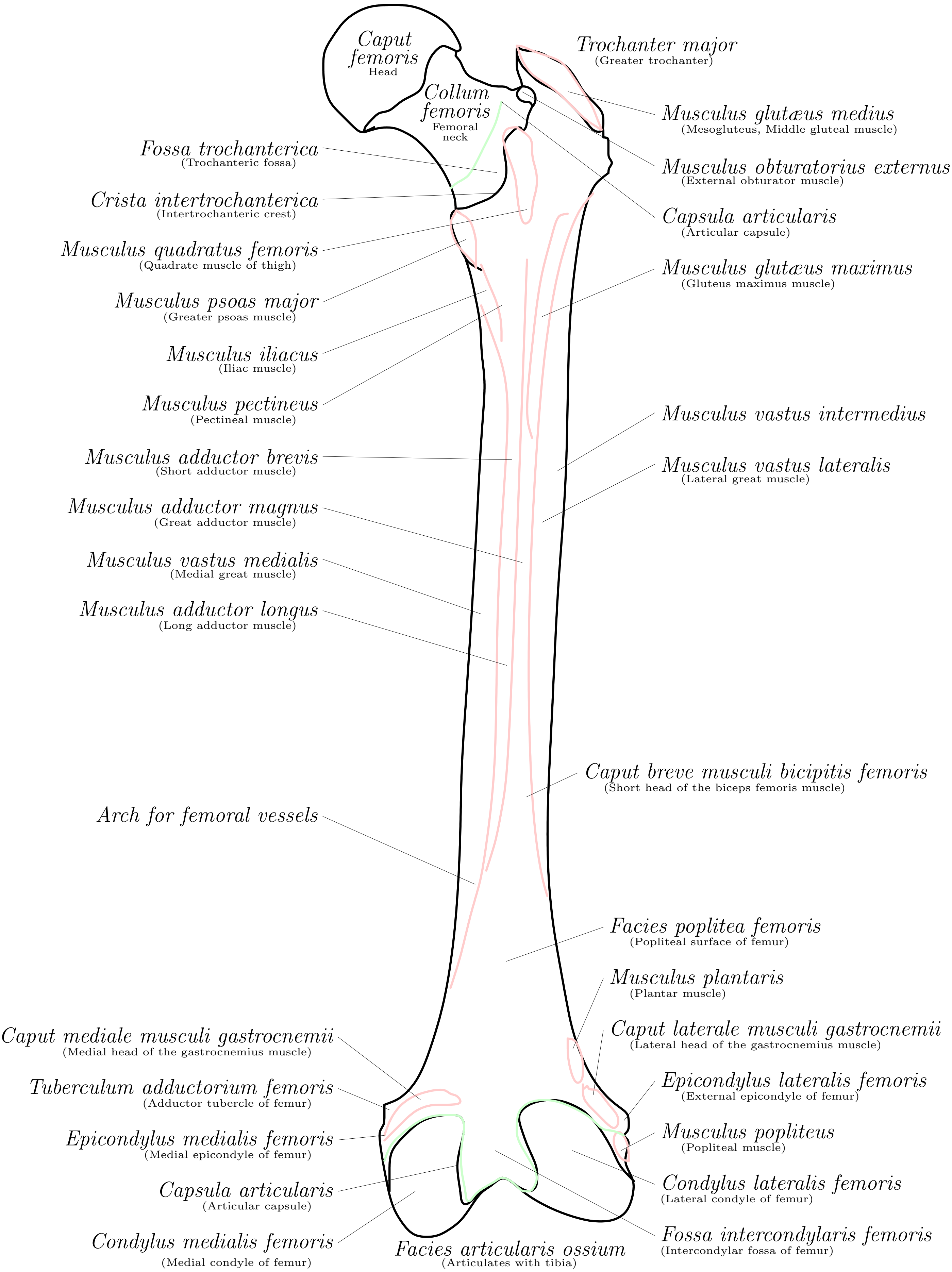

FIGURE 2. Right femur—Posterior surface

Musculus piriformis [Piriform muscle] has origin on ilium, second to fourth sacral vertebrae and insertion on upper border of greater trochanter.

Musculus gemellus inferior [Inferior gemellus muscle] originates from the tuberosity of ischium and inserts on the greater trochanter of femur. It rotates thigh laterally.

Musculus gemellus superior [Superior gemellus muscle] originates from the spine of ischium and inserts on the greater trochanter of femur. Action: It rotates thigh laterally.

Obturator [L.] is any structure, natural or artificial, that closes an opening.

Musculus obturatorius internus [Internal obturator muscle] has origin on pelvic surface of hip bone, margin of obturator foramen, ramus of ischium, inferior ramus of pubis, internal surface of obturator membrane. The insertion is on greater trochanter of femur. The action is to rotate thigh laterally.

Musculus glutæus minimus [Least gluteal muscle] has origin on lateral surface of ilium between anterior and inferior gluteal lines. Insertion: greater trochanter of femur. Action: abducts, rotates thigh medially.

Musculus glutæus medius [Mesogluteus, Middle gluteal muscle] originates on lateral surface of ilium between anterior and posterior gluteal lines. Insertion is on greater trochanter of femur. Action: abducts and rotates thigh medially.

Musculus glutæus maximus [Gluteus maximus muscle] originates posteriorly from the posterior gluteal line of the ilium, aponeurosis of the erector spinae, dorsal surface of the sacrum, coccyx, and sacrotuberous ligament. It inserts at the iliotibial band and the gluteal tuberosity of the femur. The gluteus maximus is the uppermost of the three muscles. Its action is to extend and outwardly rotate hip, and extend the trunk. The direct attachment to the sacrum it may influence the stability of the joint.

Musculus articularis genus [Articular muscle of knee] originates at the distal fourth of anterior surface of shaft of femur. Insertion: synovial membrane of knee joint. Action: lifts capsule of knee joint.

Epicondylus [Epicondyle] is an eminence upon a bone, above its condyle.

Epicondylus lateralis femoris [Lateral epicondyle of femur] is a projection from the distal end of the femur, above the lateral condyle, for the attachment of collateral ligaments of the knee. Called also external epicondyle of femur.

Epicondylus medialis femoris [Medial epicondyle of femur] is a projection from the distal end of the femur, above the medial condyle, for the attachment of collateral ligaments of the knee; called also internal epicondyle of femur.

Condylus (pl. condyli) [L., from Gr. kondylos knuckle, condyle] is a rounded projection on a bone, usually for articulation with another.

Condylus lateralis femoris [Lateral condyle of femur] is the lateral of the two surfaces at the distal end of the femur that articulate with the superior surfaces of the head of the tibia. It is also called external or fibular condyle of femur.

Condylus medialis femoris [Medial condyle of femur] is the medial of the two surfaces at the distal end of the femur that articulate with the superior surfaces of the head of the tibia. Called also internal or tibial condyle of femur, and condylus tibialis femoris.

Facies patellaris femoris (Patellar surface of femur) is the smooth anterior continuation of the condyles that forms the surface of the femur articulating with the patella; called also anterior intercondylar fossa of femur and patellar fossa of femur.

Tuberculum adductorium femoris [Adductor tubercle of femur] is a small projection from the upper part of the medial epicondyle of the femur, to which the tendon of the adductor magnus muscle is attached.

Fossa (pl. fossae), [L.] is a trench, channel, or hollow place.

Fossa trochanterica [Trochanteric fossa] is a deep depression on the medial surface of the greater trochanter that receives the insertion of the tendon of the obturator externus muscle.

Musculus obturatorius externus [External obturator muscle] originates on pubis, ischium, and superficial surface of obturator membrane. Insertion is on trochanteric fossa of femur. Action: rotates thigh laterally.

Crest is a projection or projecting structure, or ridge, especially one surmounting a bone or its border; see also crista and ridge.

Crista intertrochanterica [Intertrochanteric crest] is a prominent ridge running obliquely downward and medialward from the summit of the greater trochanter on the posterior surface of the neck of the femur to the lesser trochanter; called also intertrochanteric ridge, linea intertrochanterica posterior, and posterior intertrochanteric line.

Musculus quadratus femoris [Quadrate muscle of thigh, Quadratus femoris muscle] originates on upper part of lateral border of tuberosity of ischium; inserts on quadrate tubercle of femur, intertrochanteric crest. It adducts, rotates thigh laterally.

Musculus iliacus [Iliac muscle] originates on iliac fossa and base of sacrum; inserts on greater psoas tendon and lesser trochanter of femur. Action: flexes thigh, trunk on limb.

Musculus pectineus [Pectineal muscle] originates on pectineal line of pubis; inserts on femur distal to lesser trochanter. Action: flexes, adducts thigh.

Musculus adductor brevis [Short adductor muscle, Short h. of triceps femoris muscle] originates on outer surface of inferior ramus of pubis; insertion is on upper part of linea aspera of femur. Action: adducts, rotates, flexes thigh.

Musculus adductor magnus [Great adductor muscle] (2 parts): Deep part originates on inferior ramus of pubis, ramus of ischium. Superficial part on ischial tuberosity. Deep part inserts on linea aspera of femur. Superficial part on adductor tubercle of femur. Action: Deep part adducts thigh, Superficial part extends thigh.

Musculus adductor longus [Long adductor muscle] originates on crest and symphysis of pubis. Insertion is on linea aspera of femur. Action: adducts, rotates, flexes thigh.

Caput breve musculi bicipitis femoris [Short head of the biceps femoris muscle] is arising from the linea aspera femoris.

Facies (pl. facies) is a specific surface of a body structure, part, or organ.

Facies articularis ossium is articular surface of bone: the surface by which a bone articulates with another.

Facies poplitea femoris [Popliteal surface of femur] is the triangular lower third of the posterior surface of the femur, between the medial and lateral supracondylar lines, which forms the superior part of the floor of the popliteal fossa; called also planum popliteum femoris.

Musculus plantaris [Plantar muscle] has origin on oblique popliteal ligament, lateral supracondylar line of femur; insertion on posterior part of calcaneus. Action: plantar flexes foot.

Epicondylus lateralis femoris [Lateral epicondyle of femur] is a projection from the distal end of the femur, above the lateral condyle, for the attachment of collateral ligaments of the knee. Called also external epicondyle of femur.

Musculus popliteus [Popliteal muscle] has origin on lateral condyle of femur, lateral meniscus; insertion is on posterior surface of tibia. Action: flexes leg, rotates leg medially.

Fossa intercondylaris femoris [Intercondylar fossa of femur] is the posterior depression between the condyles of the femur; called also fossa intercondyloidea femoris, intercondylar notch of femur, and popliteal notch or incisure.

Caput laterale musculi gastrocnemii [Lateral head of the gastrocnemius muscle, Lateral gastrocnemius muscle] is arising from the lateral condyle and posterior surface of the femur, and the capsule of the knee joint.

Caput mediale musculi gastrocnemii [Medial head of the gastrocnemius muscle, Medial gastrocnemius muscle] is arising from the medial condyle of the femur and the capsule of the knee joint.

Corpus femoris [Body, Shaft] is almost cylindrical in form. It is slightly arched, so as to be convex in front.

1.2. The architecture and internal structure of the femur. John C. Koch[3] by mathematical analysis has *"shown that in every part of the femur there is a remarkable adaptation of the inner structure of the bone to the machanical requirements due to the load on the femur-head."*

It is believed that the following laws of bone structure have been demonstrated for the femur:

1. The inner structure and external form of human bone are closely adapted to the mechanical conditions existing at every point in the bone.

2. The inner architecture of a normal bone is determined by definite and exact requirements of mathematical and mechanical laws to produce a maximum of strength with a minimum of material.[4]

[3] [**Koc17**]. Cf. [**Gra18**] at `http://www.bartleby.com/107/59.html`. See also Wolff and Roux.

[4] That all is cited from [**Gra18**]. There also is the following: Diagram of the lines of stress in the upper femur, based upon the mathematical analysis of the right femur. These result from the combination of the different kinds of stresses at each point in the femur. (After Koch.) See http://www.bartleby.com/107/illus248.html, http://www.bartleby.com/107/illus251.html, etc. Cf. second half of http://www.bartleby.com/107/59.html.

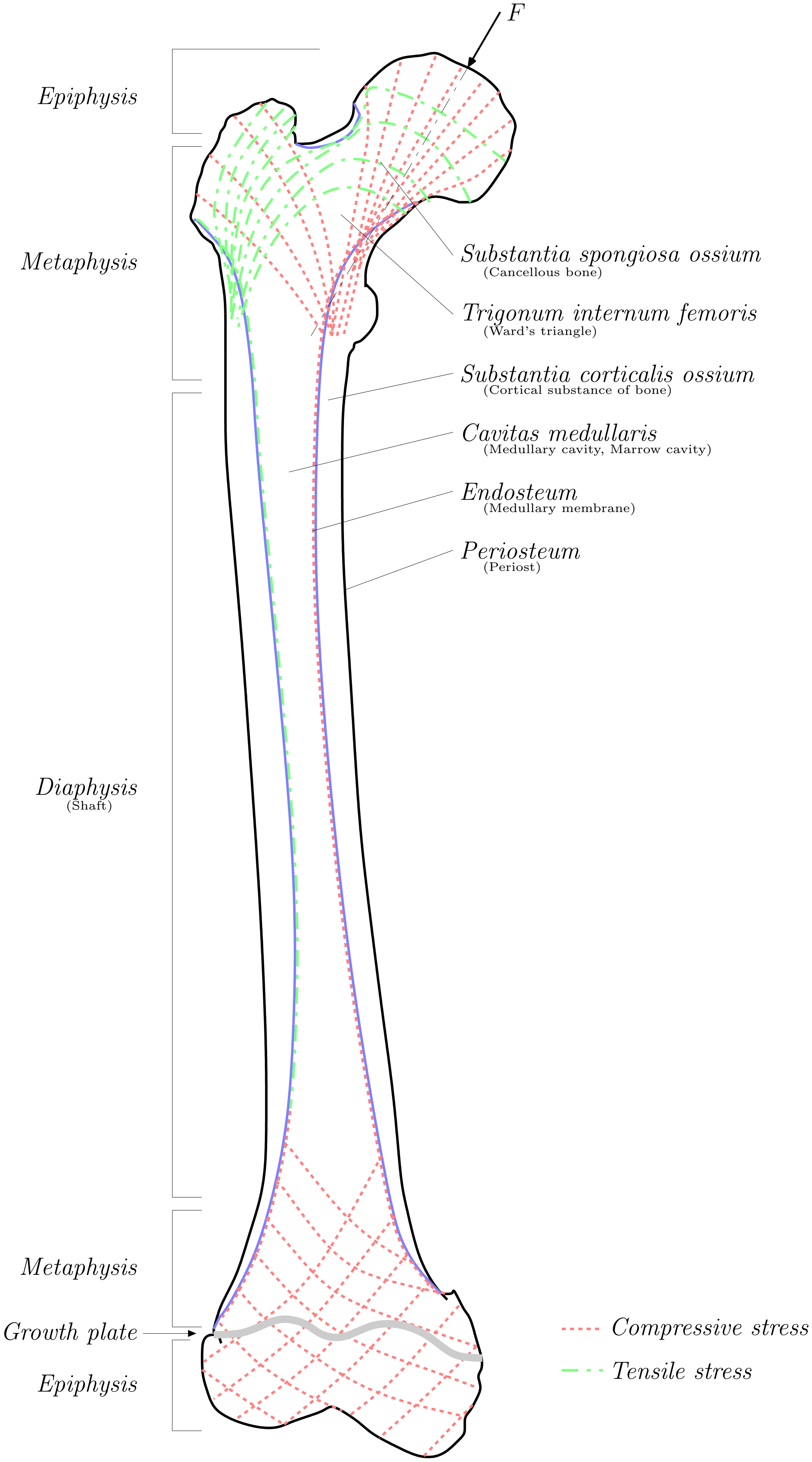

FIGURE 3. Internal structure of the right femur—Anterior surface

Trabeculae descend from the periphery of the femoral head toward the medial cortex along the direction of the resultant compressive force, exactly like the compressive trajectories obtained theoretically and by the photoelastic method. A bundle of trabeculae follows an arched course from the lateral to the medial cortex, as do the tensile trajectories derived from theory.[5]

Trigonum internum femoris [Ward's triangle] is the space formed by the angle of the trabeculae (an area of diminished density in the trabecular pattern) in the neck of the femur; a vulnerable point for fracture. It is evident by X-ray as well as by direct inspection.

Cancellus (pl. cancelli) [L., a lattice] any structure arranged like a lattice. A reticular, spongy, or lattice-like structure.

Substantia (pl. substantiae) [L., substance, called also matter] is a general anatomical nomenclature for material of which a tissue, organ, or body is composed.

Substantia spongiosa ossium [Spongy substance of bone, called also Cancellated or Cancellous bone, Spongy bone, Trabecular substance, and Substantia trabecularis ossium] is bone substance made up of thin intersecting lamellae, usually found internal to compact bone.

Corticalis [Cortical] means pertaining to or of the nature of a cortex or bark.

Substantia corticalis ossium [Cortical substance of bone] is the substance comprising the hard outer layer of a bone.

Cavitas medullaris [Medullary cavity, Marrow cavity, Medullary canal, and Medullary space] is the space in the diaphysis of a long bone containing the marrow.

Endo [L., inside, within].

Membrana (gen. and pl. membranae) [Membrane] is an anatomic nomenclature for a thin layer of tissue that covers a surface, lines a cavity, or divides a space or organ.

Endosteum [Medullary membrane] is the tissue lining the medullary cavity of a bone.

Peri (Gr., around, about).

Periosteum (Peri- + Gr. osteon, bone) [Periost] is a specialized connective tissue covering all bones of the body, and possessing bone-forming potentialities; in adults, it consists of two layers that are not sharply defined, the external layer being a network of dense connective tissue containing blood vessels, and the deep layer composed of more loosely arranged collagenous bundles with spindle-shaped connective tissue cells and a network of thin elastic fibers. Thus, the periosteum is a fibrous sheath that covers bones. It contains the blood vessels and nerves that provide nourishment and sensation to the bone.

Epiphysis (pl. epiphyses, Gr.: an ongrowth, excrescence) is the expanded articular end of a long bone, developed from a secondary ossification center, which during the period of growth is either entirely cartilaginous or is separated from the shaft by the epiphyseal cartilage. Called also apophysis ossium.

Metaphysis (pl. metaphyses) is the wider part at the extremity of the shaft of a long bone, adjacent to the epiphyseal disk. During development it contains the growth zone and consists of spongy bone; in the adult it is continuous with the epiphysis.

Diaphysis (pl. diaphyses, Gr.: the point of separation between stalk and branch) [Shaft] is the portion of a long bone formed from a primary center of ossification. It is the elongated cylindrical portion (the shaft) of a long bone, between the ends or extremities (the epiphyses), which are usually articular and wider than the shaft; it consists of a tube of compact bone, enclosing the medullary (marrow) cavity.

1.3. Sector of the shaft of a long bone. Osteon (Gr., bone) [Haversian system] is the basic unit of structure of compact bone, comprising a haversian canal and its concentrically arranged lamellae, of which there may be 4 to 20, each 3 to 7 micrometres thick, in a single (haversian) system. Such units are directed mainly in the long axis of the bone.[6]

Canalis nutricius [Haversian canal, Haversian space, Canalis nutriens, Nutrient canal of bone] is one of the freely anastomosing channels of the haversian system of compact bone, which contain blood vessels, lymph vessels, and nerves. Named for Clopton Havers, English physician and anatomist, 1650—1702

Volkmann's canal [Alfred Wilhelm Volkmann, German physiologist, 1800—1877] is a passage other than haversian canals (canales nutricii), for the passage of blood vessels through bone. It is usually transversely connecting two Haversian canals.

Haversian lamella (L., genitive and plural: lamellae) is one of the concentric bony plates surrounding a haversian canal.

Collagen fiber [collagenous fiber] is the soft, flexible, white fiber which is the most characteristic constituent of all types of connective tissue, consisting of the protein collagen, and composed of bundles

[5]See Fig. 3. Cf. [**Pau76**], [**Koc17**], [**Gra18**] at `http://www.bartleby.com/107/59.html`.

[6]Cf. [**Gra18**] at http://www.bartleby.com/107/18.html

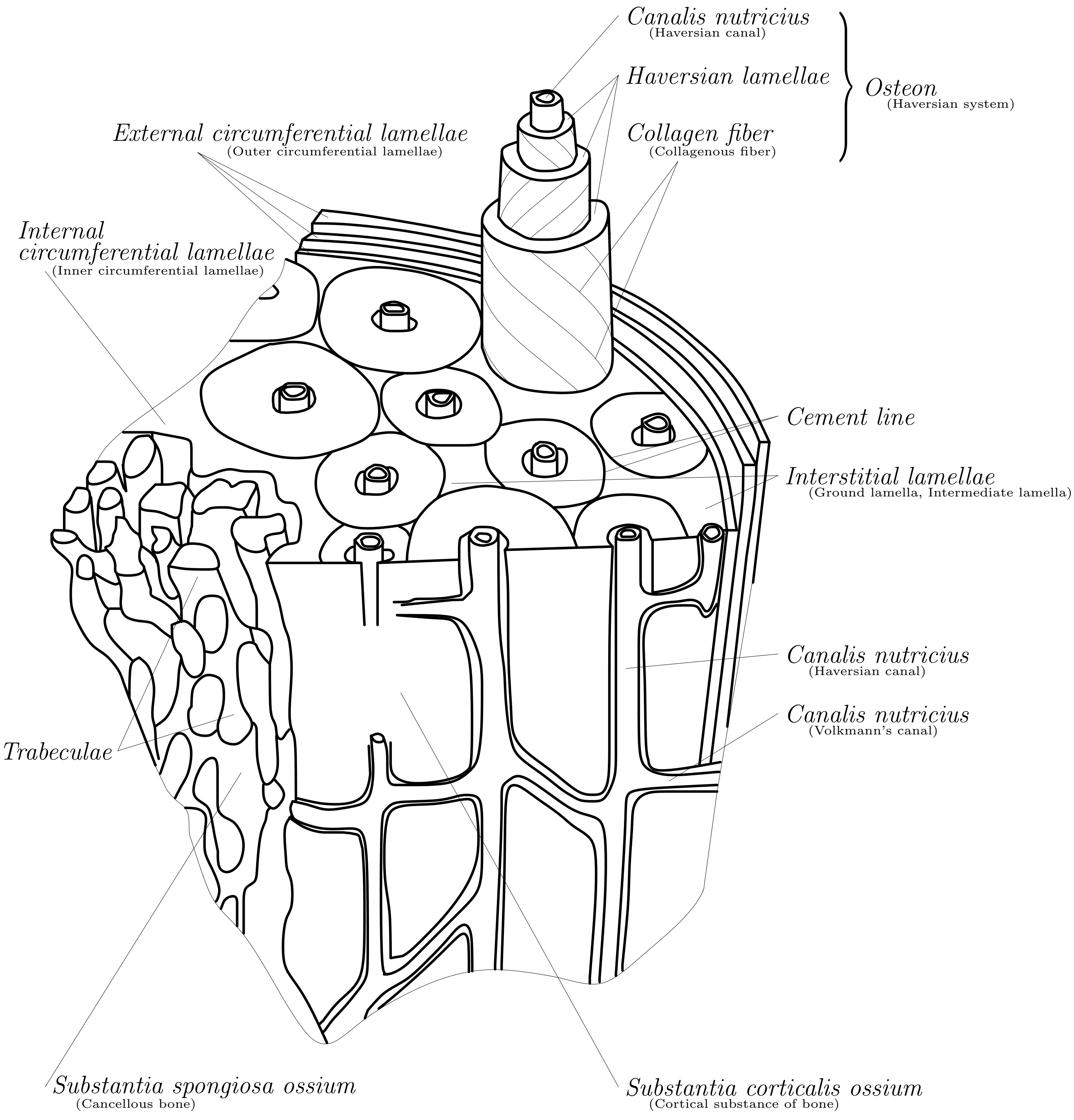

FIGURE 4. Sector of the shaft of a long bone

of fibrils that are in turn made up of smaller units (unit fibrils or microfibrils) which show a characteristic crossbanding with a major periodicity of approximately 65 nm. In describing the hierarchy of arrangement of collagen structure, the terms fiber and fibril are sometimes loosely interchanged.

Interstitial lamella (pl. lamellae) [Ground lamella, Intermediate lamella] is one of the bony plates that fill in between the haversian systems.

Cement line is a name applied to a line, visible in microscopic examination of bone in cross section, marking the boundary of an osteon (haversian system).

Circumferential lamella (gen. and pl. lamellae) is one of the layers of bone. There are *external circumferential lamellae* and *internal circumferential lamellae*.

Trabecula (pl. trabeculae) is, in anatomical nomenclature, a supporting or anchoring strand of connective tissue, such as one extending from a capsule into the substance of the enclosed organ.

Trabeculae of bone are anastomosing bony spicules in cancellous bone which form a meshwork of intercommunicating spaces that are filled with bone marrow.

2. Mathematical model of the cortical bone osteon

2.1. Introduction. Osteon (Gr., bone) [Haversian system] is the basic unit of structure of compact bone. The osteon consists of a number (may be 4 to 20) **Haversian lamellae**, *i.e.*, the concentric bony plates surrounding a haversian canal. Each of these lamellae is 3 to 7 microns thick.[7]

Haversian lamella is composed of **collagen fibers**. Collagen fiber is the soft, flexible, white fiber which is the most characteristic constituent of all types of connective tissue, consisting of the protein collagen, and composed of bundles of fibrils that are in turn made up of smaller units (unit fibrils or microfibrils) which show a characteristic crossbanding with a major periodicity of approximately 65 nm.

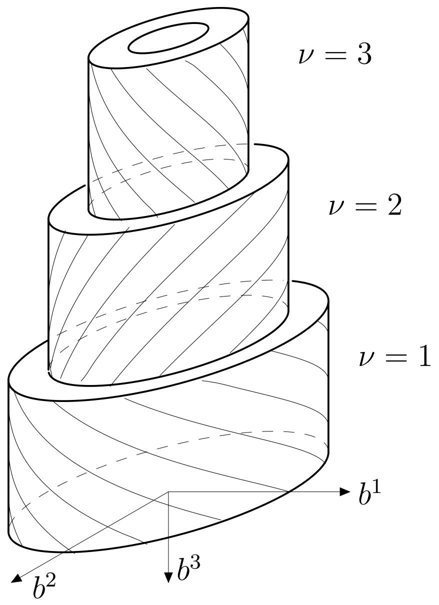

FIGURE 5. Cortical bone osteon global coordinate system

2.2. Frames of reference as a foundation of a mathematical modeling of the osteons. In the mathematical modeling it is essential to constitute a coordinate system. It is true that abstract tensor notation derives the label from *abstract* in the meaning unrelated to a specified coordinate system. Nevertheless, every mechanical modeling is connected with a body and the body has a geometry that is describable only with a coordinate system. At this stage let us look at the osteon, Fig. 5, in the b^3-direction and draw one lamella of the osteon, say $\nu = 1$, together with the global computational coordinates and one of the infinite number of local Cartesians, Fig. 6.

The relations between the coordinates of the osteon are (see carefully Fig. 6)

$$b^1 = \beta^1 \cos \beta^2,$$
$$b^2 = \beta^1 \sin \beta^2,$$
$$b^3 = \beta^3.$$
$$\beta^1 = \sqrt{(b^1)^2 + (b^2)^2},$$
$$\beta^2 = \arctan \frac{b^2}{b^1},$$
$$\beta^3 = b^3.$$
$$x^1 = \beta^1 - r_o,$$
$$x^2 = r_o \beta^2,$$
$$x^3 = \beta^3.$$
$$\beta^1 = x^1 + r_o,$$

[7]Cf. [**Gra18**] at http://www.bartleby.com/107/18.html

ξ^a — Local Cartesian coordinate system
b^a — Global Cartesian coordinate system of the osteon
β^a — Global computational coordinate system of the osteon
x^a — Global computational coordinate system of the unfolded osteon lamella

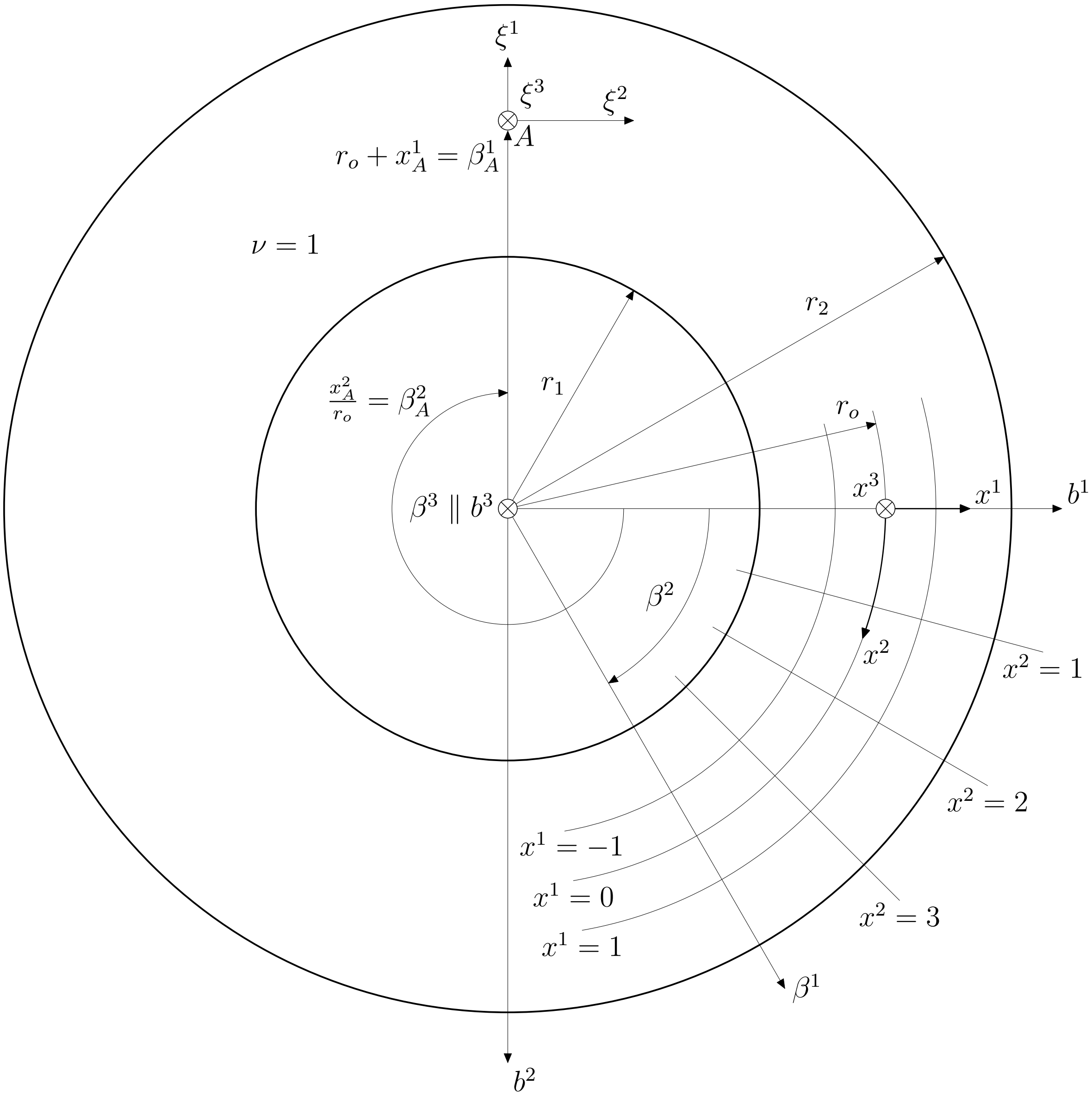

FIGURE 6. Cortical bone osteon lamella coordinate system

$$\beta^2 = \frac{1}{r_o}x^2,$$
$$\beta^3 = x^3.$$

The transformation between the x-frame and the ξ-frame we postpone to another opportunity.

The matrices of tensor transformation between the above listed frames are given[8] via the following derivatives.

$$\frac{\partial b^a}{\partial \beta^b} = \begin{pmatrix} \cos\beta^2 & -\beta^1 \sin\beta^2 & 0 \\ \sin\beta^2 & \beta^1 \cos\beta^2 & 0 \\ 0 & 0 & 1 \end{pmatrix}$$

[8][**LR89**], [**SS78**].

As

$$\frac{\partial b^a}{\partial \beta^b}\frac{\partial \beta^b}{\partial b^c} = \delta^a_c$$

we have also

$$\frac{\partial \beta^a}{\partial b^b} = \begin{pmatrix} \cos\beta^2 & \sin\beta^2 & 0 \\ \frac{-1}{\beta^1}\sin\beta^2 & \frac{1}{\beta^1}\cos\beta^2 & 0 \\ 0 & 0 & 1 \end{pmatrix}.$$

Further,

$$\frac{\partial x^a}{\partial \beta^b} = \begin{pmatrix} 1 & 0 & 0 \\ 0 & r_o & 0 \\ 0 & 0 & 1 \end{pmatrix}, \quad \frac{\partial \beta^a}{\partial x^b} = \begin{pmatrix} 1 & 0 & 0 \\ 0 & \frac{1}{r_o} & 0 \\ 0 & 0 & 1 \end{pmatrix},$$

and

$$\frac{\partial b^a}{\partial x^b} = \frac{\partial b^a}{\partial \beta^c}\frac{\partial \beta^c}{\partial x^b} = \begin{pmatrix} \cos\beta^2 & -\frac{\beta^1}{r_o}\sin\beta^2 & 0 \\ \sin\beta^2 & \frac{\beta^1}{r_o}\cos\beta^2 & 0 \\ 0 & 0 & 1 \end{pmatrix},$$

$$\frac{\partial x^a}{\partial b^b} = \frac{\partial x^a}{\partial \beta^c}\frac{\partial \beta^c}{\partial b^b} = \begin{pmatrix} \cos\beta^2 & \sin\beta^2 & 0 \\ \frac{-r_o}{\beta^1}\sin\beta^2 & \frac{r_o}{\beta^1}\cos\beta^2 & 0 \\ 0 & 0 & 1 \end{pmatrix}.$$

Now, we arrive at the constitution of the metric tensors, g_{ab}. It holds

$$\mathrm{d}s^2 = \overset{x}{g}_{ab}\,\mathrm{d}x^a\mathrm{d}x^b = \overset{\beta}{g}_{ab}\,\mathrm{d}\beta^a\mathrm{d}\beta^b = \overset{b}{g}_{ab}\,\mathrm{d}b^a\mathrm{d}b^b.$$

As the b-frame is the Cartesian one (in the Euclidian space),

$$\mathrm{d}s^2 = \mathrm{d}b^a\mathrm{d}b^a = \delta_{ab}\mathrm{d}b^a\mathrm{d}b^b$$

and thus

$$\overset{b}{g}_{ab} = \delta_{ab} = \begin{pmatrix} 1 & 0 & 0 \\ 0 & 1 & 0 \\ 0 & 0 & 1 \end{pmatrix}.$$

Transforming,

$$\overset{x}{g}_{ab} = \frac{\partial b^c}{\partial x^a}\frac{\partial b^d}{\partial x^b}\delta_{cd} = \begin{pmatrix} \cos\beta^2 & \sin\beta^2 & 0 \\ -\frac{\beta^1}{r_o}\sin\beta^2 & \frac{\beta^1}{r_o}\cos\beta^2 & 0 \\ 0 & 0 & 1 \end{pmatrix}\begin{pmatrix} \cos\beta^2 & -\frac{\beta^1}{r_o}\sin\beta^2 & 0 \\ \sin\beta^2 & \frac{\beta^1}{r_o}\cos\beta^2 & 0 \\ 0 & 0 & 1 \end{pmatrix},$$

i.e.,

$$\overset{x}{g}_{ab} = \begin{pmatrix} 1 & 0 & 0 \\ 0 & \left(\frac{\beta^1}{r_o}\right)^2 & 0 \\ 0 & 0 & 1 \end{pmatrix} = \begin{pmatrix} 1 & 0 & 0 \\ 0 & \left(\frac{x^1+r_o}{r_o}\right)^2 & 0 \\ 0 & 0 & 1 \end{pmatrix}, \tag{24}$$

the entry $\left(\frac{\beta^1}{r_o}\right)^2 = \left(\frac{x^1+r_o}{r_o}\right)^2$ being the "stretching" of the x^2-coordinate.

Similarly,

$$\overset{\beta}{g}_{ab} = \frac{\partial b^c}{\partial \beta^a}\frac{\partial b^d}{\partial \beta^b}\delta_{cd} = \begin{pmatrix} \cos\beta^2 & \sin\beta^2 & 0 \\ -\beta^1\sin\beta^2 & \beta^1\cos\beta^2 & 0 \\ 0 & 0 & 1 \end{pmatrix}\begin{pmatrix} \cos\beta^2 & -\beta^1\sin\beta^2 & 0 \\ \sin\beta^2 & \beta^1\cos\beta^2 & 0 \\ 0 & 0 & 1 \end{pmatrix},$$

and thus

$$\overset{\beta}{g}_{ab} = \begin{pmatrix} 1 & 0 & 0 \\ 0 & \left(\beta^1\right)^2 & 0 \\ 0 & 0 & 1 \end{pmatrix}.$$

Another task to look at is the *local coordinate system* of the unfolded infinitesimal ply of the lamella, ξ^a, and the connection between ξ-frame and x-frame, Fig. 7. The ξ-frame, being *Cartesian*, has the metric equal to δ_{ab} and thus the tensor transformation must be such that

$$\delta_{ab} = \overset{\xi}{g}_{ab} = \frac{\partial x^c}{\partial \xi^a}\frac{\partial x^d}{\partial \xi^b}\,\overset{x}{g}_{cd},$$

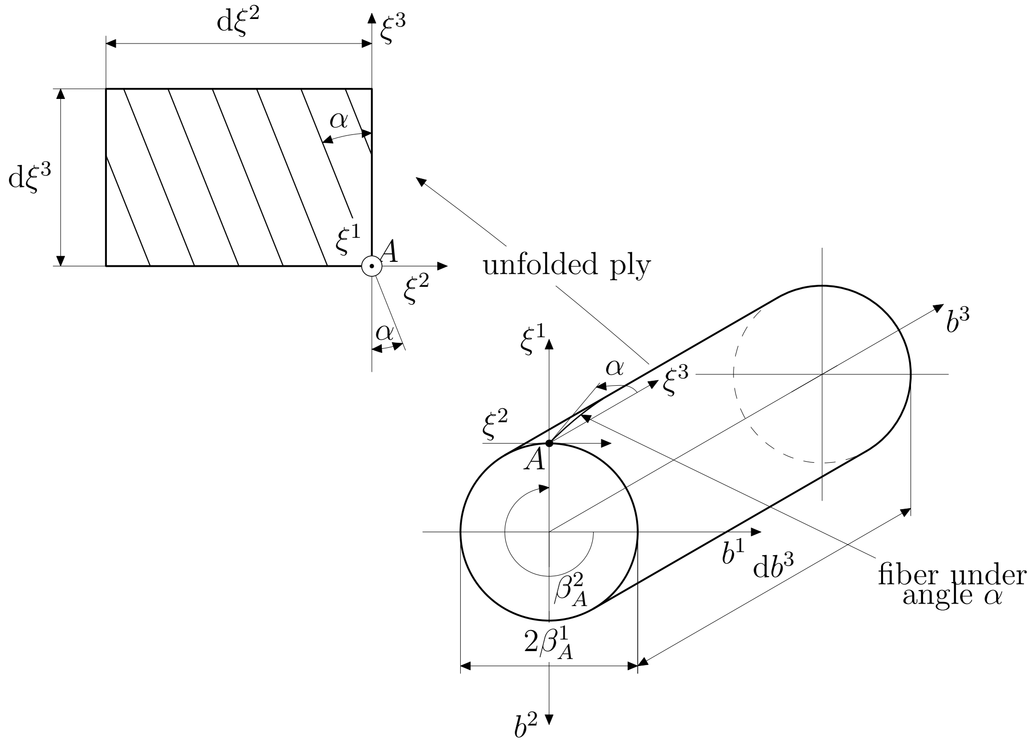

FIGURE 7. Local coordinate system ξ^a of an unrolled infinitesimal ply of a lamella of the osteon

i.e., as the directions of respective axes are alined,

$$\frac{\partial x^a}{\partial \xi^b} = \begin{pmatrix} 1 & 0 & 0 \\ 0 & \frac{r_o}{\beta^1} & 0 \\ 0 & 0 & 1 \end{pmatrix} = \begin{pmatrix} 1 & 0 & 0 \\ 0 & \frac{r_o}{r_o + x^1} & 0 \\ 0 & 0 & 1 \end{pmatrix}$$

and

$$\frac{\partial \xi^a}{\partial x^b} = \begin{pmatrix} 1 & 0 & 0 \\ 0 & \frac{\beta^1}{r_o} & 0 \\ 0 & 0 & 1 \end{pmatrix} = \begin{pmatrix} 1 & 0 & 0 \\ 0 & \frac{r_o + x^1}{r_o} & 0 \\ 0 & 0 & 1 \end{pmatrix}.$$

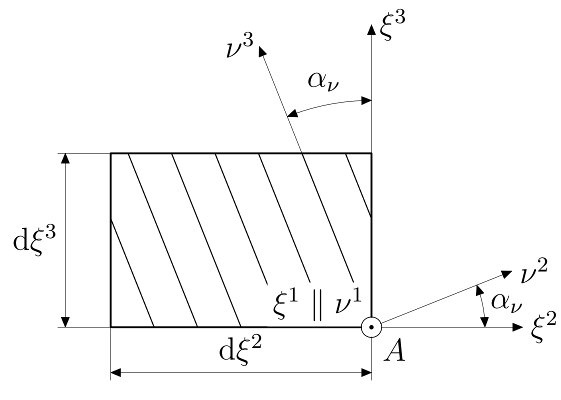

FIGURE 8. Principal material coordinate system ν^a of an unrolled infinitesimal part of the lamella

The connection of the principal coordinate system of local orthotropy, ν^a, with the local coordinate system, ξ^a, of an unrolled infinitesimal ply of a lamella of the osteon is apparent from the Fig. 8. It holds that

$$\frac{\partial \nu^a}{\partial \xi^b} = \begin{pmatrix} 1 & 0 & 0 \\ 0 & \cos\alpha_\nu & \sin\alpha_\nu \\ 0 & -\sin\alpha_\nu & \cos\alpha_\nu \end{pmatrix}, \quad \frac{\partial \xi^a}{\partial \nu^b} = \begin{pmatrix} 1 & 0 & 0 \\ 0 & \cos\alpha_\nu & -\sin\alpha_\nu \\ 0 & \sin\alpha_\nu & \cos\alpha_\nu \end{pmatrix}.$$

2.3. The stress-strain relation of a lamella of the osteon. The components of the stress tensor relevant to the ξ-frame are the physical ones, *i.e.*, the components that possess the stress units, MPa. The same holds for strains. Now, imagine that in a way the stress-strain relation of a very thin unrolled ply of an osteon lamella written in the principal coordinate system of the orthotropy was obtained.[9] Thus

$$\overset{\nu}{\sigma}{}^{ij} = \overset{\nu}{E}{}^{ijkl} \overset{\nu}{\varepsilon}_{kl}$$

and

$$\overset{\nu}{\varepsilon}_{ij} = \overset{\nu}{C}_{ijkl} \overset{\nu}{\sigma}{}^{kl}$$

are the relations derived for an infinitesimal curved block regarded, or really adjusted, as rectangular. From the entries of the metric tensor of the x-frame, see (24), we can deduced that for $x^1 \ll r_o$ there is minimal error to put

$$\overset{x}{E}{}^{abcd} = \overset{\xi}{E}{}^{abcd} = \frac{\partial \xi^a}{\partial \nu^i} \frac{\partial \xi^b}{\partial \nu^j} \overset{\nu}{E}{}^{ijkl} \frac{\partial \xi^c}{\partial \nu^k} \frac{\partial \xi^d}{\partial \nu^l}.$$

But if we take into account the opposite case, the case of an osteon where the thickness is not negligible compared with the radius, we must take deeper analysis:

$$\overset{x}{E}{}^{oprs} = \frac{\partial x^o}{\partial \xi^a} \frac{\partial x^p}{\partial \xi^b} \overset{\xi}{E}{}^{abcd} \frac{\partial x^r}{\partial \xi^c} \frac{\partial x^s}{\partial \xi^d} = \frac{\partial x^o}{\partial \xi^a} \frac{\partial x^p}{\partial \xi^b} \frac{\partial \xi^a}{\partial \nu^i} \frac{\partial \xi^b}{\partial \nu^j} \overset{\nu}{E}{}^{ijkl} \frac{\partial \xi^c}{\partial \nu^k} \frac{\partial \xi^d}{\partial \nu^l} \frac{\partial x^r}{\partial \xi^c} \frac{\partial x^s}{\partial \xi^d}.$$

That is

$$\frac{\partial \nu^a}{\partial x^b} = \frac{\partial \nu^a}{\partial \xi^c} \frac{\partial \xi^c}{\partial x^b} = \begin{pmatrix} 1 & 0 & 0 \\ 0 & \frac{r_o + x^1}{r_o} \cos \alpha_\nu & \sin \alpha_\nu \\ 0 & -\frac{r_o + x^1}{r_o} \sin \alpha_\nu & \cos \alpha_\nu \end{pmatrix}$$

and

$$\frac{\partial x^a}{\partial \nu^b} = \frac{\partial x^a}{\partial \xi^c} \frac{\partial \xi^c}{\partial \nu^b} = \begin{pmatrix} 1 & 0 & 0 \\ 0 & \frac{r_o}{r_o + x^1} \cos \alpha_\nu & -\frac{r_o}{r_o + x^1} \sin \alpha_\nu \\ 0 & \sin \alpha_\nu & \cos \alpha_\nu \end{pmatrix}.$$

Similarly,

$$\frac{\partial \nu^a}{\partial \beta^b} = \frac{\partial \nu^a}{\partial x^c} \frac{\partial x^c}{\partial \beta^b} = \begin{pmatrix} 1 & 0 & 0 \\ 0 & \beta^1 \cos \alpha_\nu & \sin \alpha_\nu \\ 0 & -\beta^1 \sin \alpha_\nu & \cos \alpha_\nu \end{pmatrix},$$

$$\frac{\partial \beta^a}{\partial \nu^b} = \frac{\partial \beta^a}{\partial x^c} \frac{\partial x^c}{\partial \nu^b} = \begin{pmatrix} 1 & 0 & 0 \\ 0 & \frac{1}{\beta^1} \cos \alpha_\nu & -\frac{1}{\beta^1} \sin \alpha_\nu \\ 0 & \sin \alpha_\nu & \cos \alpha_\nu \end{pmatrix};$$

and

$$\frac{\partial \nu^a}{\partial b^b} = \frac{\partial \nu^a}{\partial x^c} \frac{\partial x^c}{\partial b^b} = \begin{pmatrix} \cos \beta^2 & \sin \beta^2 & 0 \\ -\cos \alpha_\nu \sin \beta^2 & \cos \alpha_\nu \cos \beta^2 & \sin \alpha_\nu \\ \sin \alpha_\nu \sin \beta^2 & -\sin \alpha_\nu \cos \beta^2 & \cos \alpha_\nu \end{pmatrix},$$

$$\frac{\partial b^a}{\partial \nu^b} = \frac{\partial b^a}{\partial x^c} \frac{\partial x^c}{\partial \nu^b} = \begin{pmatrix} \cos \beta^2 & -\cos \alpha_\nu \sin \beta^2 & \sin \alpha_\nu \sin \beta^2 \\ \sin \beta^2 & \cos \alpha_\nu \cos \beta^2 & -\sin \alpha_\nu \cos \beta^2 \\ 0 & \sin \alpha_\nu & \cos \alpha_\nu \end{pmatrix}.$$

2.4. Elastic strain energy of the osteon. The *elastic strain energy* is the functional

$$a = \int_\Omega \varepsilon_{ab} \varepsilon_{cd} E^{abcd} \, \mathrm{d}\Omega,$$

where the differential element of a volume in a curvilinear coordinate system is related to the differentials of the coordinates by the square root of the determinant of the metric tensor g_{ab}, *e.g.*, in the β-frame,

$$\mathrm{d}\Omega = \left| \overset{\beta}{g}_{ab} \right|^{\frac{1}{2}} \mathrm{d}^3\beta = \beta^1 \mathrm{d}\beta^1 \mathrm{d}\beta^2 \mathrm{d}\beta^3,$$

and the invariant

$$\varepsilon_{ab} \varepsilon_{cd} E^{abcd}$$

[9] The Cartesian entries of the elastic and compliance tensor see at [**Mar06a**].

must be the function of the integrative coordinates. Nevertheless, components of the acting tensors may be relevant to any, but for all the same, coordinate system. If specified, in the case of the osteon,

$$a = \int_0^l \sum_{\nu=1}^{n_b} \int_{r_\nu}^{r_{\nu+1}} \beta^1 \int_0^{2\pi} \overset{\beta}{\varepsilon}_{ab} \overset{\beta}{\varepsilon}_{cd} \frac{\partial\beta^a}{\partial\nu^i} \frac{\partial\beta^b}{\partial\nu^j} \overset{\nu}{E}{}^{ijkl} \frac{\partial\beta^c}{\partial\nu^k} \frac{\partial\beta^d}{\partial\nu^l} \,\mathrm{d}\beta^2 \,\mathrm{d}\beta^1 \,\mathrm{d}\beta^3,$$

n_b being the number of the osteon lamellae, r_ν the inner radius of the ν-th lamella, r_{n_b+1} outer radius of the osteon, and l the regarded length of the osteon.

3. Method of cortical bone analysis

The geometry and internal structure of thigh bone have been described. At the last section a method of mathematical description of the osteon has been proposed. At this stage let us use the description to analyse a sample of the cortical bone, *e.g.*, the shaft of a thigh bone.

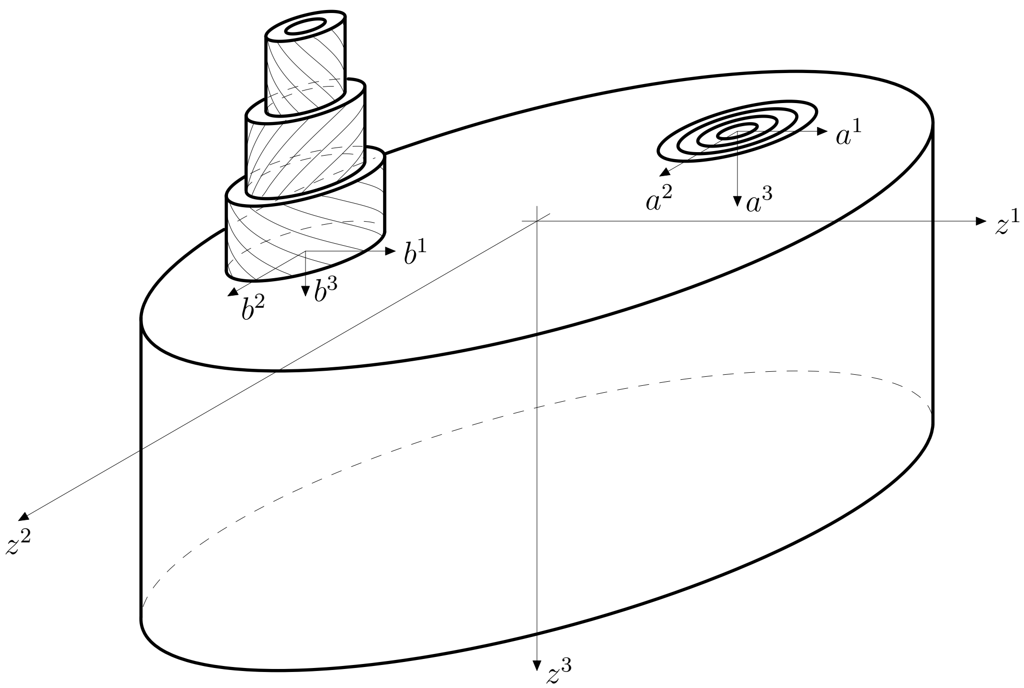

FIGURE 9. Relation between the coordinate systems of long bone osteons

3.1. Osteons of a cortical bone. Let us pursue the model according to Fig. 9—something like a number of osteons embedded in interstitial bone tissue, for our purposes considered as homogeneous isotropic material. For one osteon it holds that *elastic strain energy of the osteon* is the functional[10]

$$a_\ell = \int_{\Omega_\ell} \varepsilon_{ab} \varepsilon^{cd} E^{ab}{}_{cd} \,\mathrm{d}\Omega, \tag{25}$$

where, in the β-frame,[11]

$$\mathrm{d}\Omega = \left| \overset{\beta}{g}_{ab} \right|^{\frac{1}{2}} \mathrm{d}^3\beta = \beta^1 \mathrm{d}\beta^1 \mathrm{d}\beta^2 \mathrm{d}\beta^3.$$

Now, we must collect the set of osteons into one whole, *i.e.*, into the cylinder of the cortical diaphysis of a long bone. More for convenience than for absolute accuracy, let us assume the contour of the femur diaphysis as a hollow circular shaft with inner diameter, R_i, and outer diameter, R_o, respectively. The number of the osteons being n, every one of them, with its own global Cartesian coordinate system $(a, b, \ldots, n)$, consists of a number of lamellae, n_ℓ $(\ell = a, b, \ldots, n)$ of known winding angles, α_ν^ℓ $(\nu = 1, 2, \ldots, n_\ell)$. Besides the *global Cartesian coordinate system of the diaphysis*, z^a, consider the *global cylindrical coordinate system of the diaphysis*, θ^a.

[10][**Mar06b**]

[11]See once more [**Mar06b**].

The elastic energy stored in the hollow cylindrical shaft of the diaphysis, a, may be, as every integral, decomposed into the sum of integrals over disjunct subsets of the considered part of the diaphysis volume, Ω. Thus,

$$a = \int\limits_{\Omega} \varepsilon_{ab}\varepsilon_{cd}\mathcal{E}^{abcd}\,\mathrm{d}\Omega + \sum_{\ell=1}^{n}\int\limits_{\Omega_\ell} \varepsilon_{ab}\varepsilon_{cd}E^{abcd}\,\mathrm{d}\Omega - \sum_{\ell=1}^{n}\int\limits_{\Omega_\ell} \varepsilon_{ab}\varepsilon_{cd}\mathcal{E}^{abcd}\,\mathrm{d}\Omega,$$

$\mathcal{E}^{abcd}$ being the elasticity (stiffness) tensor of the *interstitial lamellae* modeled as a transversally isotropic material (this choice will be discussed later), E^{abcd} elasticity (stiffness) tensor of the osteons as described at another place, Ω_ℓ the volume of ℓ-th osteon. The point of expressing the elastic energy in this way is the comfortable integration over the osteons with β-frames as the chosen coordinates and over the entire cross section of diaphysis in the global cylindrical coordinate system of the diaphysis, θ^a.

CHAPTER 5

Residual stresses in blood vessels

1. Anatomy of blood vessel

The main function of blood vessels is to transport blood throughout the body. The most important vessels in the system are the capillaries which are the microscopic vessels enabling the actual exchange of water and chemicals between the blood and the tissues. The conduit vessels, arteries and veins, carry blood away from the heart and through the capillaries or back towards the heart.

The arteries and veins, which have the same basic structure, are composed of three different layers. The innermost layer is called tunica intima. It is made up of one layer of endothelial cells and is supported by an internal elastic lamina. The middle layer of an artery or vein is known as tunica media. It is the thickest layer and consists of circularly arranged elastic fiber, connective tissue and polysaccharide substances. In the case of arteries, the tunica media may contain vascular smooth muscle, which controls the calibre of the vessel. The outermost layer (tunica adventitia) is entirely made of connective tissue and contains nerves that supply the muscular layer.

Generally, it may be said that the blood vessels are anisotropic and heterogeneous structures but they are commonly modeled in a highly simplified manner.

2. Biomechanical models of blood vessel

Predominantly, the blood vessel is modeled as a cylindrical tube made of a homogeneous elastic material. There are also viscoelastic models but they are not especially popular. The elasticity of blood vessel is usually expressed in the form of a hyperelastic (Green elastic) material where

$$S^{ab} = \frac{\partial w}{\partial E_{ab}},$$

with w being a strain energy density function.

The most approved models are both the Hooke's material with the strain energy density function

$$w = \frac{1}{2} E^{abcd} E_{ab} E_{cd}$$

and Zhou-Fung model

$$w = \frac{c}{2} e^{G^{abcd} E_{ab} E_{cd}},$$

where E^{abcd} and G^{abcd} are regarded either as isotropic

$$E^{abcd} = \lambda g^{ab} g^{cd} + \mu g^{ac} g^{bd} + \mu g^{ad} g^{bc}$$

or othotropic as established above. It is evident that G^{abcd} is a dimensionless quantity while the constant c has the unit of stress. The most modern models are based on a linear combination of the two models just mentioned.

3. Residual strain in blood vessels

Let us determine residual strain in a sector of the blood vessel. The studied sector is a short cylinder and we are going to study both the state before (left hand side in the Fig. 1) and the state after executing a cut along the length of the sample (right hand side in the Fig. 1).

Now let us inverse the perspective. The blood vessel with cut be regarded as a state before deformation and the blood vessel without cut be the state after deformation that was induced by a stress of the amount of the residual stress implied on the face of the cut. The coordinate system o is to be the space coordinate system and the coordinate system ξ is to be the material coordinate space that is deformed with the body. But this time the material coordinate system is uncharacteristically the physical one that means the one with real units. Namely the coordinate ξ^2 represents angle measured in radians.

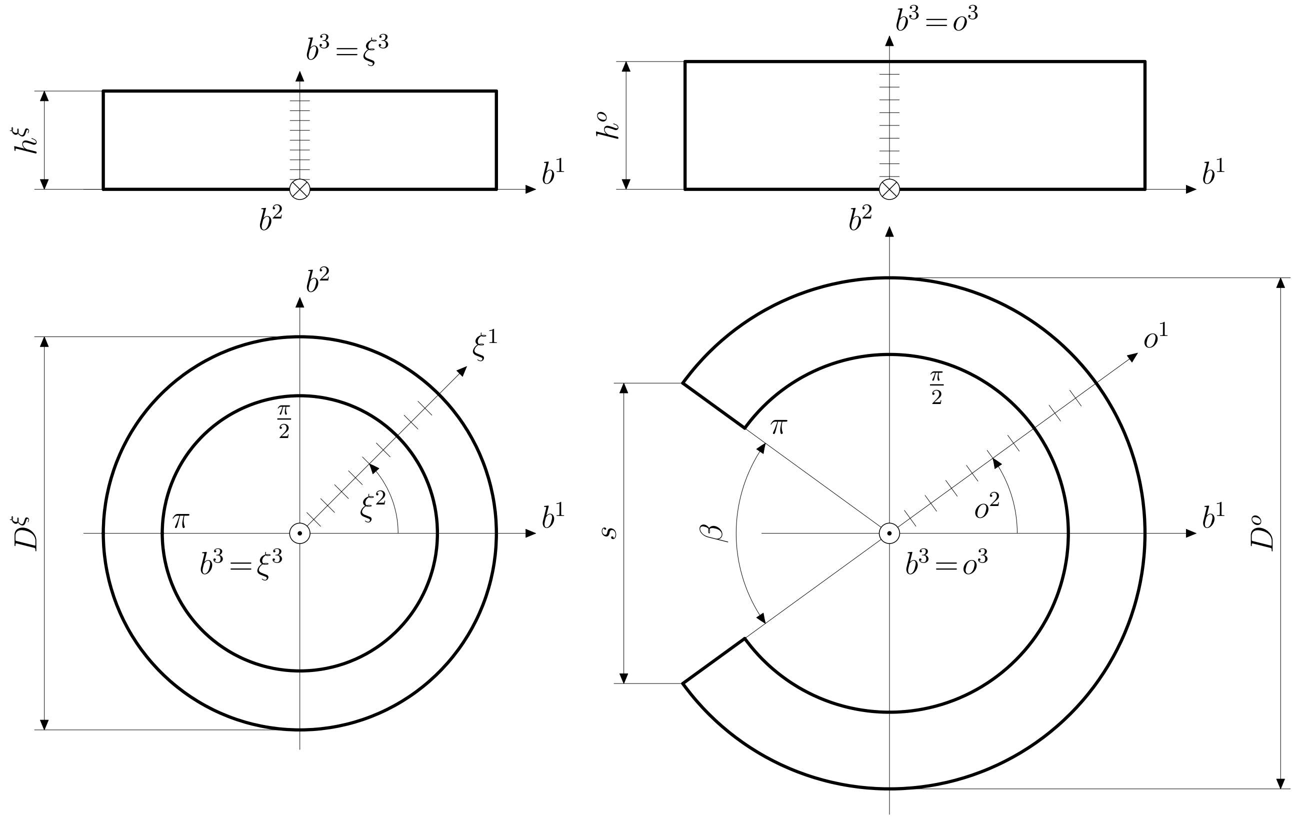

FIGURE 1. Coordinate systems of a prestressed blood vessel

Presuming the stress and consequently the strain is constant throughout the body we may expect the following relations between the coordinate systems:

$$\xi^1 = \delta o^1,$$

$$\xi^2 = \gamma o^2$$

and

$$\xi^3 = \eta o^3,$$

where

$$\delta = \frac{D^o}{D^\xi},\ \gamma = \frac{\pi - \frac{\beta}{2}}{\pi},\ \eta = \frac{h^o}{h^\xi},$$

with

$$\sin\frac{\beta}{2} = \frac{s}{D^o}.$$

As coordinate system b is the cartesian one and the relation between the coordinate systems b and ξ is

$$b^1 = \xi^1 \cos\xi^2,$$

$$b^2 = \xi^1 \sin\xi^2,$$

$$b^3 = \xi^3,$$

the metric of the cylindrical coordinate system ξ is

$$\overset{\xi}{g}_{ab} = \frac{\partial b^c}{\partial \xi^a}\frac{\partial b^d}{\partial \xi^b}\delta_{cd} = \begin{pmatrix} \cos\xi^2 & \sin\xi^2 & 0 \\ -\xi^1\sin\xi^2 & \xi^1\cos\xi^2 & 0 \\ 0 & 0 & 1 \end{pmatrix}\begin{pmatrix} \cos\xi^2 & -\xi^1\sin\xi^2 & 0 \\ \sin\xi^2 & \xi^1\cos\xi^2 & 0 \\ 0 & 0 & 1 \end{pmatrix} = \begin{pmatrix} 1 & 0 & 0 \\ 0 & (\xi^1)^2 & 0 \\ 0 & 0 & 1 \end{pmatrix}.$$

Since the relation between the coordinate systems ξ and o is known we can obtain the metric of the coordinate system o according the tensor transformation rule

$$\overset{o}{g}_{ab} = \frac{\partial \xi^c}{\partial o^a}\frac{\partial \xi^d}{\partial o^b}\overset{\xi}{g}_{cd} = \begin{pmatrix} \delta & 0 & 0 \\ 0 & \gamma & 0 \\ 0 & 0 & \eta \end{pmatrix}\begin{pmatrix} 1 & 0 & 0 \\ 0 & (\xi^1)^2 & 0 \\ 0 & 0 & 1 \end{pmatrix}\begin{pmatrix} \delta & 0 & 0 \\ 0 & \gamma & 0 \\ 0 & 0 & \eta \end{pmatrix} = \begin{pmatrix} \delta^2 & 0 & 0 \\ 0 & \gamma^2(\xi^1)^2 & 0 \\ 0 & 0 & \eta^2 \end{pmatrix}.$$

Once the metrics are known the Green-Lagrange-St. Venant strain in the coordinate system ξ is

$$\overset{\xi}{E}_{ab} = \frac{1}{2}\left(\overset{\xi}{g}_{ab} - \overset{o}{g}_{ab}\right) = \frac{1}{2}\begin{pmatrix} 1-\delta^2 & 0 & 0 \\ 0 & \left(1-\gamma^2\right)\left(\xi^1\right)^2 & 0 \\ 0 & 0 & 1-\eta^2 \end{pmatrix}.$$

4. Residual stress

Let us express the residual stress in the most simple case of the isotropic linear elastic (Hooke's) material. In the cylindrical coordinate system the 2nd Piola-Kirchhoff stress tensor is

$$\overset{\xi}{S}^{ab} = \overset{\xi}{E}^{abcd}\overset{\xi}{E}_{cd} = \left(\lambda\, \overset{\xi}{g}^{ab}\overset{\xi}{g}^{cd} + \mu\, \overset{\xi}{g}^{ac}\overset{\xi}{g}^{bd} + \mu\, \overset{\xi}{g}^{ad}\overset{\xi}{g}^{bc}\right)\frac{1}{2}\left(\overset{\xi}{g}_{cd} - \overset{o}{g}_{cd}\right),$$

where

$$\overset{\xi}{g}^{ab} = \left(\overset{\xi}{g}_{ab}\right)^{-2} = \begin{pmatrix} 1 & 0 & 0 \\ 0 & \left(\xi^1\right)^{-2} & 0 \\ 0 & 0 & 1 \end{pmatrix}.$$

After rearrangement of the terms in parenthesis we have

$$2\,\overset{\xi}{S}^{ab} = \overset{\xi}{g}^{ab}\left(\left(3-g^c_c\right)\lambda + 2\mu\right) - 2\mu\, \overset{\xi}{g}^{ac}\, g^b_c,$$

where

$$g^b_c = \overset{\xi}{g}^{bd}\overset{o}{g}_{dc} = \begin{pmatrix} 1 & 0 & 0 \\ 0 & \left(\xi^1\right)^{-2} & 0 \\ 0 & 0 & 1 \end{pmatrix}\begin{pmatrix} \delta^2 & 0 & 0 \\ 0 & \gamma^2\left(\xi^1\right)^2 & 0 \\ 0 & 0 & \eta^2 \end{pmatrix} = \begin{pmatrix} \delta^2 & 0 & 0 \\ 0 & \gamma^2 & 0 \\ 0 & 0 & \eta^2 \end{pmatrix}$$

and

$$g^c_c = \delta^2 + \gamma^2 + \eta^2.$$

Thus

$$2\,\overset{\xi}{S}^{ab} = \begin{pmatrix} 1 & 0 & 0 \\ 0 & \left(\xi^1\right)^{-2} & 0 \\ 0 & 0 & 1 \end{pmatrix}\left(\left(3-g^c_c\right)\lambda + 2\mu\right) - 2\mu\begin{pmatrix} 1 & 0 & 0 \\ 0 & \left(\xi^1\right)^{-2} & 0 \\ 0 & 0 & 1 \end{pmatrix}\begin{pmatrix} \delta^2 & 0 & 0 \\ 0 & \gamma^2 & 0 \\ 0 & 0 & \eta^2 \end{pmatrix}$$

and

$$2\,\overset{\xi}{S}^{ab} = \begin{pmatrix} \left(3-g^c_c\right)\lambda + 2\mu\left(1-\delta^2\right) & 0 & 0 \\ 0 & \left(\xi^1\right)^{-2}\left(\left(3-g^c_c\right)\lambda + 2\mu\left(1-\gamma^2\right)\right) & 0 \\ 0 & 0 & \left(3-g^c_c\right)\lambda + 2\mu\left(1-\eta^2\right) \end{pmatrix}.$$

In the coordinate system normal-tangent-axis, t^a, the entries of the stress tensor would have physical units. The transformation from the ξ coordinate system into the coordinate system normal-tangent-axis can be obtained utilising the fact that these coordinate systems are aligned, the transformation of metric is

$$\overset{\xi}{g}_{ab} = \frac{\partial t^c}{\partial \xi^a}\frac{\partial t^d}{\partial \xi^b}\,\overset{t}{g}_{cd}$$

and the latter is cartesian one, which implies

$$\frac{\partial t^a}{\partial \xi^b} = \begin{pmatrix} 1 & 0 & 0 \\ 0 & \xi^1 & 0 \\ 0 & 0 & 1 \end{pmatrix}.$$

Consequently, the stress tensor in the appropriate cartesian coordinate system is

$$\overset{t}{S}^{ab} = \frac{\partial t^a}{\partial \xi^c}\frac{\partial t^b}{\partial \xi^d}\,\overset{\xi}{S}^{cd},$$

i.e.,

$$\overset{t}{S}^{ab} = \frac{1}{2}\begin{pmatrix} \left(3-g^c_c\right)\lambda + 2\mu\left(1-\delta^2\right) & 0 & 0 \\ 0 & \left(3-g^c_c\right)\lambda + 2\mu\left(1-\gamma^2\right) & 0 \\ 0 & 0 & \left(3-g^c_c\right)\lambda + 2\mu\left(1-\eta^2\right) \end{pmatrix}.$$

CHAPTER 6

Shape analysis of lipid membranes with intrinsic (anisotropic) curvature – statistical mechanical approach

1. Cell membrane

The cell membrane (also called the plasma membrane, plasmalemma) is a semipermeable lipid bilayer found in all cells.

The cell membrane surrounds the cytoplasm of a cell and physically separates the intracellular components from the extracellular environment, thereby serving a function similar to that of skin. The cell wall plays mostly a mechanical support role rather than a role as a selective boundary. The cell membrane also plays a role in anchoring the cytoskeleton to provide shape to the cell, and in attaching to the extracellular matrix to help group cells together in the formation of tissues.

The barrier is selectively permeable and able to regulate what enters and exits the cell, thus facilitating the transport of materials. The movement of substances across the membrane can be either passive, occurring without the input of cellular energy, or active, requiring the cell to expend energy in moving it. The membrane also maintains the cell potential.

Specific proteins embedded in the cell membrane can act as molecular signals that allow cells to communicate with each other. Protein receptors are found ubiquitously and function to receive signals from both the environment and other cells. These signals are transduced into a form that the cell can use to directly effect a response. Other proteins on the surface of the cell membrane serve as markers that identify a cell to other cells. The interaction of these markers with their respective receptors forms the basis of cell-cell interaction in the immune system.

The cell membrane consists of a thin layer of amphipathic[1] lipids which spontaneously arrange so that the hydrophobic tail regions are shielded from the surrounding polar fluid, causing the more hydrophilic head regions to associate with the cytosolic and extracellular faces of the resulting bilayer. This forms a continuous, spherical lipid bilayer containing the cellular components approximately 7 nm thick, barely discernible with a transmission electron microscope.

A lipid bilayer or bilayer lipid membrane (BLM) is a membrane or zone of a membrane composed of lipid molecules (usually phospholipids, see Figs. 1 and 2). The lipid bilayer is a critical component of all biological membranes, including cell membranes, and so is absolutely essential for all known life on Earth. Its essential structure was discovered in 1925 by two Dutch physicians, E. Gorter and F. Grendel.

Support for the existence of a lipid bilayer in cell membranes came with the discovery by Alec Bangham in 1965 that phospholipids, when introduced into an aqueous environment, spontaneously form liposomes. These are small balloons of lipid bilayer which can entrap polar molecules inside them. The major force driving the formation of lipid bilayers is the hydrophobic interaction between the tails and their repulsion by water. Within the interior of the membrane the hydrocarbon tails are arranged, on average, perpendicular to the plane of the membrane. The properties of the bilayer are influenced by a variety of factors, including the lipid composition, temperature and membrane pressure.

The widely accepted model for cell membranes is the fluid mosaic model proposed by Singer and Nicolson in 1972.[2] In this model, the cell membrane is considered as a lipid bilayer where the lipid molecules can move freely in the membrane surface like fluid, while the proteins are embedded in the lipid bilayer. Some proteins are called integral membrane proteins because they traverse entirely in the lipid bilayer and play the role of information and matter communications between the interior of the cell and its outer environment. The others are called peripheral membrane proteins because they are partially embedded in the bilayer and accomplish the other biological functions.

The first step to study the elasticity of cell membranes is to study lipid bilayers. Usually, the thickness of the lipid bilayer is much smaller than the scale of the whole lipid bilayer. It is reasonable to describe

[1]From the Greek $\alpha\mu\varphi\iota\varsigma$: both and $\varphi\iota\lambda\acute{\iota}\alpha$: love, friendship.

[2][**SN72**]

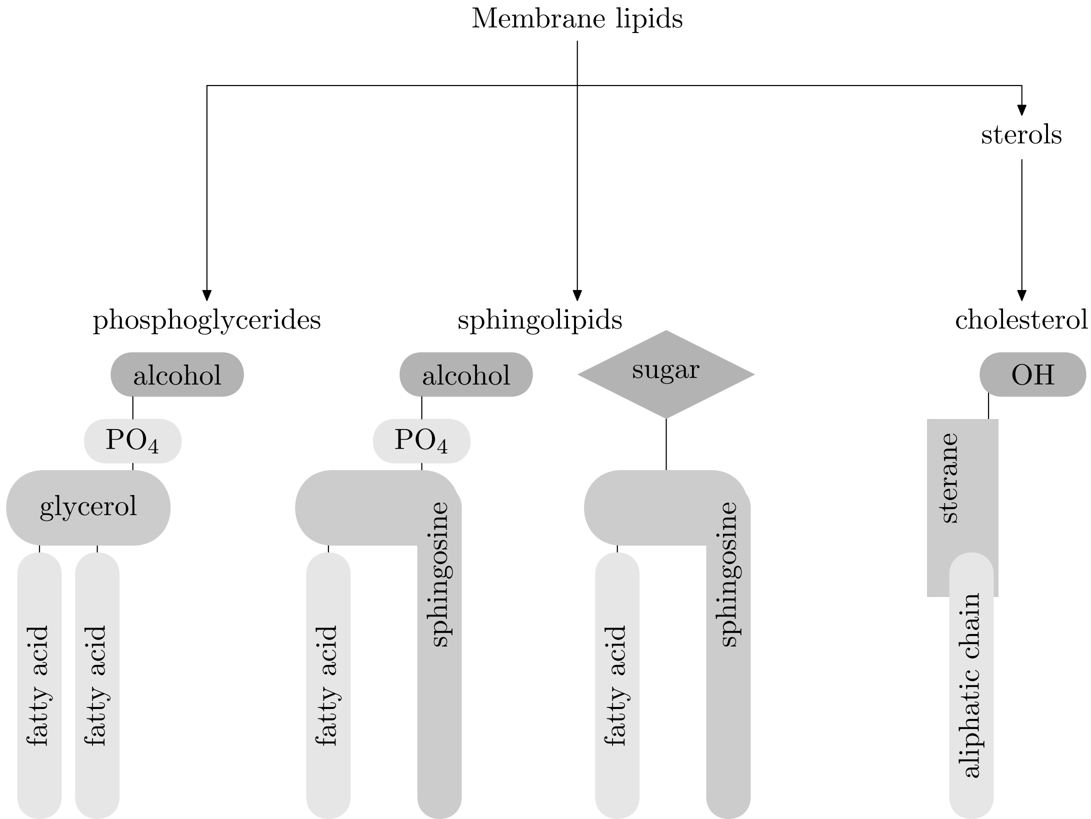

FIGURE 1. Membrane lipids

the lipid bilayer by a mathematical surface. In 1973, Helfrich[3] proposed the curvature energy per unit area of the bilayer

$$f = \frac{1}{2}k_b(c_1 + c_2 - C_o)^2 + k_g c_1 c_2,$$

where k_b and k_g are elastic constants, c_a (a=1,2) the main curvatures of a mathematical surface representing the bilayer and C_o is a phenomenological parameter called spontaneous curvature. The total free energy, known as Helfrich energy, is

$$F = \int_A f \mathrm{d}A.$$

2. Intrinsic curvature, anisotropic inclusions and embedded molecules

The system in this chapter analyzed is composed of a continuum of phospholipid molecules into which anisotropic laterally mobile molecules are embedded. It can be expected that the embedded molecules may considerably influence the membrane free energy and also the equilibrium vesicle shape (Cf. Fig. 3). The effect of the embedded molecules on the vesicle shape was also observed in experiments.[4]

The term inclusion is generally used for an entity consisting of the embedded molecule and some lipids that are significantly distorted due to the presence of the embedded molecule.

It is imagined that there exists a local membrane shape (and orientation) which fits the inclusion. We refer to this shape as to the intrinsic shape of the inclusion. The intrinsic shape is represented with the intrinsic curvature tensor B^a_b in a way described thereinafter.

3. Curvature, curvature tensor and metric

For a plane curve, the curvature at a given point has a magnitude equal to the reciprocal of the radius of an osculating circle and is a vector pointing in the direction of that circle's center. The smaller the radius r of the osculating circle, the larger the magnitude of the curvature ($1/r$) will be. A straight line has curvature 0 everywhere; a circle of radius r has curvature $1/r$ everywhere.

[3][**Hel73**]
[4][**FKIB+03**]

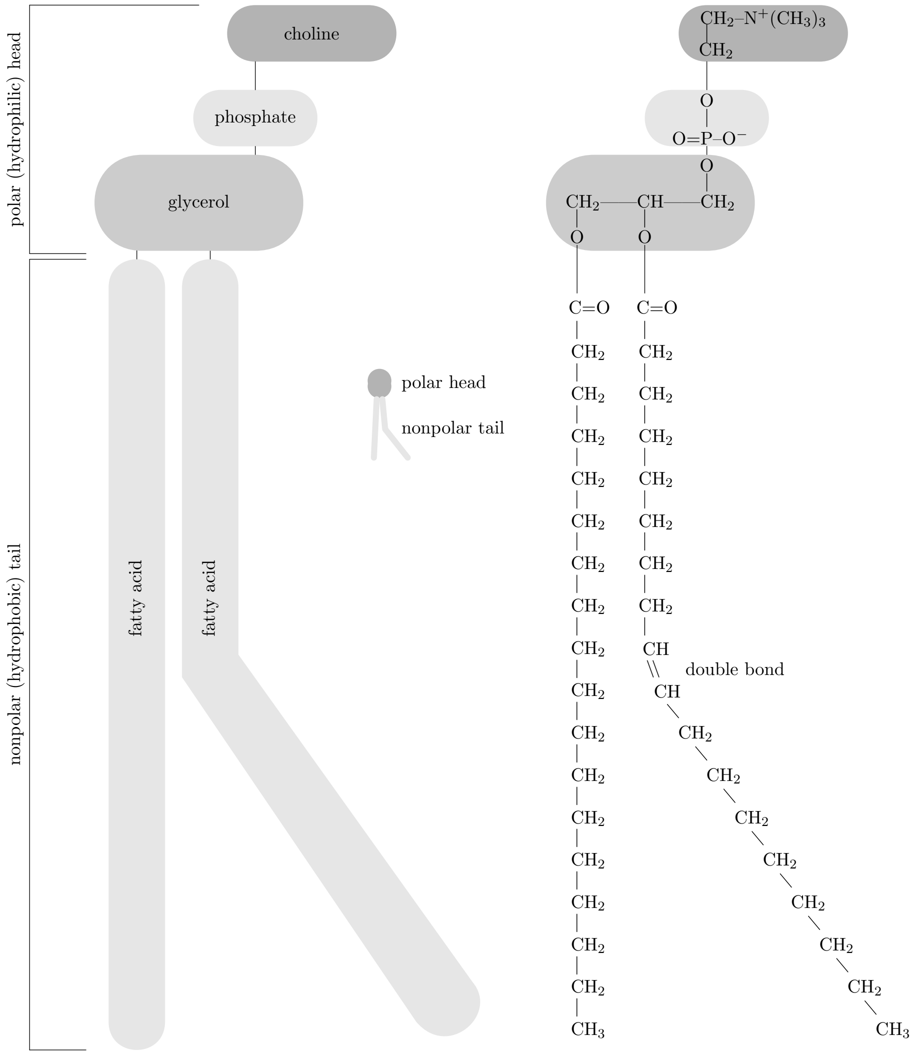

FIGURE 2. Phosphatidylcholine – phospholipid molecule

Osculating circle of a curve at a point is a circle which 1) touches the curve at that point, 2) has its unit tangent vector equal to the unit tangent of the curve at that point and 3) has its derivative of unit tangent (with respect to arc length) equal to that of the curve at that point; note, the circle and the curve must be parameterised by arc length.

For a two-dimensional surface embedded in R^3, consider the intersection of the surface with a plane containing the normal vector and one of the tangent vectors at a particular point. This intersection is a plane curve and has a curvature. This is the normal curvature, and it varies with the choice of the tangent vector. The maximum and minimum values of the normal curvature at a point are called the principal curvatures, c_1 and c_2, and the directions of the corresponding tangent vectors are called principal directions.

The Gaussian curvature, named after Carl Friedrich Gauss, is equal to the product of the principal curvatures, $c_1 c_2$. It has the dimension of $1/\text{length}^2$ and is positive for spheres, negative for one-sheet hyperboloids and zero for planes. It determines whether a surface is locally convex (when it is positive) or locally saddle (when it is negative).

The above definition of Gaussian curvature is extrinsic in that it uses the surface's embedding in R^3, normal vectors, external planes etc. Gaussian curvature is however in fact an intrinsic property of the surface, meaning it does not depend on the particular embedding of the surface; intuitively, this means that ants living on the surface could determine the Gaussian curvature. Formally, Gaussian curvature only depends on the Riemannian metric of the surface.

The mean curvature is equal to the sum of the principal curvatures over 2,

$$h = \frac{c_1 + c_2}{2}.$$

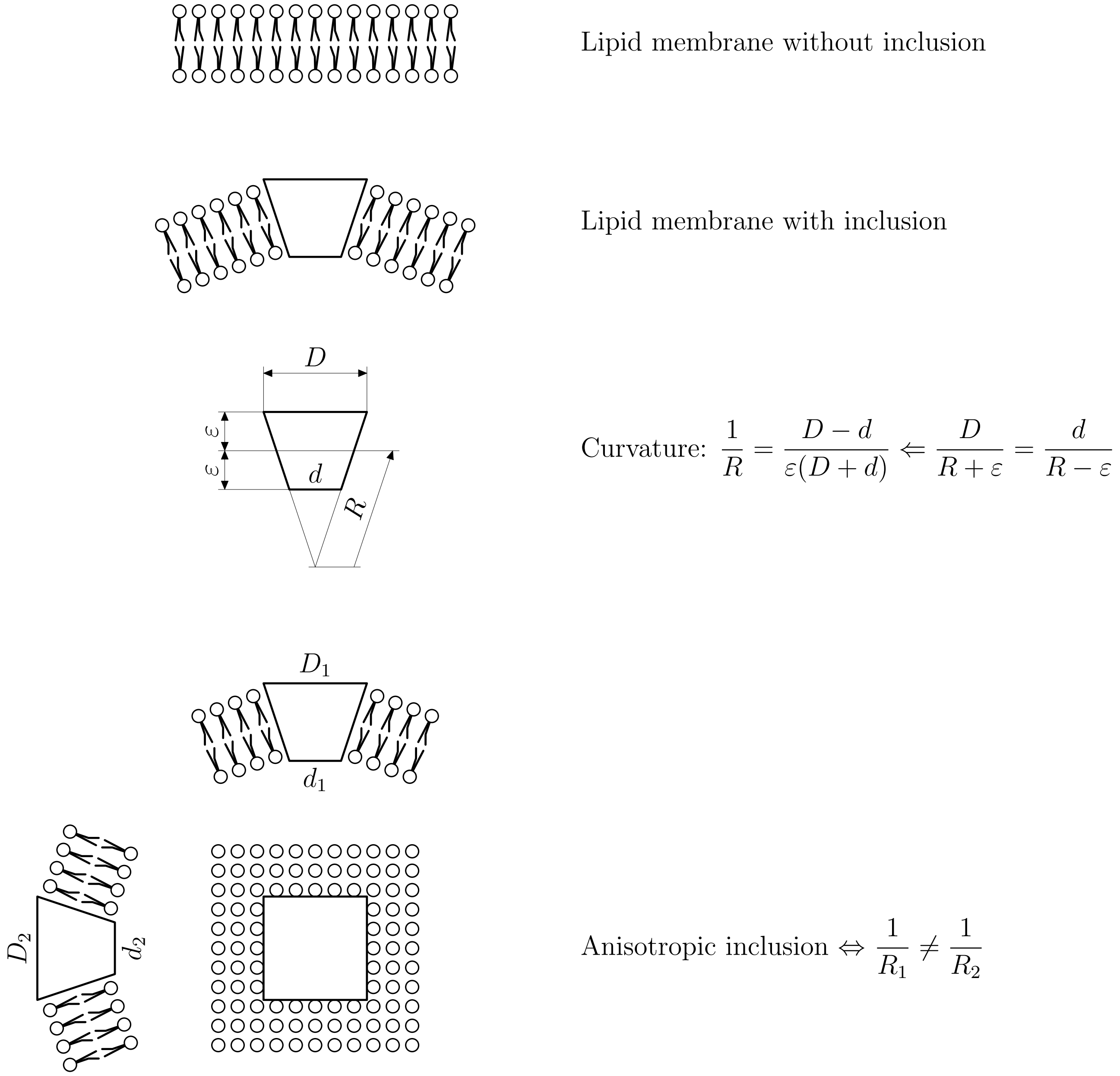

FIGURE 3. Isotropic vs. anisotropic inclusions

It has the dimension of 1/length. Unlike Gaussian curvature, the mean curvature is extrinsic and depends on the embedding, for instance, a cylinder and a plane are locally isometric but the mean curvature of a plane is zero while that of a cylinder is nonzero.

Let us imagine a two-dimensional object (biological membrane) located in the three-dimensional space. Introducing the curvilinear coordinates (u_1, u_2) lying on the surface of the membrane, position of any point on the membrane can be described as:

$$\boldsymbol{r} = \boldsymbol{r}(u^1, u^2) = (x^1(u^1, u^2), x^2(u^1, u^2), x^3(u^1, u^2)), \tag{26}$$

where x^a are cartesian coordinates in the three-dimensional space. At any point of the surface we may define two tangent vectors $\boldsymbol{r}_1$ and $\boldsymbol{r}_2$

$$\boldsymbol{r}_1 = \frac{\partial \boldsymbol{r}}{\partial u^1} = \left(\frac{\partial x^1}{\partial u^1}, \frac{\partial x^2}{\partial u^1}, \frac{\partial x^3}{\partial u^1}\right), \tag{27}$$

$$\boldsymbol{r}_2 = \frac{\partial \boldsymbol{r}}{\partial u^2} = \left(\frac{\partial x^1}{\partial u^2}, \frac{\partial x^2}{\partial u^2}, \frac{\partial x^3}{\partial u^2}\right) \tag{28}$$

and a unit normal vector

$$\boldsymbol{n} = \pm \frac{\boldsymbol{r}_1 \times \boldsymbol{r}_2}{|\boldsymbol{r}_1 \times \boldsymbol{r}_2|}. \tag{29}$$

Using the expression for metric tensor $a_{\alpha\beta}$ $(\alpha, \beta = 1, 2)$ from the differential geometry [**LR89, SS78**],

$$a_{\alpha\beta} = \boldsymbol{r}_\alpha \cdot \boldsymbol{r}_\beta, \tag{30}$$

the element area can be expressed as

$$\mathrm{d}A = |a_{\alpha\beta}|^{\frac{1}{2}} \mathrm{d}u^1 \mathrm{d}u^2. \tag{31}$$

The curvature tensor[5]

$$b^\alpha_\beta = -a^{\alpha\gamma} \frac{\partial \boldsymbol{n}}{\partial u^\gamma} \cdot \boldsymbol{r}_\beta = a^{\alpha\gamma} \partial_\gamma \partial_\beta \boldsymbol{r} \cdot \boldsymbol{n}, \tag{32}$$

where $a^{\alpha\gamma} = (a_{\alpha\gamma})^{-1}$. The main curvatures c_1, c_2 may be determined as the eigenvalues of the curvature tensor b^α_β. That means that in the coordinate system coinciding with the principal directions, the curvature tensor is diagonal:

$$b^\alpha_\beta = \begin{pmatrix} c_1 & 0 \\ 0 & c_2 \end{pmatrix}.$$

4. Koiter's energy for an elastic shell and Helfrich energy for lipid bilayer membrane

At the case of a shell, *i.e.*, three dimensional object with one dimension (thickness, 2ε) approximate zero ($2\varepsilon \to 0$) the three dimensional elastic energy may be expressed in the form of Koiter's energy for an elastic shell

$$A_a = \frac{1}{2} \int_\omega 2a \,\mathrm{d}A$$

where[6]

$$2a = \frac{\varepsilon}{4} a^{\alpha\beta\gamma\delta} \left(a_{\alpha\beta} - \overset{o}{a}_{\alpha\beta} \right) \left(a_{\gamma\delta} - \overset{o}{a}_{\gamma\delta} \right) + \frac{\varepsilon^3}{3} a^{\alpha\beta\gamma\delta} \left(b_{\alpha\beta} - \overset{o}{b}_{\alpha\beta} \right) \left(b_{\gamma\delta} - \overset{o}{b}_{\gamma\delta} \right),$$

$$a^{\alpha\beta\gamma\delta} = \tilde{\lambda} a^{\alpha\beta} a^{\gamma\delta} + \tilde{\mu} a^{\alpha\gamma} a^{\beta\delta} + \tilde{\mu} a^{\alpha\delta} a^{\gamma\beta}, \tag{33}$$

and $\overset{o}{b}_{\alpha\beta}$ and $\overset{o}{a}_{\alpha\beta}$ represent the zero energy (natural) state of the shell, *i.e.*, in our setting,

$$\overset{o}{b}_{\alpha\beta} = B_{\alpha\beta} \quad \text{and} \quad \overset{o}{a}_{\alpha\beta} = A_{\alpha\beta},$$

where $A_{\alpha\beta}$ is the metric of the bilayer without inclusions and B^β_α the curvature tensor that fits the inclusions.

The lipid layers represent really interesting material that in bending exhibits, astonishingly, linear elastic behaviour while in the surface the lipids can move freely, only with the constraint that the area of the surface is covered with a constant number of lipids, *i.e.*, the area, A, of the layer is constant. Consequently, the above formulation of the problem

$$\min_{a_{\alpha\beta}, b^\beta_\alpha} A_a$$

is, possibly, replaced with the problem

$$\min_{a_{\alpha\beta}, b^\beta_\alpha \in B} F_a$$

where

$$F_a = \int_A f \,\mathrm{d}A$$

with

$$f = \frac{1}{6} \varepsilon^3 a^{\alpha\beta\gamma\delta} m_{\alpha\beta} m_{\gamma\delta}, \tag{34}$$

and

$$m_{\alpha\beta} = b_{\alpha\beta} - \overset{o}{b}_{\alpha\beta} = m_{\beta\alpha},$$

[5] [**Cia05**]
[6] $(\alpha\beta\gamma\delta = 1, 2)$

and where

$$B = \left\{ a_{\alpha\beta}, b^{\beta}_{\alpha} : A = \text{constant} \right\}.$$

Now, (33) in (34) leads to

$$f = \frac{1}{6}\varepsilon^3 \left(\tilde{\lambda} m^{\alpha}_{\alpha} m^{\beta}_{\beta} + 2\tilde{\mu} m^{\alpha}_{\beta} m^{\beta}_{\alpha} \right)$$

and substitution

$$k_1 = (\tilde{\lambda} + 2\tilde{\mu})\frac{\varepsilon^3}{6}, \quad k_2 = 2\tilde{\mu}\frac{\varepsilon^3}{6}$$

leads to

$$f = k_1 m^{\alpha}_{\alpha} m^{\beta}_{\beta} - k_2 \left(m^{\alpha}_{\alpha} m^{\beta}_{\beta} - m^{\alpha}_{\beta} m^{\beta}_{\alpha} \right) \tag{35}$$

what can be written like

$$f = k_1 \mathrm{Tr}(m)^2 - 2k_2 \det(m).$$

5. Energy per lipid

Let us look at the elastic energy of a single lipid

$$E = f A_{\text{lipid}} = \tilde{k}_1 m^{\alpha}_{\alpha} m^{\beta}_{\beta} - \tilde{k}_2 \left(m^{\alpha}_{\alpha} m^{\beta}_{\beta} - m^{\alpha}_{\beta} \right), \tag{36}$$

where

$$\tilde{k}_i = k_i A_{\text{lipid}} \quad (i = 1, 2).$$

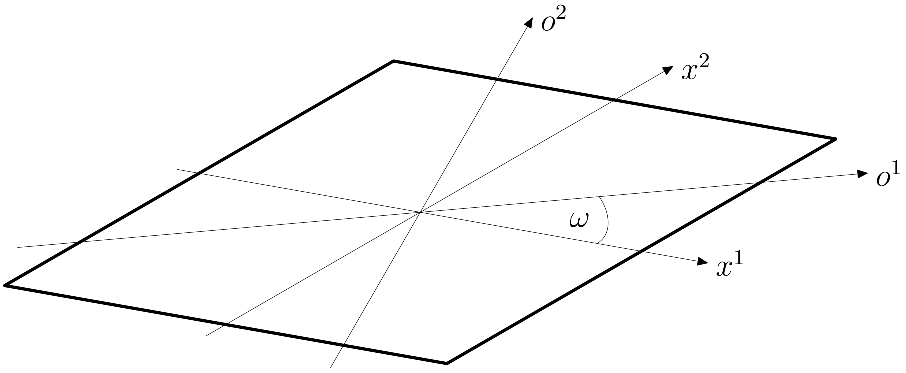

FIGURE 4. Main cartesian coordinate system of the membrane and inclusion, respectively

At the little area of a single lipid it is possible to use the local Cartesian coordinate system, x^a, aligned with the principal direction of the real curvature of the membrane or the local Cartesian coordinate system, o^a, aligned with the principal direction of the intrinsic curvature of the membrane given by the principal direction of the curvature of the inclusion. The curvature tensor of the lipid membrane in coordinate system, x^a, is diagonal with principal curvatures on the diagonal:

$$b^{\alpha}_{\beta} = \begin{pmatrix} c_1 & 0 \\ 0 & c_2 \end{pmatrix},$$

while the intrinsic curvature tensor is diagonal in the coordinate system, o^a:

$$B^{\alpha}_{\beta} = \begin{pmatrix} C_1 & 0 \\ 0 & C_2 \end{pmatrix}.$$

The coordinate systems x^a and o^a are not, generally, aligned but rotated with an angle ω, *Cf.* Fig. 4.

As

$$\overset{x}{b}{}^{\gamma}_{\delta} = \frac{\partial x^{\gamma}}{\partial o^{\alpha}} \frac{\partial o^{\beta}}{\partial x^{\delta}} \overset{o}{b}{}^{\alpha}_{\beta},$$

with

$$\frac{\partial x^{\gamma}}{\partial o^{\alpha}} = \begin{pmatrix} \cos\omega & -\sin\omega \\ \sin\omega & \cos\omega \end{pmatrix}$$

and

$$\frac{\partial o^{\beta}}{\partial x^{\delta}} = \begin{pmatrix} \cos\omega & \sin\omega \\ -\sin\omega & \cos\omega \end{pmatrix},$$

we can write, in the local Cartesian coordinates x^a,

$$m^{\alpha}_{\beta} = \begin{pmatrix} c_1 & 0 \\ 0 & c_2 \end{pmatrix} - \begin{pmatrix} \cos\omega & -\sin\omega \\ \sin\omega & \cos\omega \end{pmatrix} \begin{pmatrix} C_1 & 0 \\ 0 & C_2 \end{pmatrix} \begin{pmatrix} \cos\omega & \sin\omega \\ -\sin\omega & \cos\omega \end{pmatrix}.$$

Using the last expression in (36) together with

$$\sin^2\omega = \frac{1}{2}(1-\cos 2\omega), \quad \cos^2\omega = \frac{1}{2}(1+\cos 2\omega)$$

leads onwards to the expression of energy per single lipid in the form

(37) $$E = a(h-H)^2 + b(d^2 - 2dD\cos 2\omega + D^2)$$

where mean curvature

$$h = \frac{c_1+c_2}{2},$$

intrinsic mean curvature

$$H = \frac{C_1+C_2}{2},$$

curvature deviator

$$d = \frac{|c_1-c_2|}{2},$$

intrinsic curvature deviator

$$D = \frac{|C_1-C_2|}{2},$$

$$a = \frac{\xi}{2} = \tilde{k}_1 - 2\tilde{k}_2$$

and

$$b = \frac{\xi+\xi^*}{4} = 2\tilde{k}_2.$$

6. Statistical thermodynamics approach

6.1. Helmholtz free energy of a patch of lipid layer. For the sake of simplicity, let us consider 2 state model, *i.e.*, only two energetic levels: The minimum energy level ($\cos 2\omega = 1$):

$$E_{\min} = a(h-H)^2 + b(d^2 - 2dD + D^2)$$

and the maximum energy level ($\cos 2\omega = -1$):

$$E_{\max} = a(h-H)^2 + b(d^2 + 2dD + D^2).$$

Consider a patch of lipid layer consisting of M lipid molecules, N of this number in the state of maximal energy $E_{\max}$ and $M-N$ in the state of minimal energy $E_{\min}$. The energy of the patch is then

$$E = NE_{\max} + (M-N)E_{\min}$$

or (in the units where $kT = 1$)

$$\frac{E}{kT} = \frac{Ma}{kT}(h-H)^2 + \frac{Mb}{kT}(d^2+D^2) + \frac{b(2N-M)}{kT}2dD.$$

The number of states of the patch is

$$\sum_{N=0}^{M} \frac{M!}{N!(M-N)!}$$

and, consequently, the partition function[7]

$$Q = \sum_{N=0}^{M} \frac{M!}{N!(M-N)!} e^{-\frac{E}{kT}}$$

or

$$Q = e^{-\frac{Ma}{kT}(h-H)^2 - \frac{Mb}{kT}(d^2+D^2)} \sum_{N=0}^{M} \frac{M!}{N!(M-N)!} e^{-\frac{b(2N-M)}{kT}2dD}.$$

---

[7] [**Hil86**]

Using Newton binomial formula

$$(x+y)^M = \sum_{N=0}^{M} \begin{pmatrix} M \\ N \end{pmatrix} x^{M-N} y^N, \quad \begin{pmatrix} M \\ N \end{pmatrix} = \frac{M!}{N!(M-N)!}$$

and

$$\cosh x = \frac{e^x + e^{-x}}{2},$$

the partition function receive the form

$$Q = \left(2e^{-\frac{a}{kT}(h-H)^2 - \frac{b}{kT}(d^2+D^2)} \cosh\left(\frac{b}{kT} 2dD\right)\right)^M .$$

Helmholz free energy of the patch is then[8]

$$F_p = -kT \ln Q$$

or

$$F_p = -kTM \left(\ln 2 - \frac{a}{kT}(h-H)^2 - \frac{b}{kT}(d^2+D^2) + \ln\cosh\left(\frac{b}{kT}2dD\right)\right).$$

6.2. Helmholz free energy of the lipid bilayer. To obtain Helmholz free energy of the lipid bilayer we need to integrate over both outer and inner layer (definition of the sign of curvatures are, as well as the sign of the intrinsic curvatures, changed with the change of the layer):

$$F = \int\limits_{A_{\text{outer}}} \frac{1}{MA_{\text{lipid,outer}}} F_p \, \mathrm{d}A + \int\limits_{A_{\text{inner}}} \frac{1}{MA_{\text{lipid,inner}}} F_p \, \mathrm{d}A.$$

If $A_{\text{lipid,outer}} = A_{\text{lipid,inner}} = A_{\text{lipid}}, A_{\text{outer}} = A_{\text{inner}} = A$ and $a = b$, *i.e.*, $\xi = 2a$, then

$$F = \frac{\xi}{A_{\text{lipid}}} \int\limits_A \left((h-H)^2 + (d^2+D^2)\right) \mathrm{d}A - \frac{2kT}{A_{\text{lipid}}} \int\limits_A \ln\left(2\cosh\left(\frac{\xi}{kT} dD\right)\right) \mathrm{d}A. \tag{38}$$

7. Minimization of Helmholtz free energy of an axisymetric closed lipid bilayer

7.1. Analytical expression. In the following we shall assume that the surface is axisymmetric. In the case of rotational symmetry with respect to the axis z, the curvilinear coordinates $u^1 = \psi$ and $u^2 = \varphi$ are introduced (Fig. 5). The angle φ defines angle of the rotation around the symmetry axis while the angle ψ corresponds to a site of the meridian. Then

$$\boldsymbol{r} = \boldsymbol{r}(\psi) = \begin{pmatrix} p(\psi)\cos\psi\cos\varphi \\ p(\psi)\cos\psi\sin\varphi \\ p(\psi)\sin\psi \end{pmatrix} \tag{39}$$

where $p(\psi)$ is the distance between the center of coordinates and a certain point on the surface given via the angles ψ and φ.

According to Eq. (30), the metric tensor

$$a_{\alpha\beta} = \boldsymbol{r}_\alpha \cdot \boldsymbol{r}_\beta = \begin{pmatrix} \boldsymbol{r}_{,\psi}\cdot\boldsymbol{r}_{,\psi} & \boldsymbol{r}_{,\psi}\cdot\boldsymbol{r}_{,\varphi} \\ \boldsymbol{r}_{,\varphi}\cdot\boldsymbol{r}_{,\psi} & \boldsymbol{r}_{,\varphi}\cdot\boldsymbol{r}_{,\varphi} \end{pmatrix} = \begin{pmatrix} p^2 + p_{,\psi}^2 & 0 \\ 0 & p^2\cos^2\psi \end{pmatrix}.$$

For element area (31) it holds

$$\mathrm{d}A = |a_{\alpha\beta}|^{\frac{1}{2}} \mathrm{d}\psi \mathrm{d}\varphi = p\cos\psi \sqrt{p^2 + p_{,\psi}^2}\, \mathrm{d}\psi\mathrm{d}\varphi$$

and, utilizing axisymmetry,

$$\mathrm{d}A = 2\pi p\cos\psi\sqrt{p^2+p_{,\psi}^2}\,\mathrm{d}\psi.$$

For volume element then

$$\mathrm{d}V = \pi(p\cos\psi)^2 \frac{\mathrm{d}z}{\mathrm{d}\psi}\mathrm{d}\psi = \pi(p\cos\psi)^2\left(p_{,\psi}\sin\psi + p\cos\psi\right)\mathrm{d}\psi.$$

[8][**Hil86**]

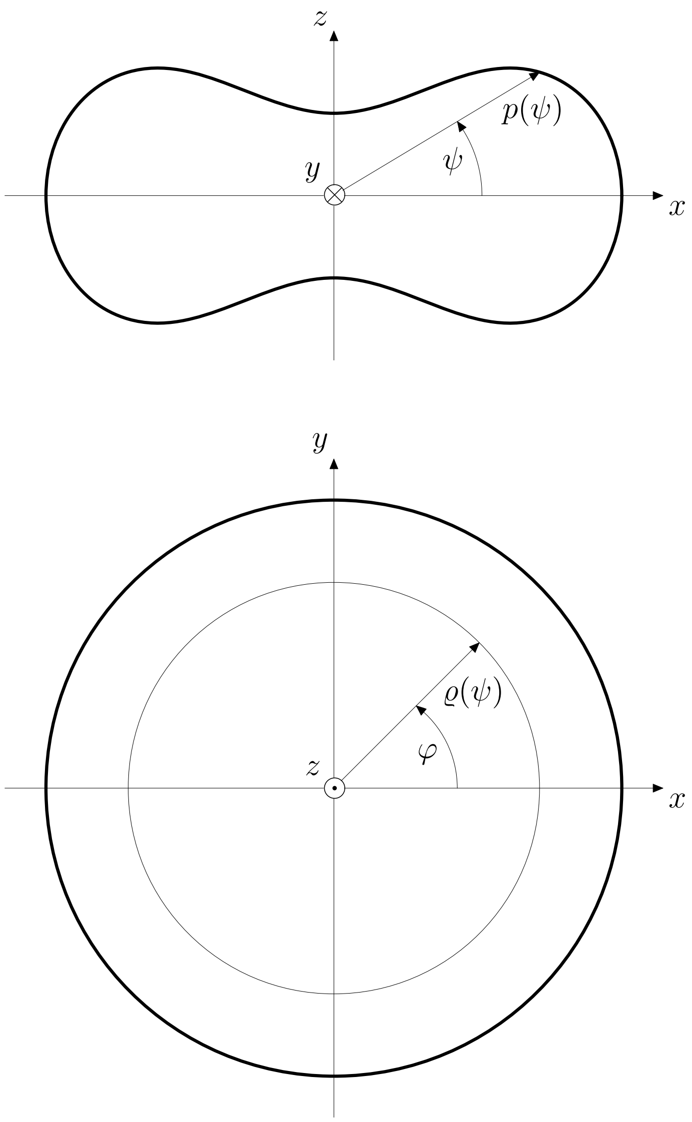

FIGURE 5. The axisymmetric surface

Curvature tensor (32), utilizing (29)

$$\boldsymbol{n} = \frac{-1}{\sqrt{p^2 + p_{,\psi}^2}} \begin{pmatrix} p\cos\psi\cos\varphi + p_{,\psi}\sin\psi\cos\varphi \\ p\cos\psi\sin\varphi + p_{,\psi}\sin\psi\sin\varphi \\ p\sin\psi - p_{,\psi}\cos\psi \end{pmatrix}$$

and

$$a^{\alpha\beta} = (a_{\alpha\beta})^{-1} = \begin{pmatrix} \frac{1}{p^2+p_{,\psi}^2} & 0 \\ 0 & \frac{1}{p^2\cos^2\psi} \end{pmatrix},$$

reads

$$b_{\alpha\beta} = \frac{1}{\sqrt{p^2 + p_{,\psi}^2}} \begin{pmatrix} 2p_{,\psi}^2 + p^2 - pp_{,\psi\psi} & 0 \\ 0 & p^2\cos^2\psi + pp_{,\psi}\cos\psi\sin\psi \end{pmatrix}$$

and

$$b_\beta^\alpha = a^{\alpha\beta}b_{\alpha\beta} = \frac{1}{\sqrt{p^2 + p_{,\psi}^2}} \begin{pmatrix} 1 - \frac{p_{,\psi}^2 - pp_{,\psi\psi}}{p^2+p_{,\psi}^2} & 0 \\ 0 & 1 + \frac{p_{,\psi}}{p}\tan\psi \end{pmatrix}.$$

Hence, the mean curvature

$$h = \frac{1}{2\sqrt{p^2 + p_{,\psi}^2}} \left(2 - \frac{p_{,\psi}^2 - pp_{,\psi\psi}}{p^2 + p_{,\psi}^2} + \frac{p_{,\psi}}{p}\tan\psi\right)$$

and curvature deviator

$$d = \frac{1}{2\sqrt{p^2+p_{,\psi}^2}} \left| \frac{p_{,\psi}^2 - pp_{,\psi\psi}}{p^2+p_{,\psi}^2} + \frac{p_{,\psi}}{p}\tan\psi \right|.$$

Consequently, we arrive at the following formulation of the constrained minimization problem for the Helmholz free energy of an axisymmetric lipid bilayer:

$$\min_{\varrho} F,$$

where

$$F = 2\frac{2\pi\xi}{A_{\text{lipid}}}\int_0^{\frac{\pi}{2}} \left((h-H)^2 + (d^2+D^2) - \frac{2kT}{\xi}\cosh\left(\frac{\xi}{kT}dD\right) - \frac{2kT}{\xi}\ln 2 \right) \mathrm{d}\psi,$$

$$h = \frac{1}{2\sqrt{p^2+p_{,\psi}^2}} \left(2 - \frac{p_{,\psi}^2 - pp_{,\psi\psi}}{p^2+p_{,\psi}^2} + \frac{p_{,\psi}}{p}\tan\psi \right)$$

and curvature deviator

$$d = \frac{1}{2\sqrt{p^2+p_{,\psi}^2}} \left| \frac{p_{,\psi}^2 - pp_{,\psi\psi}}{p^2+p_{,\psi}^2} + \frac{p_{,\psi}}{p}\tan\psi \right|.$$

with constraints

1) $$2\int_0^{\frac{\pi}{2}} 2\pi p\cos\psi\sqrt{p^2+p_{,\psi}^2}\mathrm{d}\psi = A$$

2) $$2\int_0^{\frac{\pi}{2}} \pi(p\cos\psi)^2\left(p_{,\psi}\sin\psi + p\cos\psi\right)\mathrm{d}\psi = V$$

3) $$p \geq 0.$$

The constraint 1) takes into account the constant area of the given surface; the constraint 2) the given volume enclosed within the bilayer; and the 3) is the geometrical constrain.

Let us approximate the function $p(\psi)$ with a Fourier series fulfilling the boundary condition

$$p_{,\psi}(0) = 0 \;\text{ and }\; p_{,\psi}(\frac{\pi}{2}) = 0.$$

The appropriate choice might be the trigonometric series

$$p = \sum_{k=0}^{K} a_k \cos 2k\psi.$$

The constraint minimum of the function $F(a_k)$, we try and find applying the genetic algorithm[9] on the minimization of the penalized function

$$P_k = F + M_k\left(\left| 2\int_0^{\frac{\pi}{2}} 2\pi p\cos\psi\sqrt{p^2+p_{,\psi}^2}\mathrm{d}\psi - A \right| + \left| 2\int_0^{\frac{\pi}{2}} \pi(p\cos\psi)^2\left(p_{,\psi}\sin\psi + p\cos\psi\right)\mathrm{d}\psi - V \right| + \int_0^{\frac{\pi}{2}} P(p)\,\mathrm{d}\psi \right),$$

where

$$P(p) = 0 \;\text{ if }\; p \geq 0,$$
$$P(p) = -p \;\text{ if }\; p < 0,$$

and

$$M_k > 0$$

such that

$$\lim_{k\to\infty} M_k = \infty.$$

[9] Cf. http://en.wikipedia.org/wiki/Genetic_algorithm

The GA chromosome of the problem is then

$$(a_1, a_2, \ldots, a_K)\,.$$

The problem described above was translated into GNU Octave code with the results of testing runnings depicted in Figs. 6, 7 and 8.

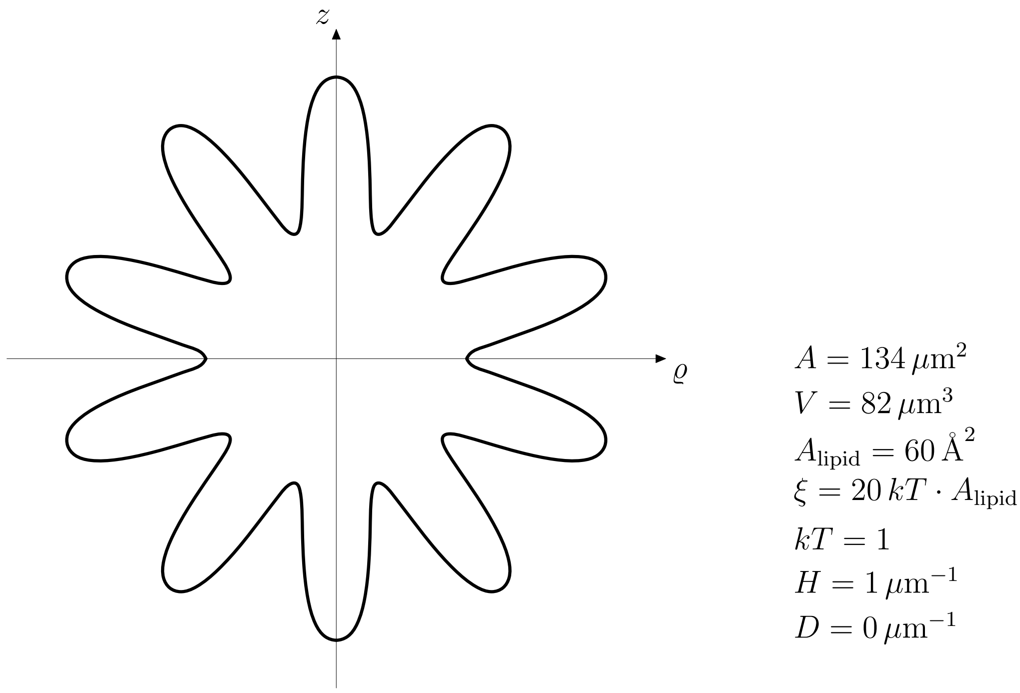

Figure 6. $H = 1\,\mu\mathrm{m}^{-1}$

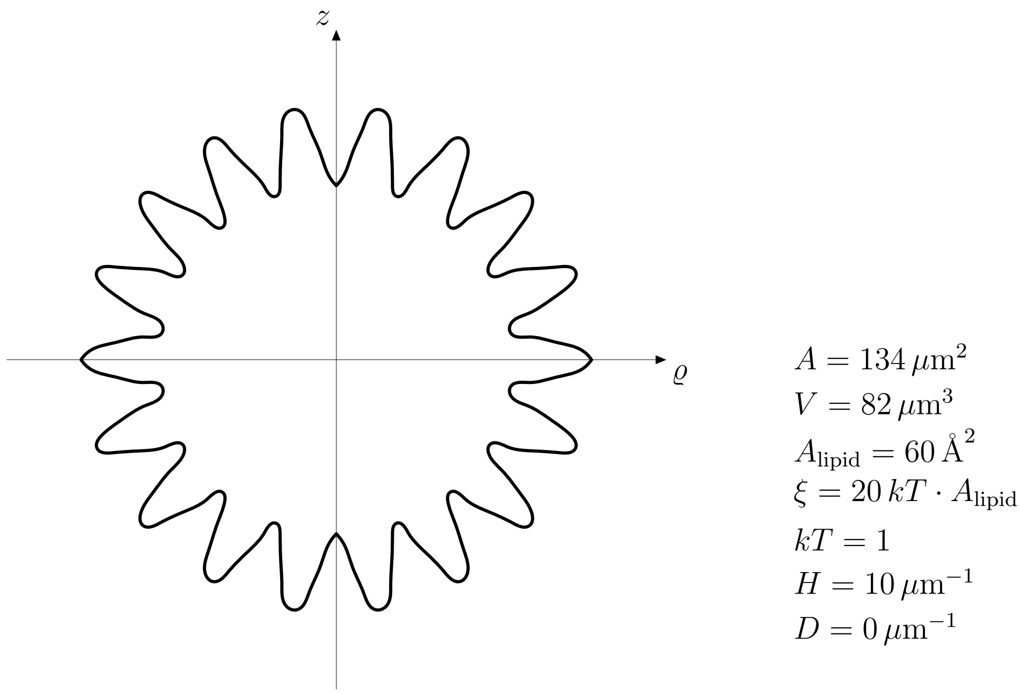

Figure 7. $H = 10\,\mu\mathrm{m}^{-1}$

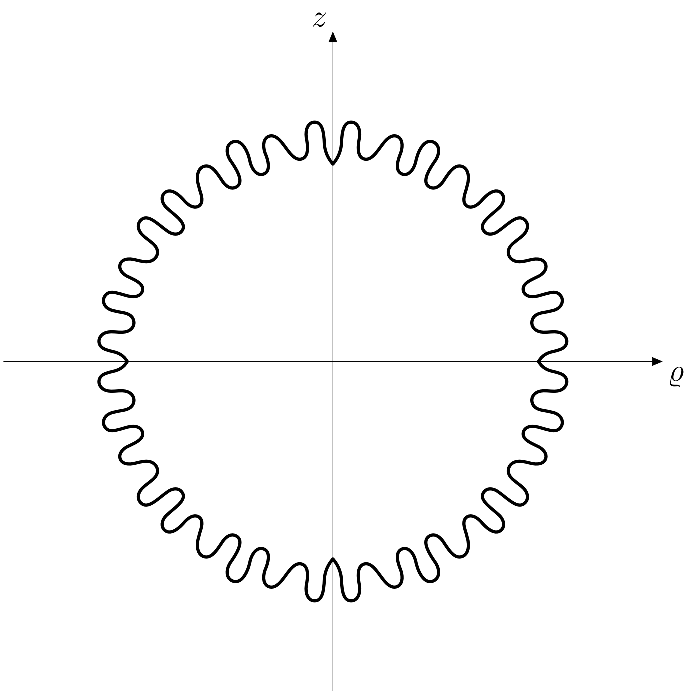

$A = 134\,\mu\mathrm{m}^2$
$V = 82\,\mu\mathrm{m}^3$
$A_{\mathrm{lipid}} = 60\,\text{Å}^2$
$\xi = 20\,kT \cdot A_{\mathrm{lipid}}$
$kT = 1$
$H = 100\,\mu\mathrm{m}^{-1}$
$D = 0\,\mu\mathrm{m}^{-1}$

FIGURE 8. $H = 100\,\mu\mathrm{m}^{-1}$

8. The shape analysis of a bilayer lipid nanotube

Let us study the shape of a bilayer lipid nanotube as depicted on Fig. 9.

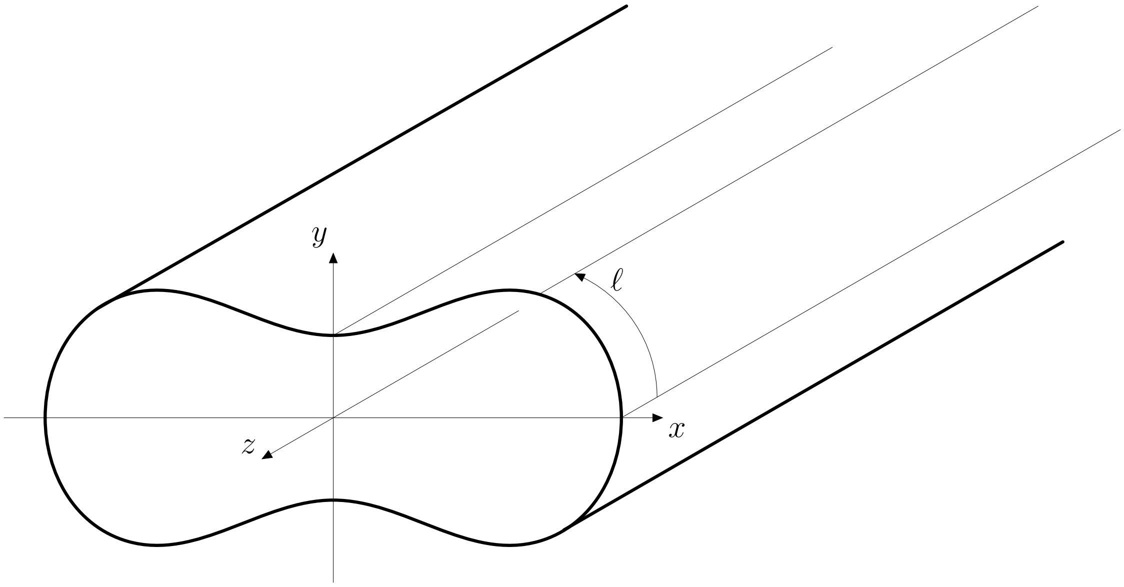

FIGURE 9. Bilayer lipid nanotube

Analysing the shape we are going to minimize the Helmholtz free energy (38)

$$F = \frac{\xi}{A_{\text{lipid}}} \int\limits_A \left((h-H)^2 + (d^2 + D^2)\right) \,\mathrm{d}A - \frac{2kT}{A_{\text{lipid}}} \int\limits_A \ln\left(2\cosh\left(\frac{\xi}{kT} dD\right)\right) \,\mathrm{d}A.$$

The mean curvature, h, and deviatoric curvature, d, depends on the main curvatures, c_1 and c_2, in the already mentioned way

$$h = \frac{c_1 + c_2}{2},$$
$$d = \frac{|c_1 - c_2|}{2}.$$

The main curvatures are entries of the diagonal form of the

$$b^\alpha_\beta = a^{\alpha\gamma} \partial_{\gamma\beta} \boldsymbol{r} \cdot \boldsymbol{n},$$

where, as can be viewed from the figure,

$$\boldsymbol{r} = (x, y, z)$$

and

$$\boldsymbol{n} = \frac{\partial_\ell \boldsymbol{r} \times \partial_z \boldsymbol{r}}{|\partial_\ell \boldsymbol{r} \times \partial_z \boldsymbol{r}|} = \frac{(x_\ell, y_\ell, 0) \times (0,0,1)}{|(x_\ell, y_\ell, 0) \times (0,0,1)|} = \frac{(y_\ell, -x_\ell, 0)}{\sqrt{y_\ell^2 + x_\ell^2}} = (y_\ell, -x_\ell, 0)\,,$$

where we have chosen the pair of curvilinear coordinates ℓ, z. Now

$$\partial_{\alpha\beta} \boldsymbol{r} = \begin{pmatrix} (x_{\ell\ell}, y_{\ell\ell}, 0) & (0,0,0) \\ (0,0,0) & (0,0,0) \end{pmatrix},$$

$$a_{\alpha\beta} = \partial_\alpha \boldsymbol{r} \cdot \partial_\beta \boldsymbol{r} = \begin{pmatrix} x_\ell & y_\ell & 0 \\ 0 & 0 & 1 \end{pmatrix} \begin{pmatrix} x_\ell & 0 \\ y_\ell & 0 \\ 0 & 1 \end{pmatrix} = \begin{pmatrix} 1 & 0 \\ 0 & 1 \end{pmatrix},$$

thus

$$b^\alpha_\beta = \begin{pmatrix} x_{\ell\ell} y_\ell - x_\ell y_{\ell\ell} & 0 \\ 0 & 0 \end{pmatrix}.$$

Using the geometrical relations

$$x_\ell = -\cos\psi$$

and

$$y_\ell = \sin\psi,$$

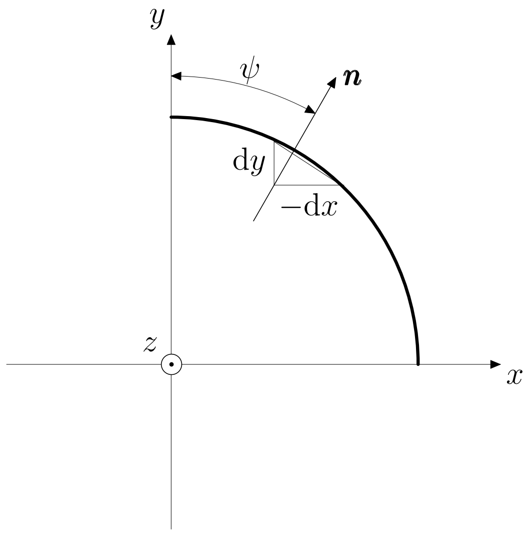

FIGURE 10. The definition of the angle ψ

where ψ is the angle made by the outer normal and the positive y-axis (Fig. 10), we get

$$b^{\alpha}_{\beta} = \begin{pmatrix} \psi_\ell & 0 \\ 0 & 0 \end{pmatrix}.$$

As the regarded nanotube is taken to be infinite the constrains on the volume and area are irrelevant here and the continuity (periodicity) condition

$$\int_L \psi_\ell \, \mathrm{d}\ell = 2\pi$$

is replaced by boundary conditions

$$\psi(0) = \frac{\pi}{2}, \quad \psi(\frac{L}{4}) = 0.$$

The boundary conditions are applied to the quarter in the first quadrant of xy-coordinat system with tube regarded as symmetrical with respect to horizontal and vertical plane, respectively. The line density of Helmholtz free energy to be minimized is then

$$\tilde{F} = \frac{\xi}{A_{\text{lipid}}} \int_{\frac{L}{4}} \left(\left(\frac{\psi_\ell}{2} - H \right)^2 + \left(\frac{\psi_\ell}{2} \right)^2 + D^2 \right) \mathrm{d}\ell - \frac{2kT}{A_{\text{lipid}}} \int_A \ln \left(2 \cosh \left(\frac{\xi}{2kT} \psi_\ell D \right) \right) \mathrm{d}\ell$$

and the minimization is to be done without any constrains but the boundary conditions. The necessary condition of the minimum is

$$\frac{\partial L}{\partial \psi} - \frac{\mathrm{d}}{\mathrm{d}\ell} \frac{\partial L}{\partial \psi_\ell} = 0$$

with

$$L = \frac{\psi_\ell^2}{2} - \psi_\ell H + H^2 + D^2 - p \ln \left(2 \cosh \left(\psi_\ell s \right) \right),$$

where

$$p = \frac{2kT}{\xi}$$

and

$$s = \frac{\xi D}{2kT}.$$

Using the fact that Lagrangean L is independent of ψ, the necessary condition takes the form

$$\frac{\partial L}{\partial \psi_\ell} = K_2,$$

K_2 being a constant, and

$$\psi_\ell - ps \tanh \left(s \psi_\ell \right) = K_2 + H = K_3$$

with, at the case that H is a constant, another constant K_3. At the case that H and D, and consequently also K_3 and s, are constants, the last equation is an equation for unknown ψ_ℓ with the solution

$$\psi_\ell = K_4,$$

where K_4 is still another constant, and

$$\psi = K_4\ell + K_5.$$

The constants are evaluated using the boundary conditions as

$$K_4 = -\frac{2\pi}{L}, \quad K_5 = \frac{\pi}{2}$$

and the solution is

$$\psi = \frac{\pi}{2} - \frac{2\pi}{L}\ell$$

which being connected with the definition of the radian through the substitutions

$$\alpha = \frac{\pi}{2} - \psi, \quad L = 2\pi R, \quad \alpha R = \ell,$$

identifies the shape as a circular tube with the radius $R = \dfrac{L}{2\pi}$.

CHAPTER 7

Shape analysis of lipid membranes with intrinsic (anisotropic) curvature – classical mechanical approach

At this chapter we model the problem described in the last chapter using classical mechanical approach. Let us start with the expression of the free energy (35)

$$f = k_1 m^\alpha_\alpha m^\beta_\beta - k_2 \left(m^\alpha_\alpha m^\beta_\beta - m^\alpha_\beta m^\beta_\alpha \right)$$

with

$$m_{\alpha\beta} = b_{\alpha\beta} - B_{\alpha\beta} = \partial_\alpha \partial_\beta \boldsymbol{r} \cdot \boldsymbol{n} - \sum_{i=1}^{N} \overset{i}{B}_{\alpha\beta} \cdot \delta(\xi^a - \overset{i}{\xi^a}),$$

where $\overset{i}{B}_{\alpha\beta}$ characterizes the intrinsic curvature of an inclusion at the spot $\overset{i}{\xi^a}$ and $\delta(\xi^a - \overset{i}{\xi^a})$ is the Dirac delta function. The last expression is built on the assumption that the natural shape of lipid bilayers is the planar one.

The model proposed uses the orientational invariants called mean curvature

$$h = \frac{1}{2} b^\alpha_\alpha, \quad H = \frac{1}{2} B^\alpha_\alpha$$

and Gaussian curvature

$$k = \left| b^\beta_\alpha \right| = b^1_1 b^2_2 - b^1_2 b^2_1, \quad K = \left| B^\beta_\alpha \right| = B^1_1 B^2_2 - B^1_2 B^2_1.$$

As the curvature of the inclusions is characterized by these two invariants, H and K, the problem of the lipid bilayer shape determination could be formulate as

$$\min_{\overset{i}{\xi^a}, \boldsymbol{r}, \boldsymbol{n}, B^\alpha_\beta} \quad F_a$$

where

$$F_a = \int_A f \, \mathrm{d}A$$

with constraints on the volume and area of the closed lipid bilayer, the area occupied by the inclusions

$$\int_A \sum_{i=1}^{N} \delta(\xi^a - \overset{i}{\xi^a}) \, \mathrm{d}A = N \cdot p,$$

with $p \in (0, 1)$ being the measure of allowed overlapping of the inclusions,

$$\overset{i}{B}_{\alpha\beta} = \overset{i}{B}_{\beta\alpha}, \overset{i}{B}{}^\alpha_\alpha = 2H, \left| \overset{i}{B}{}^\beta_\alpha \right| = K,$$

$$\boldsymbol{n} \cdot \partial_\alpha \boldsymbol{r} = 0$$

and

$$\boldsymbol{n} \cdot \boldsymbol{n} = 1.$$

CHAPTER 8

Optimization of a fibre composite

1. Stiffness maximization

Start with a one-dimensional spring, Fig. 1, and look at the connection of a force, displacement, stiffness and work of external forces.

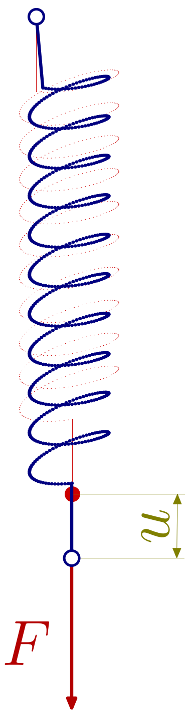

FIGURE 1. The spring

For a given force, F, the displacement

$$u = \frac{F}{k}$$

and the work done

$$W = Fu = \frac{F^2}{k}$$

is inversely proportional to the stiffness constant, k. Thus, regarding the force F as a given constant, we have the equivalence of the problem to maximize stiffness and to minimize the work done by external forces

$$\max k = \min Fu.$$

Accordingly, we can formulate the problem to maximize stifness as

$$\min(f, \hat{u}),$$

where $(.,.)$ stands for the inner product, f for external forces and $\hat{u}$ for the displacement in the state of an elastic equilibrium, *i.e.*, a solution to the Navier-Cauchy equations

$$A\hat{u} = f \tag{40}$$

as well as a minimizer of the total potential energy:

$$\Pi(\hat{u}) = \min_{u \in U} \Pi(u), \quad \Pi = \frac{1}{2}(Au, u) - (f, u), \tag{41}$$

U being a set of the statically admissible displacements. Combining (40)

$$(A\hat{u}, \hat{u}) = (f, \hat{u})$$

with (41)

$$\Pi(\hat{u}) = \frac{1}{2}(A\hat{u}, \hat{u}) - (f, \hat{u}) = -\frac{1}{2}(f, \hat{u}),$$

which means that the solution of the stiffness maximization problem fulfil the following

$$\hat{\alpha} = \arg\min_{\alpha}(f, \hat{u}) = \arg\max_{\alpha} \Pi(\hat{u}),$$

i.e.

$$\hat{\alpha} = \arg\max_{\alpha}\min_{u\in U} \Pi.$$

To incorporate the constraints, $g = 0$, constituting the set U we can build up Lagrangian $L = \Pi + \lambda g$ and write down necessary conditions of the extreme:

$$\frac{\delta L}{\delta u} = 0,$$

$$\frac{\delta L}{\delta \alpha} = 0.$$

These equations are generally nonlinear and not easy to solve. To solve these equations there is a method called alternating fulfilment of necessary equations based on the following algorithm:

1) Deliberately choose the design variables, α_0
2) Using α_k solve the elasticity problem, $\dfrac{\delta L}{\delta u} = 0 \Rightarrow u_k$
3) Using u_k solve the optimum condition, $\dfrac{\delta L}{\delta \alpha} = 0 \Rightarrow \alpha_{k+1}$
4) If $\alpha_k = \alpha_{k+1}$ you have a solution, otherwise goto item 2)

Unfortunately, this approach does not always converge, but somewhat lengthy manipulation[1] leads to another formultion of the problem

$$\hat{\alpha} = \arg\min_{\alpha}\min_{\sigma\in C} \frac{1}{2}\int_{\Omega} C_{abcd}\sigma^{ab}\sigma^{cd}\,\mathrm{d}\Omega,$$

where C is a set of statically admissible stresses, that is valid only at the case of homogeneous kinematic boundary conditions, but with much better convergence properties.[2]

2. The simplest problem of fibre composite stiffness maximization

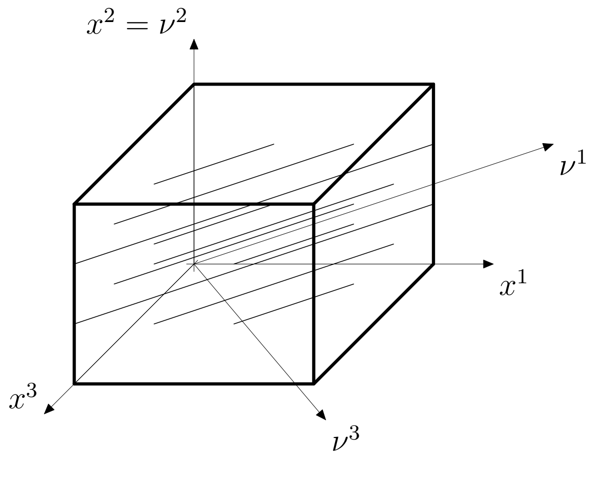

FIGURE 2. Fibre composite

[1] [**Mar06c**]
[2] [**All02**]

To illustrate the process of optimizing the fibre angle orientation, that may be continually changing along the length of the fibre, let us suppose the block from Fig. 2, tensioned with uniform stress, σ, in the direction of the x^1 axis, *i.e.*, the stress tensor of the body is

$$\sigma_{ab} = \begin{pmatrix} \sigma & 0 & 0 \\ 0 & 0 & 0 \\ 0 & 0 & 0 \end{pmatrix}$$

which solves the step 2) of the algorithm. The material properties are orthogonal with main axes of orthotropy ν^a. In the coordinate system ν^a the following relation of stresses to strains holds

$$\overset{\nu}{\varepsilon}_{ab} = \overset{\nu}{C}_{abcd} \overset{\nu}{\sigma}{}^{cd},$$

where the compliance tensor

$$\left\{ \overset{\nu}{C}_{abcd} \right\}_{\{ab\lceil cd\}} =$$

$$= \begin{pmatrix}
\frac{1}{E_{11}} & 0 & 0 & 0 & -\frac{\nu_{21}}{E_{22}} & 0 & 0 & 0 & -\frac{\nu_{31}}{E_{33}} \\
0 & \frac{1}{4G_{12}} & 0 & \frac{1}{4G_{12}} & 0 & 0 & 0 & 0 & 0 \\
0 & 0 & \frac{1}{4G_{13}} & 0 & 0 & 0 & \frac{1}{4G_{13}} & 0 & 0 \\
0 & \frac{1}{4G_{12}} & 0 & \frac{1}{4G_{12}} & 0 & 0 & 0 & 0 & 0 \\
-\frac{\nu_{12}}{E_{11}} & 0 & 0 & 0 & \frac{1}{E_{22}} & 0 & 0 & 0 & -\frac{\nu_{32}}{E_{33}} \\
0 & 0 & 0 & 0 & 0 & \frac{1}{4G_{23}} & 0 & \frac{1}{4G_{23}} & 0 \\
0 & 0 & \frac{1}{4G_{13}} & 0 & 0 & 0 & \frac{1}{4G_{13}} & 0 & 0 \\
0 & 0 & 0 & 0 & 0 & \frac{1}{4G_{23}} & 0 & \frac{1}{4G_{23}} & 0 \\
-\frac{\nu_{13}}{E_{11}} & 0 & 0 & 0 & -\frac{\nu_{23}}{E_{22}} & 0 & 0 & 0 & \frac{1}{E_{33}}
\end{pmatrix}.$$

The ν above the tensor symbol indicates that the symbol does not symbolize an abstract tensor but that it stands for the tensor components in the ν-frame of reference and $\{ij\lceil kl\}$ indicate how the entries are stored in the array, namely that the rows belong successively to the following pairs of indices ($ij = 11, 12, 13, 21, 22, 23, 31, 32, 33$) and the columns to the couples ($kl = 11, 12, \ldots, 33$).

But now, in the x coordinate system, the stiffness maximization problem of ours may be written, as the energy is uniform throughout the volume,

$$\min_{\alpha} c,$$

where

$$c = \overset{x}{\sigma}{}^{ab} \overset{x}{C}_{abcd} \overset{x}{\sigma}{}^{cd} = \sigma \overset{x}{C}_{1111} \sigma.$$

Using the transformation rule

$$\overset{x}{C}_{abcd} = \frac{\partial \nu^i}{\partial x^a} \frac{\partial \nu^j}{\partial x^b} \frac{\partial \nu^k}{\partial x^c} \frac{\partial \nu^l}{\partial x^d} \overset{\nu}{C}_{ijkl},$$

i.e.,

$$\overset{x}{C}_{1111} = \frac{\partial \nu^i}{\partial x^1} \frac{\partial \nu^j}{\partial x^1} \frac{\partial \nu^k}{\partial x^1} \frac{\partial \nu^l}{\partial x^1} \overset{\nu}{C}_{ijkl},$$

$$\overset{x}{C}_{1111} = \begin{pmatrix} \cos^2\alpha & 0 & \cos\alpha\sin\alpha & 0 & 0 & 0 & \sin\alpha\cos\alpha & 0 & \sin^2\alpha \end{pmatrix} \left\{ \overset{\nu}{C}_{abcd} \right\}_{\{ab\lceil cd\}} \begin{pmatrix} \cos^2\alpha \\ 0 \\ \cos\alpha\sin\alpha \\ 0 \\ 0 \\ 0 \\ \sin\alpha\cos\alpha \\ 0 \\ \sin^2\alpha \end{pmatrix}.$$

Thus,

$$c = \sigma^2 \left(\cos^4\alpha \frac{1}{E_{11}} + \cos^2\alpha \sin^2\alpha \left(\frac{1}{G_{13}} - \frac{\nu_{31}}{E_{11}} - \frac{\nu_{13}}{E_{33}} \right) + \sin^4\alpha \frac{1}{E_{33}} \right).$$

The necessary condition

$$\frac{\partial c}{\partial \alpha} = 0$$

reads

$$\cos^3\alpha \sin\alpha A_1 + \cos\alpha \sin^3\alpha A_2 = 0,$$

with

$$A_1 = \frac{1}{G_{13}} - \frac{\nu_{31}}{E_{11}} - \frac{\nu_{13}}{E_{33}} - \frac{2}{E_{11}}$$

and

$$A_2 = \frac{2}{E_{22}} + \frac{\nu_{31}}{E_{11}} + \frac{\nu_{13}}{E_{33}} - \frac{1}{G_{13}}.$$

The last condition permits the following solutions:

1) $\hat{\alpha}_1 = \pm\frac{\pi}{2}$ with $c_1 = \frac{\sigma^2}{E_{33}}$
2) $\hat{\alpha}_2 = 0, \pi$ with $c_2 = \frac{\sigma^2}{E_{11}}$
3) $\hat{\alpha}_{3,4} = \arctan\left(\pm\sqrt{-\frac{A_1}{A_2}}\right)$.

Which one of the solutions of necessary conditions is solution of the stiffness maximization problem depends on numerical values of the material characteristics and should be decided from the numerical values of the object function c or the study of the second derivative.[3]

3. Stiffness maximization of plates

Using the elasticity principles described above we can formulate the problem of stiffness maximization at the case of laminated multilayer Kirchhoff plates of symetric layout in symbolic form as[4]

1) The elasticity problem

$$P^{abcd} w_{cd} = q^{ab}$$

2) The necessary condition of optimum

$$w_{ab} w_{cd} R^{abcd}(\alpha_\nu) = 0$$

where w_{ab} represents Fourier series expansion coefficients of the perpendicular displacement and $R^{abcd}(\alpha_\nu)$ are functions of the design parameters, α_ν, standing for the layer orientation, see Fig. 3. The loading is expanded into Fourier series with coefficients, q^{ab}.

There is only space for citing a few results of the described problem in this lecture. The results of stiffness maximization of the laminate plate are quoted in Figs 3 through 7 where there are descriptions of the loading conditions in the caption of the figures and the optimal angles of layer orientations in the figures (only one half of the symmetric plates is depicted).[5]

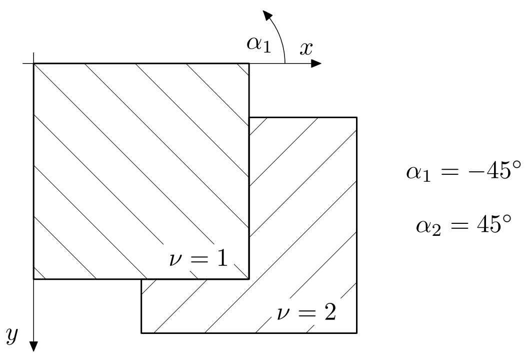

FIGURE 3. Square plate of four layers loaded by $q = q_o \sin\frac{\pi x}{a} \sin\frac{\pi y}{b}$ (Permutation of layout is possible)

[3][**Mar05**]
[4][**Mar04**]
[5][**Mar06c**]

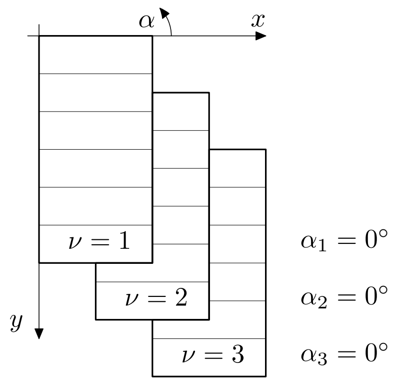

FIGURE 4. Rectangular plate (1:2) of six layers loaded by $q = q_o \sin\frac{\pi x}{a} \sin\frac{\pi y}{b}$

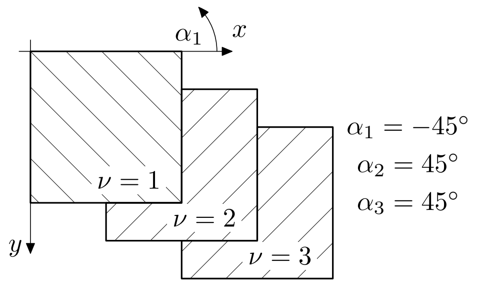

FIGURE 5. Square plate of six layers loaded by $q = q_o \sin\frac{2\pi x}{a} \sin\frac{2\pi y}{b}$ (All other layouts are possible as well)

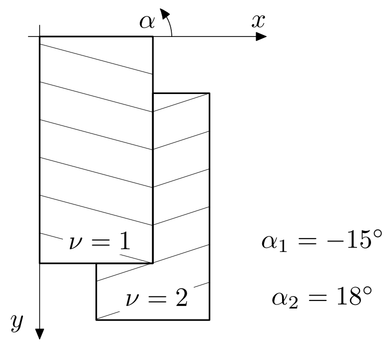

FIGURE 6. Rectangular plate (1:2) of four layers loaded by $q = q_o xy$ (The inverse layout is equivalent)

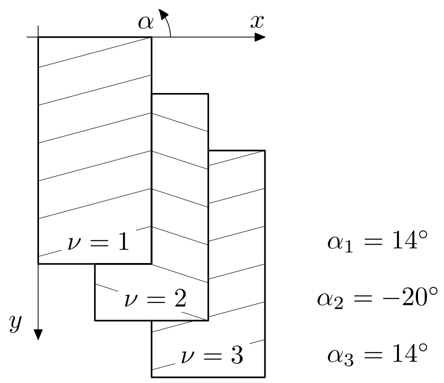

FIGURE 7. Rectangular plate (1:2) of six layers loaded by $q = q_o xy$ (The other layouts are equivalent)

4. Stiffness maximization of thick-walled anisotropic elliptic tube

At this section we are going to maximize the stiffness, by choosing winding angle of the fibre, of the thick walled fibre wound, and thus anisotropic, elliptic tube analyse in Chapter 2. The tube is optimized for three different loadings. First, under a pulling force, F, see Fig. 1, distributed evenly along the lower face. Second and third, with shearing forces T_1 (a force in the direction of the axis b^1) and T_2 (having direction of the b^2), respectively. Both of the last two forces are evenly distributed as well. Following the scheme of the alternative fulfilment of necessary condition method to perform the analysis is necessary. As this was done in Chapter 2 we can approach the necessary condition of stiffness maximum.

4.1. Stiffness maximization. Applying the method of alternating fulfilment of necessary conditions as described above leads to the necessity to solve two problems.

(1) The problem of elasticity as already solved in the form

$$\mathtt{A} = \mathtt{K}^{-1}\mathtt{P}$$

(2) The stiffness maximum condition,

$$\frac{\partial \Pi}{\partial \alpha} = 0,$$

i.e.,

$$\frac{1}{2}\mathtt{A}^T \frac{\partial \mathtt{K}}{\partial \alpha}\mathtt{A} = 0,$$

that represents, at the regarded case, one equation and we can solve it numerically, *e.g.*, using Bisection method.

At the last equation

$$\frac{\partial \mathtt{K}}{\partial \alpha} = \int_0^{\ell}\int_0^{2\pi}\int_0^{t} \mathtt{(B-Gam)'*}\frac{\partial \mathtt{Ex}}{\partial \alpha}\mathtt{*(B-Gam)*sqrt(det(gx))}\,\mathrm{d}^3 x,$$

$$\frac{\partial \mathtt{Ex}}{\partial \alpha} = \left\{ \frac{\partial \overset{x}{E}{}^{abcd}}{\partial \alpha} \right\}_{ab\lceil cd},$$

$$\frac{\partial \overset{x}{E}{}^{abcd}}{\partial \alpha} = \left(\alpha_i^a \frac{\partial x^b}{\partial \nu^j}\frac{\partial x^c}{\partial \nu^k}\frac{\partial x^d}{\partial \nu^l} + \frac{\partial x^a}{\partial \nu^i}\alpha_j^b \frac{\partial x^c}{\partial \nu^k}\frac{\partial x^d}{\partial \nu^l} + \right.$$
$$\left. + \frac{\partial x^a}{\partial \nu^i}\frac{\partial x^b}{\partial \nu^j}\alpha_k^c \frac{\partial x^d}{\partial \nu^l} + \frac{\partial x^a}{\partial \nu^i}\frac{\partial x^b}{\partial \nu^j}\frac{\partial x^c}{\partial \nu^k}\alpha_l^d \right) \overset{\nu}{E}{}^{ijkl},$$

where

$$\alpha_b^a = \frac{\partial}{\partial \alpha}\left[\frac{\partial x^a}{\partial \nu^b}\right] = \frac{\partial x^a}{\partial b^c}\frac{\partial b^c}{\partial \xi^d}\frac{\partial}{\partial \alpha}\left[\frac{\partial \xi^d}{\partial \nu^b}\right],$$

$$\frac{\partial}{\partial \alpha}\left[\frac{\partial \xi^d}{\partial \nu^b}\right] = \begin{pmatrix} 0 & 0 & 0 \\ 0 & -\sin\alpha & -\cos\alpha \\ 0 & \cos\alpha & -\sin\alpha \end{pmatrix}.$$

The last equations are stated only as a demonstration of the simplicity of the approach. For full understanding of the symbols, one must look at more detailed description of the preceding analysis.[6]

4.2. Optimized winding angles. Using the above described procedure we arrive at the following results. At the case of the pulling force, F_3, the stiffness maximizing angle seems to be 90°. For the shearing force T_1 the angle is 0° and for the shearing force T_2 it is ±45°, see Fig. 8. Even at this simple one parametric case, there is necessity at every step to choose the appropriate solution of the equation from the second step of the algorithm (as there is more than one solution of this equation.)

[6] [**Mar08**]

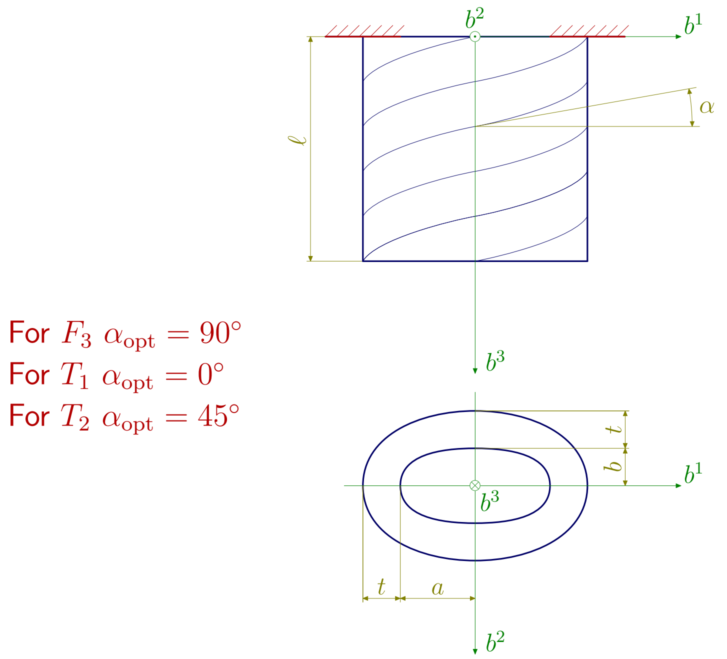

FIGURE 8. The optimum angle α for given loadings

5. Concluding remarks

As the problem of the last section is a one-parametric one, and thus an easy one, we can check the results by direct evaluation of the objective function in a set of discrete points. It must be stated the computation time was similar at both cases. The results were essentially the same. But, of course, the method of alternative fulfilment of the necessary condition is of universal usage even at the case of multilayer (multiparameter) problems. The pointwise method must be at such a case substituted by another method, *e.g.*, Genetic Algorithms. As shown in the case of plates and tubes,[7] such an approach costs much more computation time and increase of uncertainty of the quality of the solution.

[7] [**Mar06c**]

Bibliography

[All02] G Allaire, *Shape optimization by the homogenization method*, Springer-Verlag, New York, 2002.

[Ant05] Stuart S. Antman, *Nonlinear problems of elasticity*, Spiringer-Verlag, New York, 2005.

[Cau27a] Augustin Louis Cauchy, *De la pression ou tension dans un corps solide*, Exercices de Mathematiqucs (1827).

[Cau27b] ———, *Sur la condensation et la dilatation des corps solides*, Exercices de Mathematiqucs (1827).

[CGM06] Philippe G. Ciarlet, Liliana Gratie, and Cristinel Mardare, *A nonlinear korn inequality on a surface*, Journal de mathematiques pures et appliquees (2006), 1—22.

[Che00] A. V. Cherkaev, *Variational methods for structural optimization*, Springer, New York, 2000.

[Cia88] Philippe G. Ciarlet, *Mathematical elasticity. volume i: Three-dimensional elasticity*, North-Holland, Amsterdam, 1988.

[Cia05] ———, *An introduction to differential geometry with applications to elasticity*, Springer-Verlag, Berlin, 2005.

[CL03] Philippe G. Ciarlet and Florian Laurent, *Continuity of a deformation as a function of its cauchy-green tensor*, Archive for Rational Mechanics and Analysis **167** (2003), 255—269.

[Dac89] B. Dacorogna, *Direct methods in the calculus of variations*, Applied Math. Sciences, vol. 78, Springer-Verlag, Berlin, 1989.

[DN03] I. Dorland and W. A. Newman, *Dorland's illustrated medical dictionary*, W. B. Saunders Company, Philadelphia, 2003.

[FKIB+03] Miha Fošnarič, Veronika Kralj-Iglič, Klemen Bohinc, Aleš Iglič, and Sylvio May, *Stabilization of pores in lipid bilayers by anisotropic inclusions*, J Phys Chem B Condens Matter Mater Surf Interfaces Biophys **107** (2003), 12519–12526.

[Gra18] Henry Gray, *Anatomy of the human body*, Lea & Febiger, Philadelphia, 1918.

[GZ54] A. E. Green and W. Zerna, *Theoretical elasticity*, Clarendon Press, Oxford, 1954.

[Ham55] William Rowan Hamilton, *On some extensions of quaternions*, The London, Edinburgh and Dublin Philosophical Magazine and Journal of Science (4th Series) **vii—ix** (1854, 1855), 492—499, 125—137, 261—269, 46—51, 280—290, Edited by David R. Wilkins, 2001.

[Hel73] W. Helfrich, *Elastic properties of lipid bilayers: theory and possible experiments.*, Z. Naturforsch **C 28** (1973), 693.

[Hil86] Terrell L. Hill, *An introduction to statistical thermodynamics*, Dover Publications, Inc., New York, 1986.

[Koc17] John C. Koch, *The laws of bone architecture*, American Journal of Anatomy **21** (1917).

[Lov27] A. E. H. Love, *Treatise on the mathematical theory of elasticity*, Cambridge university press, Cambridge, 1927.

[LR89] David Lovelock and Hanno Rund, *Tensors, differential forms, and variational principles*, Dover Publications, Inc., New York, 1989.

[Mar04] T Mares, *Maximalizace tuhosti laminatovch desek a trubek volbou orientace vrstev*, Ph.D. thesis, Czech Technical University in Prague, Faculty of Mechanical Engineering, Department of Mechanics, Prague, 2004.

[Mar05] ———, *Laminate tube stiffness maximization by winding angle control*, Bulletin of Applied Mechanics **1** (2005), 29–54.

[Mar06a] ———, *Locally orthotropic material—the foundation of tissue mechanics*, Bulletin of Applied Mechanics **7** (2006), 151–157.

[Mar06b] ———, *Mathematical model of the cortical bone osteon*, Bulletin of Applied Mechanics **7** (2006), 159–165.

[Mar06c] ———, *Zaklady konstrukcni optimalizace*, Tomas Mares, Prague, 2006.

[Mar08] ———, *Curvilinear elasticity in biomechanics*, Czech Technical University in Prague, Faculty of Mechanical Engineering, Department of Mechanics, Prague, 2008, Habilitation thesis.

[Mik64] S. G. Mikhlin, *Variational methods in mathematical physics*, The Macmillan Co., New York, 1964.

[Pau76] Friedrich Pauwels, *Biomechanics of the normal and diseased hip*, Springer-Verlag, Berlin, 1976.

[Ped00] Pablo Pedregal, *Variational methods in nonlinear elasticity*, Society for Industrial and Applied Mathematics, Philadelphia, 2000.

[Sal01] Jean Salençon, *Handbook of continuum mechanics*, Springer-Verlag, Berlin, 2001.

[SN72] S. J. Singer and G. L. Nicolson, *The fluid mosaic model of the structure of cell membranes*, Science **175** (1972), 720.

[SS78] J. L. Synge and A. Schild, *Tensor calculus*, Dover Publications, Inc., New York, 1978.

[Tab04] Larry A. Taber, *Nonlinear theory of elasticity—aplications in biomechanics*, World Scientific, New Jersey, London, *etc.*, 2004.

[Tot05] Viktor Toth, *Tensor manipulation in gpl maxima*, arXiv:cs/0503073 **05** (2005), 1—26.

[Wal84] Robert M. Wald, *General relativity*, University of Chicago Press, Chicago and London, 1984.

[Wan05] Stefan Waner, *Introduction to differential geometry and general relativity*, Department of Mathematics, Hofstra University, 2005.

[Was75] K. Washizu, *Variational methods in elasticity nad plasticity*, 2nd ed., Pergamon Press, Oxford, 1975.